DEVELOPING AN ONCOLYTIC PRIME-BOOST VACCINE TARGETING THE TUMOUR ASSOCIATED ANTIGEN MESOTHELIN FOR THE TREATMENT OF PANCREATIC CANCER

By

Katherine Elizabeth Baxter

A thesis submitted in partial fulfillment of the requirements for the degree of Doctor of Philosophy, Specialization Microbiology and Immunology

University of Ottawa

Faculty of Medicine

December 7 2019

Supervisor

Dr Rebecca C Auer, MD

Co-Supervisor

Dr John Bell, PhD

Abstract

Pancreatic cancer (PDAC) affects 4400 Canadians each year and with 5year survival rates <8%, there is clearly an unmet need for new therapeutic approaches for treating this deadly disease. Herein I report the development of a surgical model of PDAC that recapitulates many of the hallmarks of human disease and has an immune infiltrate consisting of T cells and suppressive regulatory T cells and myeloid derived suppressor cells. This model allows the exploration of new therapeutics that can be used in combination with surgical resection of primary tumours. Furthermore, I propose that the use of neoadjuvant administration of a prime-boost oncolytic vaccine targeting a pancreatic tumour associated antigen (TAA) - mesothelin - could potentiate pancreatic tumour specific immune responses to improve patient prognosis. We demonstrate that immune tolerance to this self antigen can be broken by the complete depletion of circulating T_{regs} at the time of vaccination, which leads to the activation of a population of CD8+ T cells responsive to mesothelin. We demonstrate that these T cells respond to mesothelin expressing tumour cells *ex vivo*, and that CD8+ T cells are recruited to the site of tumour challenge. However, despite the generated CD8+ T cell response, oncolytic vaccine strategies targeting mesothelin provide no protection against Pan02 tumours, or against other mesothelin expressing murine tumour lines. I demonstrate that this is not through common tumour escape mechanisms, nor through the upregulation of suppressive immune populations. Any efficacy observed was found to be provided solely by depletion of T_{regs}, as the depletion of CD8+ T cells did not reduce protection from tumour outgrowth in vaccinated mice. While mesothelin represents a promising target, it is not an ideal target for oncolytic vaccine platforms, potentially due to its nature as a self antigen.

Acknowledgements

I couldn't have completed my PhD studies or my thesis without the help and support of my friends, family and labmates.

First, I would like to thank Dr Rebecca Auer for inviting me to join your lab and for your supervision on my project. You have been an inspiration throughout my studies and helped me to achieve my potential. Dr John Bell - thank you for your co-supervision and providing a wonderful collaborative lab environment to grow in. Dr Lee Hwa-Tai and Dr Mike Kennedy – your in-lab supervision, assistance with experiment design and willingness to revise my manuscripts and abstracts have made me a better scientist, both in the lab and out!

Christiano Tanese de Souza – I could not imagine doing my PhD without you. Thank you for the countless hours we have spent doing mouse surgeries and experiments. You made the time I spent in the lab memorable and were always there to listen.

Thank you to all the members of the Auer lab, both past and present. Almohanad – your guidance in the early stages of my work with OVs was greatly appreciated. Casey, Manahil, Leonard and Sarwat thank you for all the coffee breaks and chats, as well as being friends throughout my studies. To all other members of the Auer lab – Marisa, Andre, Meghan, Dominique, Juliana – it has been a pleasure working with you.

And finally, to my family, thank you for your ongoing love and support over the last five years, and throughout my life. You have inspired me to be the best I can be and to follow my dreams. Thank you.

Table of Contents

List of Abbreviations

5-FU = 5-Fluorouracil

ACK = Ammonium-Chloride-Potassium lysis buffer

APC = Antigen presenting cell

BCA = Bradford Colorimetric Assay

B_{reg} = Regulatory B cell

CA125 = Cancer antigen 125

CAFs = Cancer associated fibroblasts

CAR-T = Chimeric antigen receptor T cell

CD = Cluster of differentiation

CFSE = Carboxyfluorescein succinimidyl ester

Cr-51 = Chromium 51

CTLA-4 = Cytotoxic T lymphocyte associated protein 4

CTV = Cell Trace violet

CY = Cyclophosphamide

DAMPs = Damage-associated molecular patterns

DC = Dendritic cell

DCT = dopachrome tautomerase

DMEM = Dulbecco's modified Eagle's medium

FBS = Fetal bovine serum

FFPE = Formalin fixed paraffin embedded

FOXP3 = Forkhead box P3

GFP = Green fluorescent protein

GM-CSF = Granulocyte-macrophage colony stimulating factor

GVAX = GM-CSF secreting whole cell vaccine

H&E = Haemotoxylin and eosin

HLA = Human leukocyte antigen

hpi = hours post infection

HSV = Herpes Simplex Virus

i.p. = intraperitoneal

i.m. = intramuscular

i.t. = intratumoral

i.v. = intravenous

ICD = Immunological cell death

ICV = Infected cell vaccine

IFNγ = Interferon gamma

IL = Interleukin

irrB78H1GM = gamma irradiated B78H1GM cells (60Gy)

irrPan02 = gamma irradiated Pan02 cells (60Gy)

kDa = kilodalton

MAGE-A3 = Melanoma associated antigen 3

MDSC = Myeloid derived suppressor cell

MG1 = Maraba MG1 with deletions in the M and G proteins

MHC = Major histocompatibility complex

MTD = Maximum tolerated dose

MPF = Megakaryocyte-potentiating factor

MOI = Multiplicity of infection

MRD = Minimal residual disease

MRI = Magnetic resonance imaging

NK = Natural killer cell

NKT = Natural Killer T cell

OV = Oncolytic Virus

OVax = Oncolytic Vaccine

PAMPs = Pathogen-associated molecular patterns

PBMC = Peripheral blood mononuclear cell

PBS = Phosphate Buffered Saline

PDAC = Pancreatic Ductal Adenocarcinoma

PD-1 = Programmed death receptor 1

PD-L1 - PD-1 receptor ligand

PFU = Plaque forming unit

ROS = Reactive oxygen species

RPMI = Roswell Park Memorial Institute Medium

cRPMI = RPMI supplemented with 10% FBS

s.c. = subcutaneous

TAA = Tumour associated antigen

TAM = Tumour associated macrophage

TAP = Transporter for antigen presentation

TCR = T cell receptor

TGF-β = Transforming Growth Fact β

TH1 = T-helper cell 1

TH17 = T-helper 17 cell

TILs = Tumour infiltrating lymphocytes

TME = Tumour microenvironment

TNFα = Tumour Necrosis factor alpha

T_{reg} = Regulatory T cells

Trp2 = Tyrosinase-related protein 2

T-VEC = Talimogene laherparepvec

VSV = Vesicular stomatis virus

List of Fgures

List of Tables

1 Introduction

1.1 Cancer

Cancer is the second leading cause of death worldwide, accounting for an approximated 9.6 million deaths in 2018 [1]. In Canada, 1 in 2 people will be diagnosed with cancer in their lifetime [2], and while the survival rates for cancer are increasing it is estimated that 1 in 4 Canadians will die from cancer of some form. Even with the improved rates of diagnosis and treatment across a variety of cancer types, with the aging population in Canada [2,3], the overall number of Canadians diagnosed with cancer is increasing each year. With numbers this high, the economic impact of cancer is massive, upwards of $1.16 trillion dollars each year [1]. There is an immediate need for therapies that can increase survival rates and patient outcomes across all cancer types, specifically in exploring and establishing platforms that can have wide-reaching implications for health care.

Cancer is an overarching term used to describe and understand neoplastic diseases. There are six defined hallmarks of cancer that are acquired over time as normal cells progress into cancerous cells through the acquisition of a number of genetic mutations in key cellular systems [4,5]. These hallmarks are: the sustaining of proliferative potential, evading growth suppressors, resisting cell death, enabling replicative immortality, inducing angiogenesis and finally activating invasion and metastasis [6]. Further than the hallmarks of cancer as initially defined by Hanahan and Weinberg in 2000, the interactions with the tumour stroma and the hallmarks of the tumour microenvironment are just as important when defining, diagnosing, and treating cancer [4]. Specifically the cancer-associated fibroblasts (CAFs), pericytes, extracellular matrix, endothelial cells, myeloid cells and lymphocytes each play an important role in establishing the hallmarks of cancer and lead to therapeutic and immune evasion, eventually leading to

progression of disease and death [4]. CAFs are especially important in the case of the tumour stroma of breast and pancreatic carcinomas and have been associated with the initiation, growth and metastasis of these tumours as well as leading to resistance to tumour-directed therapies [4,7]. New therapeutics being developed therefore need to consider both the tumour itself, as well as the microenvironment in which the tumour is found and how they interact with the rest of the body.

1.1.1 The role of the immune system in cancer progression

The immune system plays a critical role in cancer surveillance as well as cancer progression. The importance of the immune system is such that in 2011, Hanahan and Weinberg wrote a next generation of "The Hallmarks of Cancer" that included two emerging hallmarks – reprogramming metabolism and evasion of immune destruction [5]. The first role of immune cells was identified through the invasion of bone-marrow derived cells including macrophages, neutrophils, mast cells and myeloid progenitor cells which infiltrated early into neoplastic lesions and inevitably helped to progress tumour development [5]. Its dual role in cancer was first identified in the late 70s, and was fully fleshed out by Dunn et al in the early 2000s [8]. This came after a long debate in which arguments for a promoting, suppressive or null role in cancer progression were rampant [9]. This theory – that of immunoediting [8] – can be divided into three stages, wherein the role of the immune system switches from one that actively controls cancer and eliminates cancer cells to one that is no longer able to target tumours and has actively become an essential component in the suppressive tumour microenvironment(TME) [9]. These three stages are: elimination, equilibrium and escape.

In elimination, the earliest stage of immunoediting, the immune system is fully competent and capable of eliminating tumour cells. The role of the immune system in the immunogenicity of

tumours was first fleshed out in a comparison between immunocompetent and immunodeficient mice [10]. In the immunocompetent mice, T cell editing of highly immunogenic antigens led to the development of tumours that were less immunogenic, whereas those that developed in the immunodeficient mice had tumours that grew out quickly but continued to express model antigens [11,12]. These studies also showed that the early anti-cancer immune response during the elimination phase relies on the expression of type I and type II interferons which play distinct roles in the activation and maintenance of CD4+ and CD8+ T cell responses [8,9,13] as well as the presentation of recognition molecules such as NKG2D which is essential for the innate NK cell response to tumours [9,14,15].

The equilibrium stage is characterized by a shift in the immune response from one of tumour elimination towards one of immune-mediated dormancy [9]. This stage has been less studied than the other two stages due to the paucity of models in which it can be fully explored [10]. Two landmarks studies in 2007 and 2011 using a mouse model of fibrosarcoma and p53 mutations led to an understanding of the role of Th1-mediated immunity and demonstrated that tumour dormancy is a prolonged process [16,17]. The equilibrium phase is reliant on the balance between anti-tumour responses driven by IL-12 and IFNγ and tumour promoting cytokines including IL-23 and IL-10 [9,16]. This process can be further defined by the relative balance between immunosuppressive cells (i.e., T_{regs}, MDSCs, NKT cells) and tumour-targeting immune cells (CD8+ T cells, NK cells) [18].

The final stage of immunoediting is that of escape – defined by the progressive outgrowth of immune-edited tumours and the establishment of the immunosuppressive TME [9]. In this stage the immune system is no longer capable of restricting tumour outgrowth due to immunoediting which enable the tumour cells to evade immune recognition through various mechanisms [9,19].

This stage is the one in which most therapeutics would be delivered, and the reason many therapeutics, including immunotherapies fail as the tumours have been edited and evolved a plasticity allowing them to grow continuously.

1.1.2 Pancreatic Cancer

Pancreatic ductal adenocarcinoma (PDAC) is an invasive epithelial neoplasm with ductal and/or glandular differentiation [20]. It is also one of the most lethal solid malignancies worldwide [3,20]. Last year 5500 Canadians were diagnosed with pancreatic cancer, and 4800 died [2], resulting in one of the highest mortality rates, with a 5 year survival rate of only 8% [2,3,21].

Unfortunately due to a lack of effective screening techniques [22], and the fact that it is relatively hard for pathologists to differentiate early stage tumours from pancreatitis and non-malignant cysts[20], most patients are only identified in late stages of cancer. In fact, in Canada 56.7% of new PDAC cases were only identified in stage IV leading to very reduced treatment option s[2]. Current treatment options are limited to chemotherapy, radiation and surgery, though there has been a push towards developing and testing immunotherapies for treating pancreatic cancer. Historically 5-fluorouracil (5-FU) was the chemotherapy most used to treat PDAC, however in 1997 gemcitabine became the standard treatment after a number of clinical trials showed increased survival time [23–25]. Recently gemcitabine combination therapies [25] including the addition of nab-paclitaxel [26,27] or capecitabine[28], as well as the combination therapy FOLFIRINOX – composed of 5-FU, leucovorin, oxaliplatin and irinotecan[26,29], are being employed in the clinic. Chemoradiation is also employed for locally advanced unresectable PDAC[29].

Staging of cancer has become key in identifying which treatment option is available to patients. PDAC can be classified as stage 0-II being resectable, III locally advanced/unresectable or IV

which is metastatic and unresectable [30]. Unfortunately only 20% of patients are eligible for surgery, which is the only known curative treatment [30,31]. This leaves the majority of patients facing chemotherapy or chemoradiation, which have thus far proven to be ineffective [26,27,29,30], as PDAC is known to be one of the most chemoresistant cancers[30]. This chemoresistance has been attributed to the innate tumour heterogeneity and plasticity associated with pancreatic cancer [30], as well as the dense stromal environment known as the desmoplasia surrounding the tumour[30,32].

There has recently been a push towards developing immunotherapies that can specifically target PDAC, however more research is required to understand the role of immune cells, and how they interact in the TME in order to better apply these therapeutics in the clinic. These therapies require a deeper understanding of the immune component in patients as well as the use of pre-clinical models of PDAC.

1.1.3 Surgical Resection of Pancreatic Cancer

Surgical resection of PDAC currently remains the only potentially curative treatment option for patients; with 5 year survival rates increasing from 8% to 15% for patients who receive surgical resection[31]. However, even with the best possible treatment options – combining surgical resection with chemotherapy, as was done in a large phase III clinical trial combining surgery with adjuvant gemcitabine[33] – most patients recur in the form of metastatic disease and local recurrence[31,34,35].

While in many cases a splenectomy is required in conjunction with a distal pancreatectomy to insure a negative margin resection and clearance of regional lymph nodes, spleen preserving operations are associated with better outcomes and decreased rates of mortality and morbidity following surgery[39–43]. No long term effect on overall survival or tumour progression has been observed[44]; however, the immediate postoperative complications are consistently lower,

and result in shorter hospital stays for patients[45,46]. This improved outcome has been associated with the maintenance of immune surveillance [39–41,47], and some groups have recommended that the spleen be preserved when possible[45,46].

1.1.4 Preclinical Models of PDAC

Pre-clinical models have been developed to understand PDAC and to explore therapeutics. These include xenograft models, genetic models and syngeneic models, each with their own benefits and disadvantages for studying the various aspects of PDAC. Xenograft models represent human tumours and can be divided into two categories: tumour-derived patient xenografts and transplantable tumour cell lines including MiaPaca and PANC-1 cells [48]. While these models do represent human tumours with the clinical tumour progression, they need to be injected into immunocompromised mice, either athymic nude mice lacking a thymus, or severe combined immunodeficient (SCID) mice lacking both B and T cells[48].In xenograft models the innate immune system is still intact, however they cannot be used to evaluate immunotherapies and in fact due to the differences in stroma and immune components of the TME, they do not closely resemble what occurs in the clinic[49]. Furthermore, while tumour derived xenografts have been found to more closely resemble results observed in the clinic [50], transplantable xenograft lines mimic clinical outcomes in less than one third of cytotoxic drugs evaluated [51]. In comparison, genetic models of PDAC are highly representative of clinical tumours [52]. KPC is a genetic model of PDAC which involves a constitutively active Kras and p53 point mutation murine model grows in immunocompetent mice, and represent naturally occurring tumours that model human tumour progression [52], however the variable timing of tumour development makes it difficult to study experimental therapies.

Syngeneic models were developed in mice and are grown in immunocompetent mice meaning they can be used to study the interactions of the host immune system with the tumour [53]. This

allows for the study of multiple therapeutics including immunotherapies in a model where the timeline can be controlled. Depending on the site of injection, e.g. subcutaneous or orthotopic, different aspects of tumour growth can be studied. Subcutaneous injection of PDAC cells has less direct comparison with clinical disease; however it is easy to monitor [53]. Orthotopic injection of syngeneic cell lines in the head, body or tail of the pancreas has led to models that are capable of modelling human PDAC progression in the correct TME; however this poses the problem of developing an injection technique and monitoring tumour outgrowth [53]. Various groups have tried to overcome these problems through injection in Matrigel© to avoid spread[53], and monitoring tumour outgrowth with imaging systems like magnetic resonance imaging (MRI)[53] or transducing the cells with a luciferase reporter transgene[54].

Currently Pan02 cells and 6606PDA cells represent the two best characterized syngeneic PDAC models that exist. 6606PDA cells were first isolated in 2006 by Tuveson from p48/Kras G12D mice [55], and develop into globular differentiated tumours that have pancreatic acinus and duct-like structures. However this cell line is very slow growing, and relatively non- invasive [53]. Pan02 cells are the most commonly used murine model of PDAC, and were created by Corbett et al in the 1980s through the injection of 3-methyl cholanthrene into the pancreas of C57Bl/6 mice [56]. These cells formed more aggressive tumours that had a lobular growth pattern but overall were less differentiated than 6606PDA cells [53]. Pan02 cells have been used in many PDAC models and are used in the study of both primary tumours in addition to metastatic tumours. While mice injected with Pan02 cells orthotopically tend to die of primary tumour burden before the occurrence of visible metastases, several groups have developed models of metastatic PDAC using this cell line. Wang et al passaged Pan02 lines through the liver by injecting them orthotopically into the pancreas and collecting any hepatic metastases at endpoint, then reseeding

those tumour cells into the pancreas[57] resulting in a more aggressive and more metastatic line. Splenic injections of Pan02, followed by a hemi-splenectomy have also been used to model hepatic metastases [58,59]. Pre-clinical models of PDAC allow us to investigate therapeutics and understand disease progression, but the model needs to maintain the balance between measuring biological and immunological responses while still representing clinical significance.

Several pre-clinical models exist to model pancreatic disease in mice, and to understand metastatic PDAC patterns. These models span from nude-mouse models using human cancer to syngeneic models that allow investigation into the immune system [36–38]. Ideally models that use an orthotopic technique would mostly closely model the tumour microenvironment present in the pancreas. In nude mice, Hwang et al optimized a technique for suturing tumours grown subcutaneously onto the tail of the pancreas, and then utilized this model to explore the effects of splenectomies without tumour resection on tumour growth. This model was repeated using the syngeneic Pan02 cell line in immunocompetent mice [36,37]. Hwang et al's orthotopic Pan02 and MiaPaca tumour models explored the importance of spleen preservation at the time of tumour engraftment, and tumour take-rates as well as growth rates were increased in the absence of the spleen [36,37]. Tepel et al developed a partial pancreatectomy model using human PDAC in the head of the pancreas [60] and Ni et al developed a partial pancreatectomy model in the tail of the pancreas of nude mice, however this model involves the total resection of the tail and spleen [61]. Both models allowed the exploration of combinations of chemical adjuvant therapy and the exploration of xenograft surgery models, but neither was performed in immunocompetent mice, nor did they investigate the importance of maintaining immunosurveillance. There is a lack of clinically-relevant models of PDAC in

immunocompetent mice that fully allow for the exploration of immunotherapies, in a conjunction with the only known curative therapy – surgical resection.

1.2 The Immune Response to Pancreatic Cancer

The immune response to cancer is an integral part of both cancer development, and any immunotherapy aimed at developing an anti-tumour response. During the elimination, equilibrium and escape phases of cancer development, various components of the immune system are involved in the pro- and anti- tumour responses. Pancreatic cancer is no exception, and therefore has a well defined innate and adaptive response against the tumour as well as a strong immunosuppressive component that allows the tumour to escape immune control, and in many cases evade cancer therapies.

1.2.1 Innate Response

While a strong emphasis is placed on the adaptive immune response to PDAC, the innate response - specifically that of mature dendritic cells (DCs), activated pro-inflammatory macrophages of the M1 phenotype and natural killer (NK) cells - is an essential component to an effective anti-tumour immune response [62]. NK cells in particular play an important role in anti-tumour immunity in PDAC patients, and higher numbers of circulating NK cells have been associated with prolonged survival in patients [63]. One of the key mechanisms of acquired tumour resistance to an elevated immune response is the down regulation of MHC I [19], however this adaptation makes them vulnerable to recognition and elimination by NK cells[62]. In 2007, Pandha et al collected a number of resected PDAC tissues and identified that many samples had reduced HLA I and transporter for antigen presentation (TAP), both mutations making the tumours vulnerable to NK cells [64]. Furthermore, it was found that NK activating receptors, particularly NKG2D, was reduced in pancreatic tumour tissues indicating that tumour-

infiltrating NK cells had impaired functionality within the tumour [65]. Therapies targeting these cells may prove to be essential to developing an effective treatment for PDAC patients.

1.2.2 Adaptive Immune Response

The adaptive immune response is an essential component of anti-tumour immunity, and effective anti-cancer immune responses require cytotoxic CD8+ T cells, Th1 helper T cells and the presence of tumour-targeting B cells. During the elimination and equilibrium stages of tumour development, inflammatory cytokines and the recruitment of these populations along with the innate component lead to an immune stimulatory environment that favours the elimination of tumour cells[62], however as the equilibrium phase progresses into the escape phase many of these populations become suppressed and non-functional[19,62]. These cells are not eliminated, and can still be found both within the tumour, draining lymph nodes and in circulation. In PDAC, which is defined by the overexpression of multiple well known antigens, a positive correlation has been found between humoral responses to these antigens and a favourable prognosis[62]. A number of studies on PDAC patients have found tumour-reactive adaptive cell subsets in the peripheral blood mononuclear cells (PBMCs) of patients including IgG Muc-1 specific antibodies[66], both antibodies and T cells reactive to alpha enolase[67,68] and even ENO-1 specific TH17 helper cells[69]. In most cases, the presence of these cells in the periphery were correlated with better survival [62,66].

Circulating levels of anti-tumour cells can have correlative value, but do not represent the subsets that have infiltrated into tumours. While getting PDAC samples is not always easy, as the majority of patients do not undergo surgical resection, many groups have investigated how levels of infiltrating lymphocytes may have better prognostic value than merely investigating circulating and humoral responses. Fukunaga et al found that in most cases PDAC tumours were

more highly infiltrated with CD4+ T cells than with CD8+ cells, however when both subsets were infiltrated into the tumours the patients had better survival rates[70]. Tewari et al evaluated the prognostic value of tumour infiltrating lymphocytes using tumour microarrays of 81 PDAC patients undergoing surgical resection and consistently found that higher numbers of CD3+, CD8+ and CD20+ cells positively correlated with improved survival [71]. As CD4+ T cell intratumoral infiltration can represent two very different subsets of T cells - both helper cells and regulatory cells which have opposing anti- and pro-tumour effects respectively - further investigation was needed into the nature of the T cells infiltrating into PDAC tumours. Tang et al investigated both the circulating and tumour/tissue infiltrating levels of CD8+ T cells, CD4+ T cells and specifically T_{regs} in PDAC patients as well as in healthy individuals. They found that while there were no significant differences in circulating levels of all three types of T cells, there was a significant increase in all three T cell subsets in tumours samples over healthy pancreatic tissues[72]. They found a positive correlation between CD4+ infiltration and T_{reg} infiltration, and a negative correlation between the number of CD8+ infiltration and T_{reg} infiltration indicating potentially an increasing regulatory role within the tumour. Their data also agreed with the previous data indicating that high CD8+ infiltration within the PDAC tumours was associated with a better prognosis, but further added that if the T_{reg} numbers were equivalently increased, there was a worse prognosis[72].

The presence of an anti-tumour adaptive immune response represents both a better prognosis, as seen by clinical data, as well as a potential target for therapeutic strategies. It also indicates that this tumour must have a strong immunosuppressive compartment within the TME that allows the tumour to escape immunosurveillance and tumour targeting lymphocytes.

1.3 Immunosuppression

In order to escape immunosurveillance, tumours create an environment that limits the efficacy of the immune response. This includes both intrinsic factors, including the upregulation of inhibitory immune ligands such as PD-L1 and downregulation of activating ones[64], the secretion of cytokines and factors that inhibit immune function and recruitment as well as a physical blockade against immune infiltration[19,62]. Furthermore, tumours can induce both a local and systemic immunosuppressive environment characterized by the recruitment and activation of immunosuppressive or "pro-tumour" immune cells, which further limit immunotargeting of the tumour cells by activated effector cells[19,62]. These cells are included in the tumour extrinsic component of immune evasion and lead to tumour escape as well as the inefficacy of many therapeutic strategies.

1.3.1 Immunosuppressive Cell Subsets

The key immunosuppressive cell subsets involved in promoting tumour outgrowth are regulatory T cells (T_{regs}), myeloid derived suppressor cells (MDSCs), tumour associated macrophages (TAMs) and regulatory B cells (B_{regs}) [19]. T_{regs} are CD4+ T cells that are defined by the expression of the IL-2 receptor alpha (CD25) and the transcription factor Forkhead box P3 (Foxp3). They have a role in self tolerance, and in healthy individuals promote the suppression of autoimmunity[62,73] through the secretion of the cytokines IL-10, IL-35 and TGF-β as well as through direct cell-to-cell contact[19,62,73]. T_{regs} have increased expression across many tumour types [74], and help to produce a TME that favours the progression of tumours [62]. When they were investigated in murine models of cancer, it was found that T_{regs} contribute to the early establishment and progression of tumours [75–77], and depletion of this subset of T cells was able to restore and even enhance anti-tumour immunity [19]. In human studies, the ratio of

effector T cells to regulatory T cells is highly correlated to patient outcomes, and an increase in the number of regulatory T cells is indicative of a poor prognosis [78].

MDSCs are immature myeloid cells that are released from the bone marrow during the course of chronic inflammation [79]. These cells not only promote the development of T_{regs} and the polarization of macrophages [79], but also work to directly suppress both innate and adaptive arms of the anti-tumour immune response [62]. MDSCs secrete inhibitory cytokines specifically TGF-β and IL-10, sequester cysteine, express arginase-1 which depletes systemic arginine - an amino acid essential for T cell and NK cell protein synthesis, increase reactive oxygen species (ROS) and impair T cell homing to the site of tumour[62,79], thereby limiting immune responses through multiple mechanisms.

TAMs, which are promoted within the TME by MDSCs [79], have pro-tumorigenic properties and higher frequencies of these cells have been associated with a poorer prognosis in patients across a wide variety of tumour types [19,62]. Macrophages display two distinct phenotypes: M1 which are pro-inflammatory in nature, and M2 which tend towards an anti-inflammatory phenotype. In tumours, the TAMs are polarized towards the M2 phenotype due to secreted factors in the TME, specifically the IL-10 and TGF-β, and further contribute to the immunosuppressive environment with the secretion of anti-inflammatory cytokines and upregulation of surface-expressed inhibitory ligands [62].

A new player in the immunosuppressive field is that of B_{regs}. Similar to T_{regs}, these regulatory adaptive immune cells were identified by the role that they play in limiting autoimmunity in inflammatory bowel disease, rheumatoid arthritis and autoimmune encephalomyelitis [80]. Unlike T_{regs}, they are not defined by any particular CD or transcription factor expression but rather solely by their ability to produce IL-10 and TGF-β[80]. While their role in cancer is not

fully defined[81], they have begun to be investigated in murine models of melanoma and breast cancer. In these murine models, B_{regs} induce the conversion of non-regulatory CD4+ T cells to T_{regs} through the secretion of TGF-β, and elimination of this subset blocked the development of lung metastases in a melanoma metastasis model [81]. While their role in human cancer remains to be defined, they invariably play a role in creating an immunosuppressive environment. The presence or absence of any of these subsets within the local TME, as well as systemically in cancer patients have prognostic value in determining patient outcomes, as well as stage and the presence of metastases. Each plays an essential role in tumours evading immune detection, and in tumour progression which need to be investigated in tumour types and when evaluating potential cancer therapeutic strategies.

1.3.2 Immunosuppression in PDAC

Measuring the circulating and tumour infiltrating immunosuppressive subsets in PDAC patients has revealed how important a role each plays in the progression of primary tumours and the rate at which PDAC tumours metastasize in patients. Starting with the circulating levels of cytokines, immunosuppressive biomarkers and suppressive immune cells, many studies have been able to use these levels for prognostic value, both alone and in association with other immune subsets. In 2016, a number of PDAC patient blood samples were collected and high levels of baseline IL-6 and IL-10, as well as an increase in the amount of CTLA-4 positive cells were both associated with a shortened overall survival rate [82]. Both T_{regs} and MDSCs - which are the main producers of these cytokines, and which express inhibitory biomarkers - were found to be increased in circulation [62,83,84], and were markers of a poor prognosis. In fact, the levels of MDSCs were found to be directly correlated to an increased level of T_{regs}, as well as increased levels of Arg-1 [83]. Furthermore, the correlation to poor prognosis and increased MDSC

expression was not limited to patient studies, but has also been observed in murine studies [85]. In murine models of spontaneous PDAC, MDSCs were increased in pre-cancerous lesions, and the levels increased in circulation, in draining lymph nodes and within the tumours themselves as they progressed [85]. T_{regs}, which demonstrate increased levels in the blood of PDAC patients - up to 8.1% from healthy levels of 2.47% - have been identified as a marker for increased metastasis [84], and have been identified within tumour samples and their draining lymph nodes in patient samples [86]. Finally, while T_{regs} and MDSCs appear to be the key suppressive subsets involved in PDAC progression and metastasis, TAMs also play a role in tumour progressions and an increase in M2 polarized TAMS has been associated with a poor prognosis, and a marker of lymph node metastases in PDAC patients[87]. PDAC represents a highly complex tumour type, with a strongly immunosuppressive local environment which expands to a systemic immunosuppression as the cancer progresses. This immunosuppression may play a key role in determining which therapies should be pursued as research in this field progresses.

1.4 Cancer Immunotherapy

Immunotherapy is an emerging therapeutic in the cancer field that aims to take advantage of the host's own immune system to target primary tumours as well as metastases. The concept of immunotherapy is not a new one, and was in fact first pioneered by Dr William B. Coley in 1910 with the use of bacterial toxins injected into sarcoma tumours [88]. The next big advancement in immunotherapy came with the characterization of cancer immunosurveillance, first identified in the 1950s by Ehrlich and expanded upon by Burnet and Thomas, wherein it was understood that cancer cells develop quite frequently but are recognized and killed by the host's natural immunity [89,90]. Cancer itself only develops when this process is weakened or when cancer evades the immune system. The final piece of the puzzle came into play in the early 2000s with

the concept of cancer immunoediting[8,19] in which the dual role of the immune system – as both a suppressor of tumour outgrowth as well as the role of immunosuppressive cells in facilitating tumour progression – was fully recognized.

All of these breakthroughs led to the theory that both tumour associated antigens (TAAs), as well as neoantigens present within the tumour, may shape the immune response[91], but recognizes that the natural host immune responses may prove to be ineffective against cancer due to the heterogeneity, constant evolution and complexity of the TME[19]. Immunotherapy aims to increase or take advantage of this natural immunity and improve it to achieve durable responses that display memory, thereby treating both the primary tumour as well as limiting recurrence. A number of different therapies have been developed to harness the immune potential, each with their own limitations and with the possibility of improvement through combination therapy as well as a deeper understanding of the mechanisms behind positive responses.

1.4.1 Checkpoint blockade

T cell activation is a tightly controlled process with many regulatory processes involved. In order to avoid collateral damage from over activation, as well as to limit autoimmunity, a number of so-called inhibitory checkpoints are in place during the activation process[19]. Cancer takes advantage of these checkpoints to limit T cell activation within the TME, and this inhibitory pathway has become a leading target for cancer immunotherapy - checkpoint blockade. The first identified checkpoint was cytotoxic T-lymphocyte-associated protein 4 (CTLA-4) which was identified in the 1980s [92]. This protein, which is found both on activated effector T cells and T_{regs} competes with CD28 for binding of B7 ligands. Once bound it inhibits T cell proliferation and IL-2 secretion [93]. This protein became the first target of checkpoint blockade and ipilimumab – the antibody targeting CTLA-4 - became the first in class checkpoint inhibitor that

received FDA approval in 2011[19]. While it was found to be effective in the treatment of multiple cancer types, specifically melanoma, head and neck cancers and non-small cell lung cancer, treatment with ipilimumab caused significant immune related toxicities that could only be managed with systemic steroid therapy [19]. The next two checkpoints discovered were programmed death receptor (PD-1) which was cloned in 1992[94] and its ligand PD-L1 which was identified shortly after. In fact, the ligand PD-L1 was found to be constitutively expressed by many tumours, and its expression on tumours is further induced and upregulated by IFNγ [19]. Targeting this pathway has the potential to unleash activated tumour reactive T cells, and thus began the development of pembrolizumab and nivolumab which target PD-1 as well as atezolizumab which targets the ligand PD-L1. Furthermore, as this checkpoint occurs later in the T cell activation response than CTLA-4 it has been tolerated better in patients[95,96], and due to their non-overlapping mechanisms has also been used in combination with anti-CTLA-4 blockade[19]. Checkpoint blockade represented a massive leap forward in cancer immunotherapy, but due to the reliance on pre-existing tumour reactive T cells has not had the same widespread effectiveness in all cancer types. In PDAC, which is known to be a non-immunogenic tumour that boasts a strongly immunosuppressive TME, checkpoint blockade has had limited efficacy [97]. In fact, rather than being used as a monotherapy, combination therapy with other immunotherapies such as vaccination, or even combination with traditional therapies like chemotherapy and radiation, is potentially a leading route forward to increase the efficacy of therapy and overcome resistance in PDAC [97].

1.4.2 Whole Cell Vaccines

Cancer vaccines goes beyond checkpoint blockade in that rather than simply trying to unleash a pre-existing immune response to cancer, cancer vaccines work to stimulate a specific anti-

tumour immune response, through eliciting novel responses or boosting the pre-existing lymphocytes[62,98]. They aim to activate T and B cells against TAAs through the engagement of both the innate and adaptive arms of the immune system [98]. Cancer vaccines can take many forms including DNA or peptides of the specific antigen [62] as well as whole tumour cells or antigen pulsed/transduced DCs [62,98]. The issue with cancer vaccines lies in identifying novel or effective TAAs as the target of vaccination. Whole cell vaccines, in all their various forms, overcome this problem by presenting irradiated tumour cells directly to the immune system allowing all TAAs to be presented equally and allowing the host immune system to select the most immunogenic antigen(s) [62]. The two subsets of whole cell vaccines are autologous vaccine, or those derived from a patient's own tumour, and allogeneic vaccines which are derived from tumour cell lines [62]. Autologous tumour cells represent the exact tumour cells in a patient's specific cancer, however they present multiple difficulties in applying them in the clinic including low numbers, risk of contamination and the fact that many cancer patients are not eligible for surgical resection meaning that in many cases, especially with PDAC, there is no source of cells to prepare the vaccine [62,99]. This is where allogeneic based vaccines come in: like autologous whole cell vaccines, TAAs do not need to be identified, the cells grow well *in vitro*, haplotype matching does not need to be performed as the host's immune cells will still be performing the antigen presentation [100] and finally allogeneic cells can be easily modified to express helper cytokines or antibodies to further stimulate an anti-tumour immune response [62,101]. Two allogeneic whole cell vaccines are being investigated in the clinic for the treatment of PDAC - GVAX and Algenpantucel-L[62,98,102]. Algenpantucel-L is a vaccine that consists of two live, irradiated human allogeneic pancreatic cancer lines, both of which express murine α-1,3-galactosyltransferase[62,103]. This transduced protein results in the synthesis of α-

galactosyl surface proteins which trigger antibody-dependent cell toxicity which results in the rejection of cancer cells [62,102]. This vaccine achieved a one year survival rate of 86% in resected PDAC patients when used in combination with radiation [62,104], and patients with a positive response were found to have demonstrated a humoral immune response[103]. This vaccine has since gone into Phase II clinical trials [102]. GVAX is another whole cell vaccine composed of two allogeneic human cancer lines that both express GM-CSF [62,102,105]. This vaccine is able to recruit lymphocytes, eosinophils and monocytes to the site of vaccination, and to the site of the tumour [105]. The vaccine is able to efficiently prime the immune response against TAAs as the secreted GM-CSF allows DCs to more efficiently present the antigen to T cells, resulting in their activation [62,105]. In the clinic, GVAX has been found to be safe and induce potent immune responses in a Phase I/II clinical trial [62,102,105], however in an expanded Phase II trial, no survival benefit was observed after 2 years [106]. Future studies have looked into combining GVAX with other immunotherapies including checkpoint blockade [107] and antigen-specific boosting of the immune response stimulated with GVAX [107,108]. Whole cell vaccines represent a novel form of cancer immunotherapy that does not rely on pre-existing anti-tumour immunity, and which has shown some promise in treating patients with PDAC.

1.4.3 Oncolytic Viruses

Oncolytic viruses (OV) are replication competent viruses that selectively replicate in and lyse cancer cells, but do not replicate in healthy cells [109,110]. The hallmarks of cancer, which allow cancer cells to grow undetected, or in an immunosuppressed environment lead to a permissive environment for viral replication of viruses that would otherwise be eliminated by the immune system [110]. The introduction of OVs into the tumour microenvironment causes cellular damage of the cancer cells and a pro-inflammatory environment defined by an

abundance of pathogen associated molecular patterns (PAMPs) and damage associated molecular patterns (DAMPs) that promotes the phagocytosis of dead or dying virally infected cells, and can lead to both the breaking of tolerance towards cancer cells and the direct elimination of cancer cells[109]. The selection and efficiency of OVs is linked to specific viral biology as well as host-virus interactions, and therefore each virus can have a different mechanism of action within the TME [110]. The nature of the TME as well as the immunogenicity, genomic complexity, speed of intratumoral propagation of the virus, and viral capacity of controlling immune responses should be considered prior to the selection of a specific virus [109].

OV therapies have multiple advantages over other therapies. Due to the multiple pathways targeted there is a lower likelihood of developing resistance, their inherent nature of replicating in tumours and tumour-associated tissues, but not healthy tissues, makes them less toxic than other therapies, and finally safety features can be built in[110]. The disadvantage of using OVs for cancer therapy include the suboptimal delivery methods and inefficient viral infection due to heterogeneous phenotypes / variable permissiveness of different cancers[110].

OVs can be divided into two large classes: 1) viruses that naturally prefer replication in cancer cells and are generally non-pathogenic to humans including parvovirus, myxoma virus, Newcastle Disease virus, reovirus and Seneca valley virus; and 2) viruses that are genetically manipulated to limit replication in normal cells which included measles virus, poliovirus, Vaccinia virus, adenovirus, Herpes Simplex virus and rhabdoviruses (including vesicular stomatis virus (VSVΔ51) and Maraba MG1 virus (MG1)) [110]. These viruses can be further modified with the inclusion of transgenes such as GM-CSF, interleukins, interferons, 4-1BB and CD40L[111]. The first OV to be approved for use in the United States was Talimogene laherparepvec(T-VEC) which was approved for use in stage III and IV melanoma in 2015. T-

VEC is a type I herpes simplex virus that has been modified to replicate only in tumour cells, have enhanced MHC I loading and finally to secrete GM-CSF [112]. This virus has a dual mechanism of action which includes the direct lysis of tumour cells as well as inducing local immunity against the tumour cells with the increased accumulation of dendritic cells in the TME [112]. An initial phase II clinical trial in patients with advanced melanoma demonstrated low toxicity, and had an objective response rate of 26% [113] and led to further clinical trials which eventually led to the approval of the virus in melanoma patients, but was found to be better at controlling locoregional tumours rather than having systemic effects when used as a monotherapy [112]. However the response rate observed between different lesions, without observed viral spreading between the lesions indicated a reliance on an induced anti-tumour immunity [109]. As such T-VEC was then combined with other immunotherapies - specifically the checkpoint blockade of CTLA-4 and PD-1. When combined with ipilimumab response rates in melanoma patients rose to 39%, and when combined with pembrolizumab response rates were even higher at 68%, with 33% of patients achieving full remission[109,114,115].

1.4.3.1 Oncolytic Viruses as immunotherapeutic agents

The viral immunotherapy component of OVs became more relevant as more and more clinical trials indicated that positive responses relied on developing an anti-tumour immune response [109,110]. Anti-viral immunity - including the strong inflammatory response - were initially seen as being a potential issue to be overcome due to the implications in limiting efficacy of virus spread, entry and replication in tumours [110], however the use of syngeneic models and clinical evidence emphasized that these viruses were inducing an anti-tumour immune response in addition to the anti-viral response. Vaccination and injection of viruses exploits both innate and adaptive immunity, and the cytokines and chemokines stimulated during viral infection mirror

those required for an anti-tumour response, and when they are used effectively to redirect the response against tumours, they act as *in situ* vaccines against tumours [110]. Viral immunotherapy relies on the inflammatory cascade, induction of immunogenic cell death (ICD) through the release of DAMPs (calreticulin, HMGB1 and ATP) and TAAs to stimulate an adaptive immune response. At the same time, intratumoral administration of OVs rather than systemic administration can lead to complement and antibody mediated destruction of tumour cells [110]. In multiple pre-clinical models, OVs have been shown to induce both NK cell and CD8+ T cell mediated immunity [116]. In syngeneic B16 melanoma murine models, both Diaz et al and Miller et al demonstrated tumour regression following intratumoral (*i.t.*) injection of VSV and HSV respectively which was dependent on the recruitment and activation of cytotoxic CD8+ T cells and NK cells [117,118]. Reovirus efficacy in prostate cancer was also found to be T cell and NK cell dependent [119,120], leading to the conclusion that therapeutic efficacy of OVs is based on NK cell activation and cytotoxicity as well as the stimulation of CD8+T cells to develop an anti-tumour immune response [121].

OVs are an emerging immunotherapy with multiple modes of action at inducing anti-tumour immunity. Their use in the clinic has revealed beneficial effects both as a monotherapy, and with combination therapies.

1.4.3.2 Prime-Boost Platform

Oncolytic Vaccines (OVax) expand on the use of OVs as a cancer therapy and further push the use of them as an emerging immunotherapy. They involve the expression of TAAs within the virus to drive the immune response against the tumour. In this case, to block viral replication within the tumour, anti-TAA specific CD8+ T cells as well as anti-viral T cells would be recruited to the tumour and would drive tumour-specific killing [122]. Certain viruses were

found to be better at priming such an immune response. In the case of VSV and adenoviruses, Adenovirus encoding a TAA was found to extend the survival of mice challenged with melanoma, whereas VSV encoding the same antigen was not [122]. The development of the heterologous prime-boost platform, which utilizes two different viruses each expressing the TAA, drives the immune response against the tumour, rather than towards an anti-viral response [122,123]. In this case when adenovirus was used to prime the response and VSV was introduced to boost the response an increase in median and long term survival in mouse models was observed [122,123]. An adenovirus has been consistently chosen as an ideal priming vector due to its ability to induce strong CD8+ T cell responses [123]. However the CD8+ T cells induced by adenovirus vaccination tend to be those of effector and effector memory subsets rather than central memory T cells [124]. This means that in order to not compromise the effector response, there needs to be prolonged intervals before boosting this response. Rhabdoviruses, which are unable to prime immune responses potentially due to their sensitivity to type I interferons [123] were found to be excellent at boosting responses, and could in fact boost the adenovirus-primed T cell responses at their peak levels without compromising the effector response [124]. This boost was defined by T cells that displayed increased functionality through increased cytokine and granzyme B release as well as an increase in the amount of CD127+CD62L+ central memory T cells [124]. This increase in boosting functionality has been attributed by Bridle and Wan to the cross-presentation of antigen by DCs as well as the ability of VSV to directly infect B follicular cells in the spleen which leads to antigen presentation by both the B cells and neighbouring DCs within the B cell follicle, where central memory T cells are known to reside [124]. Maraba MG1 rhabdovirus has been shown to have a similar phenotype to its related rhabdovirus VSV, but has consistently outperformed VSV in *in vitro* and *in vivo* experiments.

Therefore Pol et al postulated that a heterologous prime-boost vaccine utilizing an adenovirus prime and a Maraba MG1 boost would provide an improved OVax [123]. They targeted a melanoma TAA and found that the prime-boost platform led to T cell specific responses above 30% in circulating blood and resulted in 20% cured mice in a B16 lung metastases model [123]. To translate this into the clinic, human MAGE-A3, a cancer testis antigen, was encoded into the platform and resulted in the expansion of antigen specific CD4+ and CD8+ T cells in macaques, with no adverse effects observed [125]. This TAA has since moved into first-in human clinical trials targeting solid human malignancies that express MAGE-A3 [126,127]. Therefore, the heterologous prime-boost OVax platform utilizing an adenovirus prime and a Maraba MG1 boost represents an ideal immunotherapy capable of inducing strong and long-lasting T cell responses against the TAA without stimulating strong anti-viral responses. The next step involved is identifying the ideal TAA that can be applied to multiple cancer types in both murine models and which can be translated to the clinic.

1.4.3.3 Dopachrome Tautomerase

Dopachrome Tautomerase (DCT) or tyrosinase-related protein 2 (Trp2) is a pigmentation protein found in melanocytes [128]. Its function is to reduce the oxidative stress produced during melanogenesis, and it has been found to have high expression in melanoma [129,130].As such, DCT has been used as a proof-of-concept target antigen for immunotherapy. The human form of DCT has been encoded into the Maraba MG1 platform (MG1hDCT) and used in the heterologous OVax model to therapeutically treat B16 – a murine melanoma line expressing murine Trp2 [122,129]. This model took advantage of the xenoantigen hDCT to break immune tolerance and demonstrated efficacy in stimulating an anti-DCT immune response >40%, and extended survival [123]. However, Zhang and colleagues hypothesized that using the murine

form Trp2 in mice may result in reduced or absent efficacy due to the peripheral tolerance that would limit the stimulation of high affinity CD8+ T cells [131,132]. They found that the fusion of GFP to the Trp2 protein was able to break immune tolerance through the ubiquitin-proteasome pathway which resulted in better MHC I binding, presentation to CD8+ T cells and recruitment of helper CD4+ T cells [131,132].

1.4.3.4 Mesothelin

Mesothelin is a 40kDa cell surface glycoprotein differentiation antigen that is present on mesothelial cells lining the pericardium, the pleura and the peritoneum in both humans and mice[133]. The mesothelin gene encodes a 69kDa precursor protein that is processed into the membrane-bound mesothelin and the secreted megakaryocyte-potentiating factor (MPF) [133]. The protein is anchored to the membrane by a glycosylphosphatidyl inositol linkage [134]. While it is not a mutant antigen that is specific to cancer, mesothelin is known to be highly upregulated in many types of cancers including mesothelioma, ovarian, and pancreatic cancers [133–135]. In fact in PDAC, mesothelin expression is increased in up to 95% of all tumours tested [20], potentially making it an ideal target for immunotherapies.

While the function of mesothelin is relatively unknown, a number of studies have been performed to understand the protein. The first such study, by Bera and Pastan in 2000 used mutant mice where the mesothelin gene was inactivated through replacement with a neomycin resistance gene [136]. Despite the fact that non-mutant mice demonstrated tissue-specific mesothelin expression at various points during development and adult life, the mesothelin null mice which expressed no mesothelin mRNA or protein demonstrated normal development and reproduction n[136]. Therefore, mesothelin was deemed a non-essential protein for normal development. However, research into ovarian cancer has led to an understanding of one of the

roles mesothelin plays in cancer and tumour development. MUC16/CA125 is a very large cell surface mucin that is shed and has been used to monitor response to therapy in ovarian cancer[137]. Initially demonstrated by Rump et al, CA125 was found to bind to surface mesothelin on mesothelial cells of the peritoneum with very high affinity [138]. Furthermore, in other studies using MUC16-expressing ovarian cancer lines, mesothelin was found to bind with both the soluble and surface bound forms of MUC16 with a binding affinity (Kd) of 5nm[139]. These studies into the interaction of mesothelin with MUC16/CA125 have shed light on a potential adhesion role for mesothelin and indicate that this protein may be essential for tumours spreading throughout the peritoneum leading to peritoneal carcinomatosis.

Taken together, mesothelin's non-essential role in normal development but important role in tumour development, as well as its limited expression on healthy cells have opened up the possibility that it may be an ideal tumour associated antigen for targeted immunotherapies. It has been used as a target in a number of strategies both pre-clinically and within clinical trials. These include immunotoxins [140–142], vaccines [105,143], chimeric monoclonal antibodies, antibody-drug conjugates and chimeric antigen receptor T cells. The GVAX vaccine, described above, has since been boosted in the clinic with CRS-207 - a *Listeria monocytogenes* developed by Aduro Biotech that expresses mesothelin and secretes mesothelin into the cytosol of antigen presenting cells while stimulating both the innate and adaptive immune system [140,144]. This combination has been demonstrated to be well tolerated in the clinic and has induced immune activation as well as mesothelin-specific T cell responses in patients [144,145]. However, when this combination was investigated in a phase 2b clinical trial, no survival benefit was observed compared to patients receiving traditional chemotherapy [146]. This result is similar to that observed with CAR-T therapies targeting mesothelin, in which disease stability has been

achieved in patients for up to 5 months, but no overall reduction in tumour size has been occurred[147]. Mesothelin represents a TAA which shows a lot of potential promise as a target for immunotherapy, where the use of the OVax which combines oncolytic potential with T cell targeting may provide the necessary push towards an effective therapy.

1.4.3.5 Oncolytic viruses in the surgical setting

On top of their role in cancer immunotherapy as either a monotherapy or combination therapy, oncolytic viruses have been identified by Tai et al as the ideal therapy for use in the perioperative setting surrounding cancer surgery [148]. While surgical resection of primary solid tumours is a mainstay of cancer therapeutics, it has been shown to induce an immunosuppressive period that contributes to cancer outgrowth and metastases [149–151]. This perioperative period is a critical time for therapeutic intervention. OVs have been identified as a potential therapeutic due to the physiological immune stimulus that they present - one which could not be mimicked without the use of multiple cytokines *in vivo [148]*. The immunosuppressive environment induced by surgical stress is defined by specifically a decrease in the activation and cytotoxicity of both NK cells [116,148–151] and CD8+ cytotoxic T cells [152], both of which are stimulated by OV therapy, as described above. Tai et al explored the use of two OVs - both pre-clinical parapox virus (ORFV) and clinical JX-594 - in two models of surgical stress [151]. In a B16 melanoma lung metastases model, surgically stressed mice display increased lung metastases 3 days post surgery. Mice treated with either OV prior to surgery displayed reduced lung metastases following surgical stress, a phenomenon which was further demonstrated in a 4T1 spontaneous lung metastases model [151]. Furthermore, through the use of NK cell depletion, it was found that the decrease in lung metastases was reliant on both direct oncolysis of tumours as well as through NK cell mediated lysis of tumours. This NK cell activation in surgically stressed mice

was characterized both by increased cytotoxicity, measure via an *ex vivo* Cr-51 release assay and through IFNγ release[151]. Maraba MG1, the oncolytic rhabdovirus being investigated in the prime-boost setting[123], demonstrates a similar mechanism of action of overcoming surgery-induced NK cell suppression, and is able to attenuate the development of lung metastases following surgery in both the 4T1 and B16 metastases models[153]. In the case of MG1, the activation of NK cells relied on activating conventional dendritic cells[153]. OVax have the addition of targeting the CD8+ T cells response against the TAA, leading to the possibility of their use in the perioperative setting to overcome both NK cell and CD8+ T cell suppression [116,148]. As PDAC surgery is currently the best treatment option when possible, combination therapies need to be developed during this period to improve survival rates beyond 20% [33]. Combining the OVax heterologous prime-boost platform targeting mesothelin, which is highly upregulated in most PDAC, could represent a feasible approach to further improve survival rates for patients facing this diagnosis.

1.5 Rationale and Hypothesis

1.5.1 Rationale

Oncolytic vaccines are an ideal therapy that combines the oncolytic potential of viruses with their ability to elicit adaptive immune responses against tumour antigens, and to stimulate large inflammatory responses. The heterologous prime-boost approach has shown a great deal of promise in pre-clinical models but remains to be targeted specifically to PDAC, and has not been evaluated in the setting of a self antigen. The use of mesothelin, a self-antigen that is highly upregulated on multiple forms of cancer and specifically on >90% of PDAC tumours, makes it an ideal antigen to target with this platform. Furthermore, the success of OVs in the surgical

setting and in combination therapies allows this platform to potentially have far reaching implications for single immunotherapy, or combination therapies in the treatment of PDAC.

1.5.2 Hypothesis

A prime-boost vaccine platform can be utilized to generate an anti-mesothelin immune response for the treatment of pancreatic ductal adenocarcinoma (PDAC).

1.5.3 Aims

1. To develop a surgical model of pancreatic cancer that recapitulates clinical PDAC wherein the effect of an immunotherapy on tumour-specific immune responses, metastatic disease and survival can be investigated.
2. To identify the factors required for generating a robust immune response following vaccination with an Adenovirus prime and Maraba MG1 boost targeting the TAA mesothelin.
3. To investigate the efficacy of the prime-boost vaccine platform targeting mesothelin in the treatment of a murine PDAC model and understand how it relates to the anti-tumour immune response.

1.5.4 Significance

My proposed project addresses a serious gap in the knowledge of therapeutics for pancreatic cancer and explores the mechanisms of and barriers to efficacy of cancer vaccines in the context of a pancreatic cancer model.

2 Material and Methods

2.1 Cell lines and viruses

B16F10 (murine melanoma), HEK293T (human embryonic kidney) and Vero (monkey kidney) cell lines were obtained from American Type Culture Collection (ATCC: Manassas, VA). Pan02

(murine pancreatic adenocarcinoma - PDAC), TH04 (murine PDAC), and MC38 (murine colon adenocarcinoma) were obtained from Drs Carolina Ilkow and John Bell (Ottawa Hospital Research Institute, Ottawa). STOSE (murine spontaneously transformed ovarian surface epithelial) and ID8 (murine ovarian cancer) were obtained from Dr Barbara Vanderhyden (Ottawa Hospital Research Institute, Ottawa). Cell lines were maintained in Dulbecco's modified Eagle's Medium (DMEM, Corning Cellgro) supplemented with 10%fetal bovine serum (FBS, Seradigm). B78H1GM (murine melanoma) cells were obtained from Dr Elizabeth Jaffee (John Hopkins Institute, Baltimore MD) and were maintained in Hyclone™ Roswell Park Institute Memorial Institute (RPMI) Medium (GE healthcare) supplemented with 10%FBS, 1% L-glutamine and 0.1% β-mercaptoethanol. All cells were regularly confirmed to be free of mycoplasma contamination by Hoescht staining (Thermofisher) as per manufacturer's protocol and/or by e-Myco™ VALiD Mycoplasma PCR Kit (iNtRON Biotechnology, Sangdaewon-Dong, South Korea).

Rhabdoviruses (MG1, MG1-IL12) were propagated from seed stocks in Vero cells and viral titers were obtained via plaque assays as previously described [154]. The engineered MG1-meso virus once developed was maintained in a similar manner. Adenoviruses (AdhDCT, AdmesoGFP) were propagated and quantified by Dr Kyle Stephenson (McMaster University, Hamilton, ON) and shipped to the lab on dry ice. The Adenovirus - Maraba MG1 prime boost platform is a patented product of Turnstone Biologics (New York, NY). GM-CSF secreting vaccinia virus (JX-594) was provided to the lab by Dr John Bell (Ottawa Hospital Research Institute, Ottawa ON).

2.2 Engineering Maraba viruses

A codon optimized plasmid containing murine mesothelin (pAdShuttle Mesothelin) was created by Dr Kyle Stephenson at McMaster University. Murine mesothelin was PCR amplified to add *Mlu1* (Primers listed in Appendix 8.2) and cloned into the rhabdovirus Maraba MG1 backbone. The recombinant Maraba MG1 mesothelin was rescued as described elsewhere [129,153]. The AdmesoGFP and MG1-meso sequences are provided in Appendix 8.3, and were codon optimized from the published sequence (NCBI Gene ID: 56047).

2.3 Western Blot

Proteins were collected using NP-40 lysis buffer supplemented with 1X complete protease inhibitor. Subsequent lysate was measured for protein concentration by Bradford Colorimetric Assay (Pierce^{TM} BCA Protein Assay Kit 23225). Proteins were then run on a Western blot and transferred to a PVDF membrane. Membranes were blocked with 5% milk for 1 hr, followed by incubation with primary antibody for 1 hr (β-Actin, anti-VSV, Cas-9) or overnight (C-ERC/Mesothelin and anti-GFP). Appropriate secondary was then added for 1 hr, and the blots were visualized with Pierce ECL (Thermofisher 32209). Antibodies and dilutions are listed in Appendix 1.

2.4 Single- and Multi- Growth Curves

Single- and multi- step growth curves were performed as previously described[129] to assess the *in vitro* ability of the virus to grow and spread, respectively. Briefly, Vero cells were plated and were infected at an MOI of 10 (single-step) or 0.01 (multi-step). Supernatant were collected from individual wells at 4, 6, 8 ,10, 12, 24, 48 and 72 hrs respectively. The supernatants were subsequently titered to reveal viral replication and viral spreading. All curves were run in duplicate with both MG1-meso and the parental MG1 virus.

2.5 Viability Assays

Viability of cells was measured by two methods. The viability of cells for injection, or of collected tissues was determined by enumerating the proportion of Trypan-blue (Sigma T8154) excluding cells as a percentage of the total number of cells. Cytotoxicity assays were performed on the indicated cell lines at multiplicity of infection (MOI) as indicated and measured by resazurin-metabolism assay (alamarBlue™ Thermofisher), with non-infected cells as controls for viable cells.

2.6 ELISAs

Cytokine secretion was measured in the supernatants of cells by ELISA. For GM-CSF ELISAs (R&D MGM00), cells were cultured for 24hrs with or without an infection of MOI 10, supernatants were collected, and overall GM-CSF was measured. For IFNγ secretion, supernatants were collected after incubation of splenocytes with target peptides, tumour cells or CD3/CD28 stimulation for 18hrs.

2.7 Animals

Female C57BL/6 mice 6 weeks of age were purchased from Charles River Laboratories. Animals were housed in pathogen-free conditions and all studies performed were in accordance with institutional guidelines at the Animal Care Veterinary Service facility of the University of Ottawa (Ontario). The Animal Care Committee of the University of Ottawa approved this study. Mice were euthanized by intraperitoneal (IP) injection of Pentabarbital Sodium (65mg/kg).

2.7.1 Depletions

In vivo depletions of immune subsets were performed on C57Bl/6 mice. Depletion of regulatory T cells was achieved with a single dose of 50µg anti-CD25 (Clone PC61.5, Biolegend) with low dose cyclophosphamide (100mg/kg, The Ottawa Hospital, Ottawa, ON) delivered in a 200µl

volume *i.p.* one day before further vaccination. The depletion of CD8α T cells was achieved with 100µg of antibody (Clone 2.43, BioXcell, West Lebanon, NH) injected *i.p.* at days -2, -1 and +1 surrounding tumour cell challenge, and was continued at 100µg *i.p.* twice a week thereafter. The depletion of MDSCs was achieved with 100µg of anti-GR1 antibody (Clone RB6-8C5, BioXcell, West Lebanon, NH) injected *i.p.* at days -1 and +1 surrounding tumour challenge and was continued at 100µg twice weekly thereafter. The depletion of B cells was achieved with 200µg of anti-CD20 antibody (Clone SA271G2, Biolegend) injected *i.v.* 1 day before tumour challenged and continued every 20 days at the same dose. All depletions were confirmed through flow cytometry of saphenous blood.

2.8 Vaccination Platform

Mice were vaccinated according to the established regimen [123], receiving 2e8pfu AdmesoGFP *i.m.*, followed by a boost of 1e8pfu MG1-meso *i.v.* seven days after the prime. When other viruses were used (AdhDCT, MG1EGFP) they were used at similar dosing levels. As per Leao et al, regulatory T cells were depleted one day prior to vaccination [59]. GVAX, consisting of 2e6 B78H1GM and 2e6 Pan02 (irradiated at 60Gy) combined 1:1, was injected subcutaneously into both hind limbs at day 0, followed by either a GVAX boost at day 7 prepared similarly, or an *i.v.* MG1-meso boost. Prophylactic vaccination was performed 7 days prior to tumour challenge; whereas therapeutic vaccination was started 14 days post intrapancreatic injection.

2.9 Collecting murine tissues

At endpoint, murine tissues were collected and processed. Spleens were collected, manually dissociated and passed through a 70µm filter. Blood was collected from living mice through saphenous bleeds or at endpoint through a cardiac puncture into heparinized tubes. Tumours (both pancreatic and subcutaneous) were collected and were placed in dissociation media

consisting of RPMI supplemented with 10% FBS, Collagenase I (Sigma) and DNase I (Sigma). Following manual dissociation and incubation for 1 hr, the resulting mixture was passed through a 70μm filter. All tissues were subsequently incubated in ammonium chloride-potassium (ACK) lysis buffer to lyse red blood cells, before processing for analysis.

A section of tumours, both pancreatic and subcutaneous, were fixed in formalin (Fisher Chemical, SF100-20) for 48 hrs prior to paraffin embedding and sectioning by the University of Ottawa Histology Core Facility.

2.10 T cell stimulation

2.10.1 Peptide stimulations

Processed splenocytes and saphenous blood were incubated with viral and tumour associated peptides(listed below) for 5 hours in RPMI supplemented with 10% FBS and with β-mercaptoethanol in the case of saphenous blood at a concentration of $1x10^6$ splenocytes or 75ul of blood to 5ug of peptide. After 1 hour of incubation 1ug/ml brefeldin A (GolgiPlug™ BD Pharmingen, 555029) was added to the wells, as previously described (Ananth 2016). As a positive control, 0.1μg/ml of phorbol 12-myristate 13-acetate (PMA, Sigma P8139) and 1μg/ml of Ionomycin (Sigma I0634) was used in the place of peptide stimulation. The following peptides were used: VSVn – RGYVYQGL H2-Kb restricted (MBL International)[155], Meso 1 – LSIFKHKLD H2-Kb restricted[59], Meso 2 – LIWIPALL H2-Kb restricted[59], and Meso 3 – GQKMNAQAI H2-Db restricted[134] (all from BiomerTech).

2.10.2 Tumour cell stimulations

Target Pan02 tumour cells were incubated with 100U of recombinant murine IFNγ for 18hrs. These cells were subsequently collected with Trypsin, washed twice in RPMI supplemented with 10% FBS (cRPMI) and plated in V-bottom dishes at $3x10^5$ cells/well. Processed splenocytes or

saphenous blood was added to the wells, and the resulting target-effector cells were incubated for 5hrs in either cRPMI or cRPMI supplemented with β-mercaptoethanol in the presence of 1ug/ml brefeldin A (GolgiPlug™ BD Pharmingen, 555029).

2.11 Flow cytometry staining and analysis

Tissues were processed as described above and resuspended in FACS buffer in single cell suspension. Staining was performed in round bottomed tubes, or in V-bottom plates for large sample sizes. Cells were treated with Purified Rat Anti-Mouse CD16/CD32 (Mouse BF Fc Block™) to block Fc receptors and were subsequently stained with Fixable Viability Stain 510 (BD). They were then stained with extracellular markers, as indicated by experiment and outlined in Appendix 8.1. For intracellular staining of IFNγ and TNFα cytokines, cells were subsequently permeabilized and fixed in BD Cytofix/Cytoperm™ (BD) following the manufacturer's protocol prior to staining with intracellular markers. In the case of T_{regs}, intranuclear Foxp3 staining was performed following fixation and permeabilization of the nucleus using the eBioscience™ Foxp3/Transcription Factor Staining Buffer Set (00-5523-00) according to the manufacturer's protocol. Samples were subsequently analyzed by flow cytometry on a BD LSR Fortessa™ or BD Celesta™ cytometer. Data analysis was performed on FlowJo v10 (FlowJo, LLC, Ashland, OR).

2.12 Immunohistochemistry and H&E

Murine tissues were collected and fixed as described above. Sample sections were stained by hematoxylin and eosin (H&E) for histological analysis or were stained by immunohistochemistry for CD3 (Rabbit Anti-CD3,Abcam ab5690), CD4 (Rabbit Anti-CD4, Abcam ab183685) using the Dako EnVision+ System (K4000), CD8 (eBioscience 14-0808-80) using biotinylated Rabbit Anti-Rat IgG (ab6733). Both systems were visualized with ImmPACT™ DAB (SK-4105) and

counterstained with hematoxylin. All samples were analyzed by a certified pathologist for tissue identification, analysis and validation.

2.13 Tumour Implantations

2.13.1 Subcutaneous Tumours

Mice were subjected to 2.5% isofluorane (Baxter Corp.) for induction of anesthesia. Briefly their right flank was shaved, and 2.5e5 Panc02 cells in a volume of 100µl PBS was injected subcutaneously into the exposed flank. Mice were followed until endpoint, with tumour measurements using calipers occurring every other day. Endpoint was declared when tumours reached a size >15mm by 15mm. Volume was calculated as [length X width^2]/2.

2.13.2 Orthotopic Pancreatic Tumours

Routine perioperative care (including anesthesia and pain management) was performed as previously described [116]. Briefly, mice were subjected to 2.5% isofluorane (Baxter Corp.) for induction and maintenance of anesthesia. Hair was removed from the surgical site with Nair™ or by shaving. For all surgical procedures, the surgical site and surrounding area are prepared with Betadine®□ surgical scrub, 70% alcohol, and Betadine®□ surgical paint. Following a mid-line incision (1-3 cm) the tail of the pancreas was identified and isolated using a cotton swab moistened with saline. A 30G ½ inch needle (Hamilton, Reno 7655-07, Model 1705RN syringe, Hamilton 7803-07, length 0.625" needle) was used to inject Panc02 cells in a total volume of 10µl of PBS into the tail of the pancreas. Following removal of the needle the injection site was inspected to ensure no leakage prior to cleaning the injection site with saline and returning the pancreas to the abdominal cavity. The underlying muscle and skin are then sutured using 5.0 Polysorb™ absorbable suture (Covidien) or 9mm stainless steel wound clips (BrainTree Scientific) respectively. The clips were removed 7 days following tumour injection.

2.14 Tumour immune infiltrate analysis

2.14.1 Cultrex Plugs

Pan02 cells were collected and injected subcutaneously into the left flank of vaccinated mice in 100µl PBS and 100ul Cultrex (R&D Systems 3447-020-01). After three days, the plugs were surgically excised from the subcutaneous layer and placed in dissociation media comprised of RPMI supplemented with 10% FBS, Collagenase I and DNase I. Following a 1hr incubation, the resulting cell dissociate was passed through a 70µm strainer and analyzed using FACS staining and flow cytometry.

2.14.2 Tumours at endpoint

Tumours at endpoint (>15x15 mm) were collected, weighed and divided into two sections. Half was formalin fixed as described above, and the other half was dissociated and analyzed by flow cytometry. Formalin fixed tumours were subsequently paraffin embedded and immune infiltrate was analyzed by IHC. RNA was isolated by FFPE extraction (Qiagen), and qPCR was performed to measure mesothelin expression.

2.15 *In vivo* cytotoxicity assay

Splenocytes from naive mice were isolated, stained with CFSE (5µm) or CellTrace Violet™ (Thermofisher C34557). CFSE-labelled splenocytes remained unpulsed, and CTV labelled splenocytes were subsequently pulsed with Meso 1 peptide. Labelled splenocytes were then combined in a 1:1 ratio and were injected i.v. into naive and vaccinated mice. Injected mice were sacrificed 18hrs post injection and percent specific lysis was calculated using as [1-(Average of Naive mice ratio/Experimental mouse ratio) x100].

2.16 RNA analysis

Messenger RNA was collected from cells in culture using the RNeasy Plus Mini Kit (Qiagen 74134), and from paraffin embedded samples using the RNeasy FFPE kit (Qiagen 73504). mRNA was subsequently reverse transcribed into cDNA using the High Capacity Reverse Transcription Kit (Applied Biosystems 4374967). All cDNA was analyzed by qPCR using the SsoAdvanced^{TM} Universal SYBR (BioRad 1725271) and primers for the genes listed in Appendix 8.2. All tested genes were normalized to the housekeeping genes β-Actin and GAPDH, and ΔΔCT was calculated and plotted as fold change over experimental controls.

2.17 Surgical Models

Primary tumours were resected by laparotomy on day 15 ($1x10^5$ cells implanted cells) or day 20 ($1x10^3$ and $1x10^4$ implanted cells). Briefly, mice are anesthetized and prepared as described above prior to making a 1-1.5cm mid-line incision starting at the umbilicus and cutting upward towards the sternum. A 1-1.5 cm midline incision is then made through the muscle along the linea alba to ensure minimal bleeding. The tail of the pancreas and adjacent area is then located and isolated with sterile saline soaked cotton swab. The tumour along the splenic portion of the pancreas is isolated from the splenic artery using sutures and removed, keeping the mesenteric pancreas intact using sutures (5.0 Polysorb™ absorbable sutures (Covidien) or PDS II suture (Ethicon Z423)). Any bleeding observed in the abdomen was located and sutured (arteries) or cauterized to limit mortality post-surgery. The surgical incision was closed as described above using vicryl sutures and staples. All mice undergoing surgery received pre- and post-operative care including daily wellness and injections of buprenorphine (0.05mg/kg) subcutaneously (SC) 1hr pre-op and every 8 hours for 2 days following surgery.

2.18 Peritoneal Weight

The entire contents of the peritoneal cavity including tumour tissue was removed and weighed and normalized to body weight (peritoneal weight / total body mass x 100%) to determine the overall tumour burden present.

2.19 Statistical Analysis

One-way analysis of variance (ANOVA) with Tukey post hoc tests or Student's T test were performed for all data. A P-value of <0.05 was considered significant. Survival was plotted as a Kaplan-Meier survival curve and statistical differences assessed by log-rank tests.

3 Results

3.1 Spleen preserving distal pancreatectomy maintains immune function in a surgical model of pancreatic adenocarcinoma

The surgical resection of pancreatic tumours remains one of the most effective strategies for PDAC, [31]. However, the paucity of easily adopted murine models with surgically resectable pancreatic disease which recapitulates PDAC pathology is limiting the investigation of strategies which may improve surgical interventions, as all current models requires transfected or xenogenic cell lines[34,36,37,54]. Therefore, we sought to develop a model that represents clinical aspects of PDAC and also maintains immune function and immune surveillance to better understand the impact of potential immunotherapies.

3.1.1 Orthotopic injection of Pan02 cells into the tail of the pancreas results in a localized pancreatic tumour that demonstrates many hallmarks of clinical PDAC

The well characterized Pan02 cells which display many hallmarks of PDAC disease and can be used in immunocompetent mice were chosen for model development. As a first step, various

concentrations of Pan02 cells were injected into the surgically exposed pancreatic tail (Figure 1A). A visual examination of tumour revealed the consistent development of a resectable tumour burden at 15- and 20-days post seeding (Figure 1B, Table 1). The tumour burden assessed (Figure 1C) by weighing the peritoneal contents further confirmed a cell concentration dependent increase in tumour burden (Figure 1D), demonstrating both the outgrowth of primary pancreatic tissue as well as the development of metastases within the peritoneal cavity. Histological examination of formalin fixed/paraffin embedded (FFPE) tumours confirmed a dose related increase in tumour burden, as small tumours were observed in mice injected with $1x10^3$ Pan02 cells (Figure 2A), but established tumours were present in mice injected with $1x10^4$ and $1x10^5$ Pan02 cells (Figure 2B and C). The development of peritoneal disease was not a result of leakage from the injection site as 0/5 mice developed disease when the pancreatic tail was resected immediately following tumour cell injection suggesting the metastatic disease is a natural progression of the implanted orthotopic tumours (Table 1 "Immediate Resection").

Histological examination of resected tumours revealed 5 of the 9 established histological features associated with invasive carcinoma as described by Hruban and Fukushima[20] were present in 9 of 10 animals examined. In particular we consistently observed disruption of the lobular structure of the pancreas, a haphazard growth pattern and the development of glands adjacent to vessels in the tumour sections (Figure 3A) where as additional hallmarks such as intravascular invasion and glands touching fat were only present in selected tumour sections (Figure 3B). Taken together, these results suggest that orthotopic injection of Pan02 cells into the tail of the pancreas results in a pancreatic disease which accurately and consistently recapitulates human pathology (Figure 3C).

A

B

C

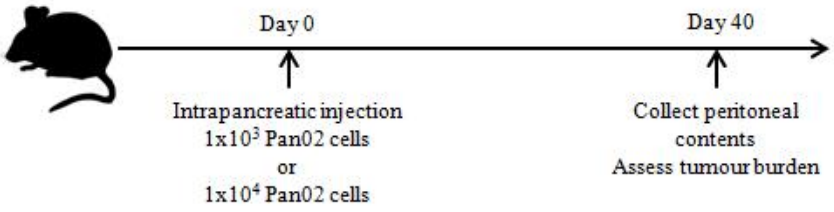
Day 0
Day 40
Intrapancreatic injection
1x10^3 Pan02 cells
or
1x10^4 Pan02 cells
Collect peritoneal
contents
Assess tumour burden

D

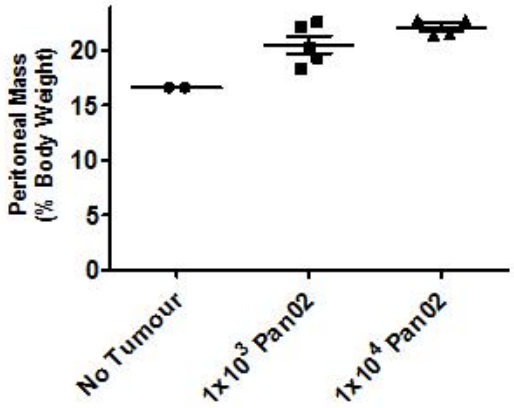
Peritoneal Mass
(% Body Weight)
20
15
10
5
0
No Tumour
1x10^3 Pan02
1x10^4 Pan02

Figure 1: Injection of Pan02 cells into the tail of the pancreas. (A) A single cell suspension of Pan02 cells (10μl) was injected into the tail of the pancreas using a Hamilton syringe. (B) Representative images of pancreatic tumour burden (indicated by forceps) at time of surgical resection. (C) Timeline of injection of Pan02 cells and quantification of tumour burden. (D) Tumour burden was quantified as an increase in peritoneal weight relative to total body weight of mice receiving $1x10^3$ (n=5) or $1x10^4$ (n=4) as compared to naïve mice(n=2) 40 days post injection.

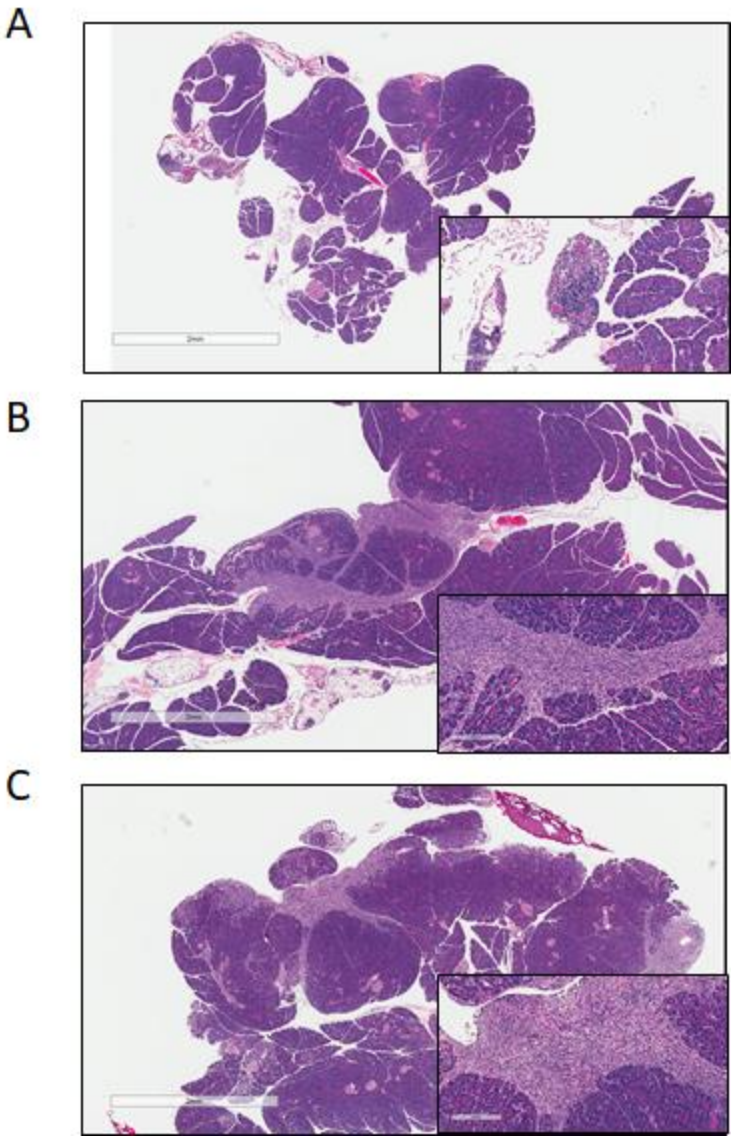
A
B
C

Figure 2: Orthotopic injections of Pan02 cells result in tumour burden. The tail of the pancreas was excised as described in the methods, fixed in paraffin and stained with H&E to reveal tumour burden after injection of (A)$1x10^3$ (B)$1x10^4$, and (C)$1x10^5$ Pan02 cells (30X magnification scale bar = 2mm, inset 200X magnification, scale bar = 200μM). Representative images from mice measured in two separate experiments, n=5 per group.

A

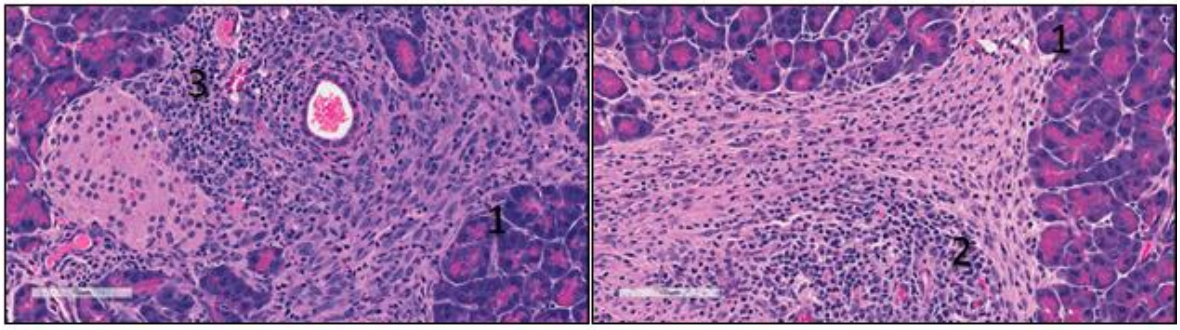

B

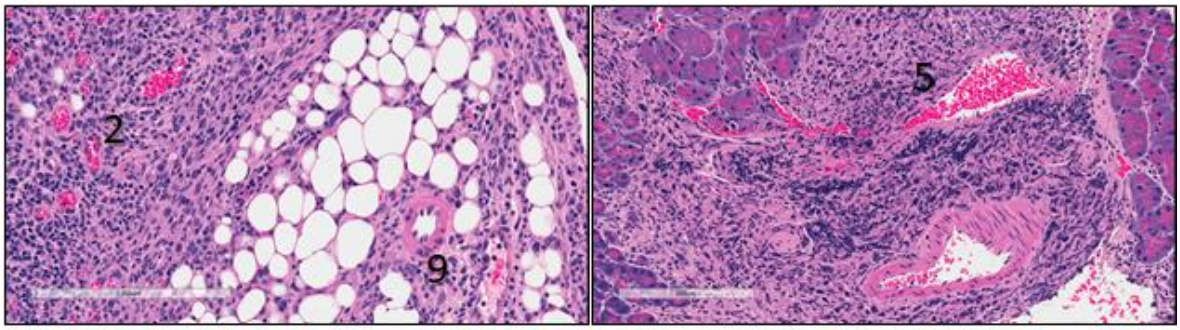

C

		Benign Gland	Invasive Carcinoma	Orthotopic Pan02 tumour
1	Disruption of lobular structure	No	Yes	Yes
2	Haphazard growth pattern	No	Yes	Yes
3	Glands adjacent to vessels	No	Yes	Yes
4	Perineural invasion	No	Yes	Advanced only
5	Intravascular invasion	No	Yes	Yes
6	Nuclear variation	No	Yes	No
7	Intraluminal necrosis	No	Often	No
8	Incomplete glands	No	Often	No
9	Gland touching fat	No	Yes	Sometimes

Figure 3: Clinical hallmarks of PDAC are evident in orthotopic Pan02 tumours. Primary pancreatic tumours of Pan02 (A and B) injected cells were stained using a hematoxylin and eosin (H&E) to investigate the histopathology of the tumours (A - Magnification100X scale bar 100µm, B- Magnification 200X scale bar 200µm). (C) Clinical hallmarks of disease compared across PDAC and the Pan02 model – adapted from Hruban et al 2007[20].

Table 1: Incidence of primary and metastatic disease in the surgical model

		Immediate Resection	$1x10^3$	$1x10^4$	$1x10^5$
Day 15/20 post injection	Orthotopic Tumour	0/5	4/5	11/12	18/18
	Peritoneal disease	0/5	0/5	1/12	5/18
Post-surgery	MRD outgrowth	0/5	2/5	4/5	5/5
	Peritoneal disease	0/5	2/5	4/5	5/5

3.1.2 Orthotopic Pan02 tumours are highly infiltrated with immune cells

A number of studies have previously shown that lymphocytic infiltration is strongly correlated with patient outcomes in PDAC [156–158]. To study the TME, IHC staining of T cells was optimized in the spleen (Figure 4), and subsequently used on paraffin embedded tumour samples (Figure 5). Finally flow cytometry was used to further characterize immune subsets (Figure 6). The TME of the orthotopic Pan02 tumours was highly infiltrated with CD45+ immune cells 20 days after implantation. CD3+ T cells, CD19+ B cells and a CD11c+ subset represent the majority of the infiltrate with MDSCs and NK cells present in lesser numbers (<10%) (Figure 6A). The CD3+ T cells included both CD4+ and CD8+ T cells and this immune infiltrate is limited to the tumour tissue with few immune cells observed in the surrounding healthy tissue (Figure 5). Interestingly, while the baseline activation of CD8+ T cells, as defined by CD69 expression, was similar between tumour bearing and tumour naive mice, the amount of PD-1 expression was significantly increased on tumour infiltrating CD8+ T cells as compared with matched spleens, suggestive of increased activation or exhaustion (Figure 6C, p=0.0007). Furthermore, regulatory T cells ($CD45^+$ $CD3^+$ CD4+ CD25+ FoxP3+) expand systemically and

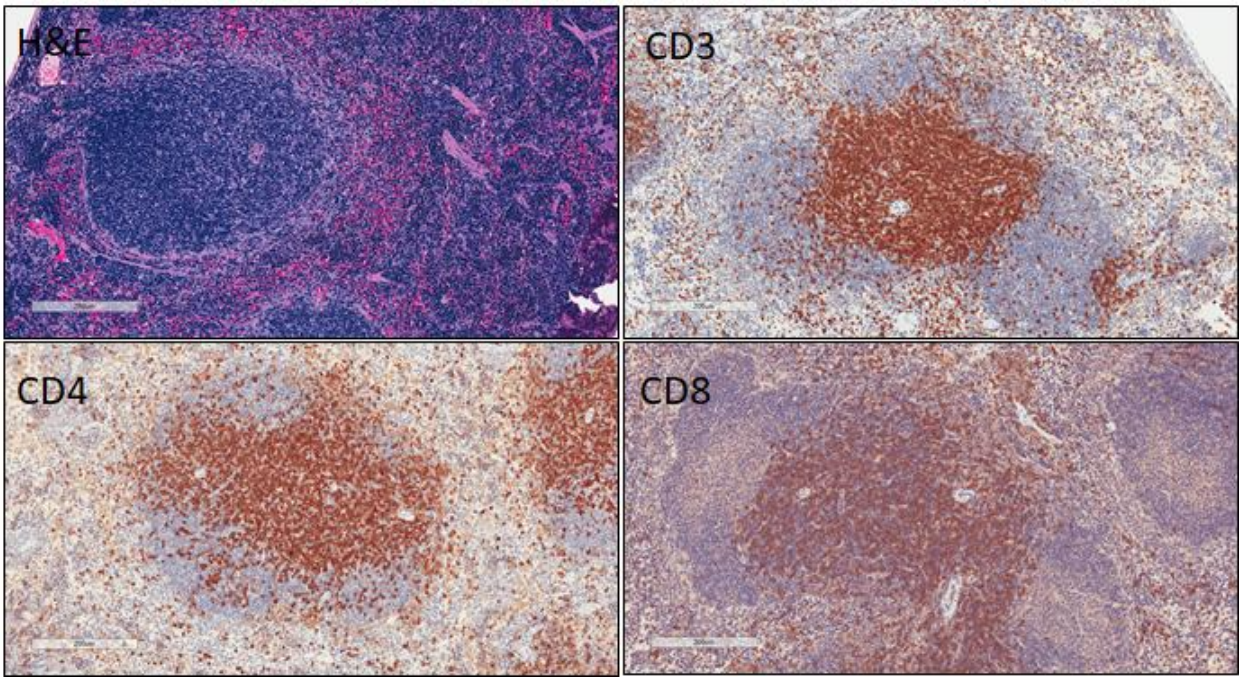
H&E
CD3
CD4
CD8

Figure 4: Immunohistochemistry optimization on the spleen. The staining of T cells and subsets was optimized on the spleen of C57Bl/6 mice. Staining of H&E, CD3, CD4 and CD8 (as indicated) confirms that the antibodies can detect T cell subsets within the white pulp of the spleen. Magnification 200X, scale bar =200 µM.

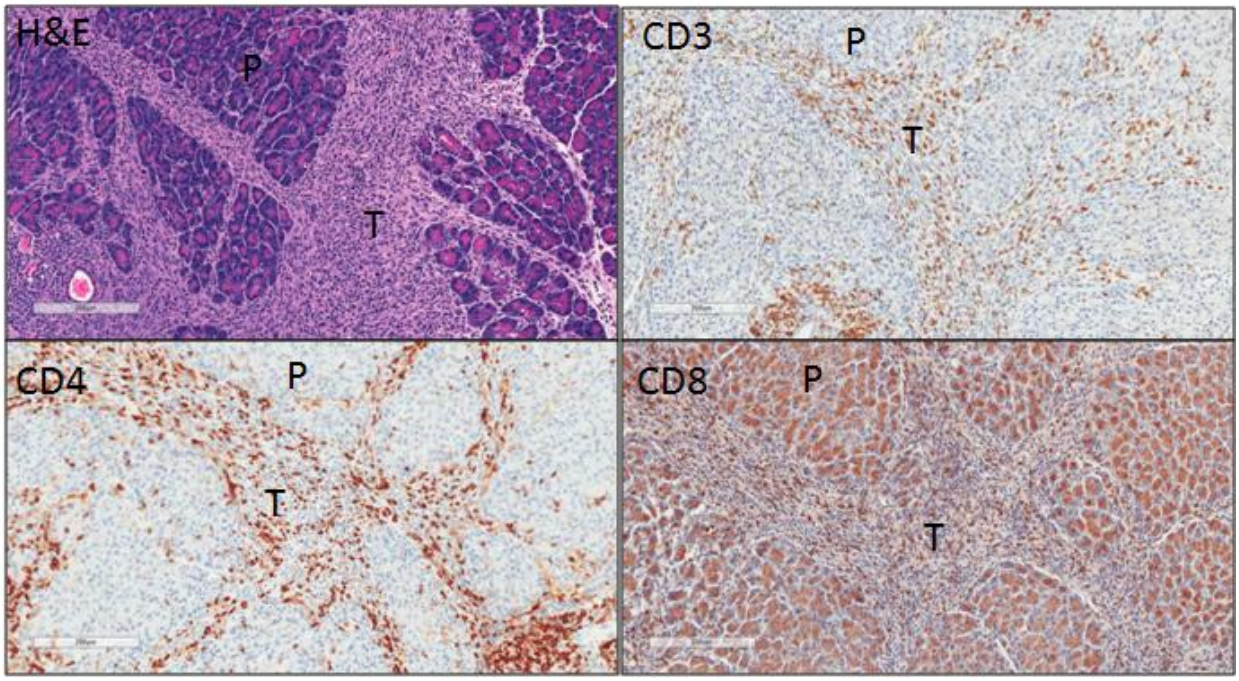
H&E
P
T
CD3
P
T
CD4
P
T
CD8
P
T

Figure 5: Immune cells infiltrate primary Pan02 tumours. tumour IHC was performed as described. Serial sections of tumour (T) and surrounding healthy pancreas (P) collected 20 days post orthotopic injection stained by H&E, anti-CD3, anti-CD4, and anti-CD8 as marked. Images representative of all mice (n=5). Magnification 200X, scale bar =200 μM.

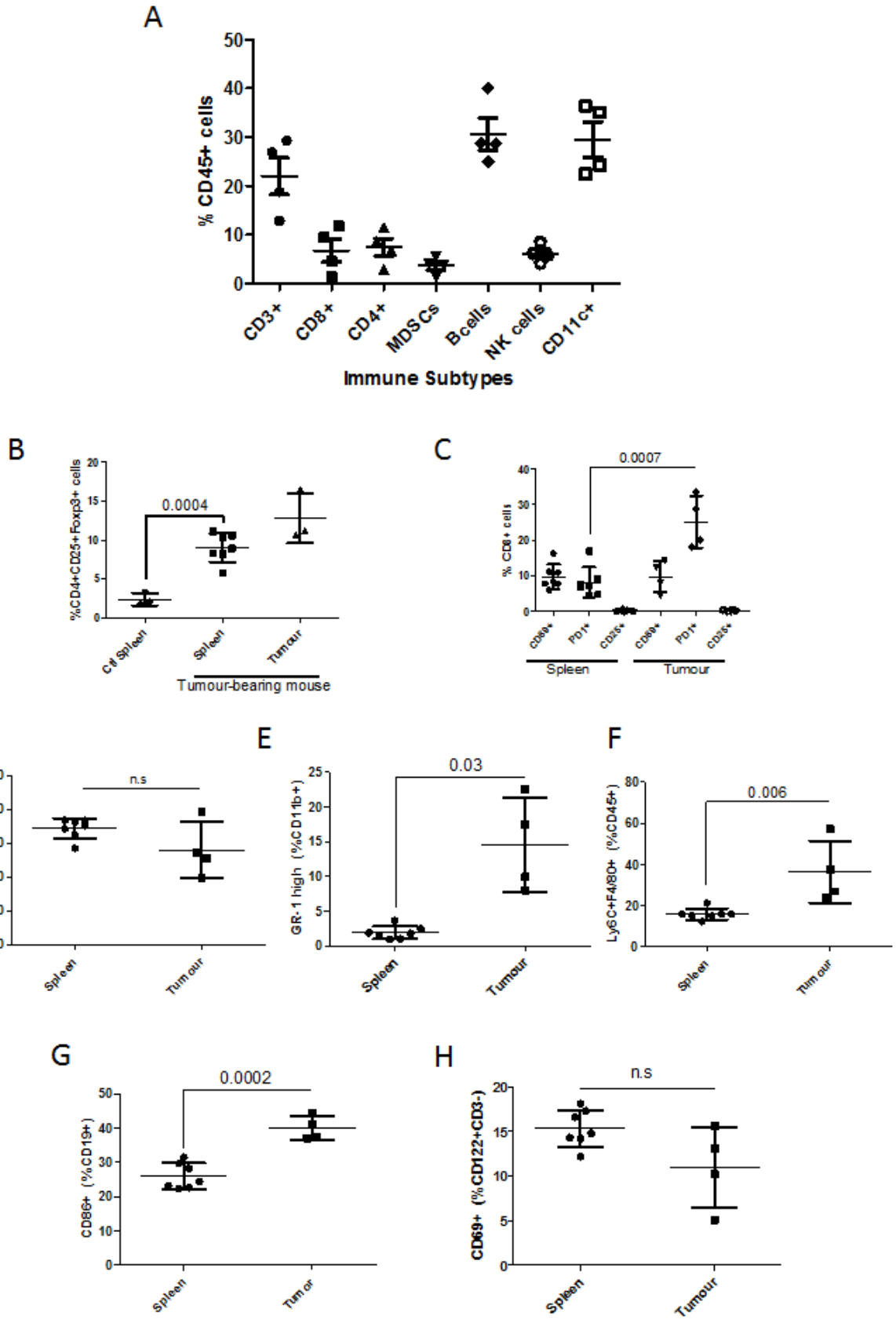
A
% CD45+ cells
CD3+
CD8+
CD4+
MDSCs
Bcells
NK cells
CD11c+
Immune Subtypes
B
%CD4+CD25+Foxp3+ cells
0.0004
C# Spleen
Spleen
Tumour
Tumour-bearing mouse
C
0.0007
% CD8+ cells
CD69+
PD1+
CD25+
Spleen
Tumour
D
CD19+ (%CD45+)
n.s
E
GR-1 high (%CD11b+)
0.03
F
Ly6C+F4/80+ (%CD45+)
0.006
G
CD86+ (%CD19+)
0.0002
H
CD69+ (%CD122+CD3-)
n.s

Figure 6: Orthotopic Pan02 tumours are highly immune infiltrated. (A) Summary of flow cytometry of immune subsets infiltrating into the Pan02 tumour microenvironment at day 20 post injection (n=4). (B) Regulatory T cell infiltrate into tumours and circulating in tumour-bearing mice as compared to a healthy control (n=3-7). (C) Activation of CD3+CD8+ cells within the spleen (n=7) and tumours (n=4) of tumour bearing mice at day 20 post injection. (D) B cells in circulation (spleen) compared with tumour infiltration levels. (E) Increased GR-1high CD11b+ cells are present within the Pan02 tumours compared to splenic levels. (F) Macrophages (Ly6C+F4/80+) are present within the tumour microenvironment. (G and H) Differences in key activation markers were observed in lymphocytic populations. (G) Increased CD86+ was observed on tumour infiltrating B cells as compared to the splenic levels. (H) NK cells had decreased surface expression of CD69 as compared to splenic NK cells. Student's paired t test was used to calculate significance and is indicated on the graphs.

infiltrate the TME as measured by flow cytometry, indicating a potential immunosuppressive mechanism (Figure 6B, p=0.0004).

In addition to T_{regs}, a number of cell types with potentially immunosuppressive actions were found within the TME including CD19+ B cells, MDSCs and macrophages (Figure 6D-F). Consistent with this finding both the B and NK cell populations found within the TME were differentially activated in comparison to their circulating counterparts (Figure 6G and H). For example, CD86 was significantly increased on tumour-infiltrating B cells (p=0.0002) whereas CD69+ was decreased on CD3-CD122+ NK cells comparison to the respective circulating populations.

Together these data suggest orthotopic Pan02 tumours are infiltrated with a large number of immune cell populations including both effector and suppressive populations and demonstrate histopathology consistent with human PDAC.

3.1.3 Orthotopic Pan02 tumours can be surgically resected without removal of the spleen

To be eligible for surgical intervention, patients typically must have localized disease without visible spread of disease within the peritoneal cavity and onto surrounding organs [22]. Notably, mice receiving injections of either $1x10^4$ or $1x10^5$ cells consistently developed pancreatic tumours without peritoneal disease or splenic metastases by day 20 and 15 respectively. Partial pancreatectomies were performed in both groups. The lighter tumour burden at the time of surgery (day 20) in mice implanted with $1x10^4$ cells was associated with a lower recurrence rate following surgical removal of the primary tumour. In contrast, a dose of $1x10^5$ consistently had a higher tumour burden at the time of surgery (Day 15) with 28% of mice (5/18) representing "open and close" type surgeries due to more extensive tumour burden and organ adhesion at the site of tumour injection (Table 2). Interestingly, in the first cohort of surgical experiments, 50%

(4/8) of mice developed ulcerating lesions within 1 week of surgical resection of the primary tumour. These lesions are characterized by hair loss, skin erosion and full thickness abdominal wall defects. Further investigation suggested that leakage of pancreatic enzymes from the pancreatic remnant had occurred when Polysorb™ absorbable sutures were used to tie off the proximal pancreatic duct,leading to pancreatic fistulisation through the abdominal wall (Figure 7). The use of slowly absorbing PDS II sutures, which are commonly used in clinical partial pancreatectomies[159] completely prevented the occurrence of pancreatic fistulas in subsequent surgical cohorts (0 /13 animals) (Table 2). At 20 days following surgical resection, mice were euthanized, and peritoneal disease was investigated. All mice exhibited visible peritoneal disease and an increased peritoneal mass to total mass ratio post op (Figure 8A-C, n=5, 21% body weight vs 23.1% body weight, p= 0.04), with the largest burden of disease occurring with $1x10^4$ mice receiving surgery at day 20, and $1x10^5$ mice receiving surgery at day 15.

Table 2: Occurrence of skin lesions following partial pancreatectomies

Suture	Occurrence of Lesions
5.0 absorbable suture	4/8
PDS II suture (Ethicon Z423)	0/13

Figure 7: Mice receiving partial pancreatectomies develop lesions. Using Polysorb™ absorbable sutures, 50% of mice developed lesions characterized by hair loss, skin erosion and full thickness abdominal wall defects, consistent with a pancreatic fistula. Representative image of lesion appearing within one week of surgery. Full summary in Table 2.

3.1.4 Spleen viability and cytokine secretion are intact following surgery

Due to the benefits of spleen preservation and the possibility of using the spleen as a tool to measure immune function post-operatively we sought to examine whether splenic function, particularly basic viability and T cell functionality, were maintained following surgery. Following the timeline in Figure 8A, mice were sacrificed 20 days following resection of the tail of the pancreas. Histological examination of the spleen by a pathologist revealed all the key structures of the spleen to be intact, including the rep pulp (RP), white pulp (WP) and marginal zones (MZ), as labelled in Figure 9A, which is a representative image of a total of 10 mice examined. Of note, an accumulation of blood and erythrocytes was observed within the red pulp of the spleen following surgery (Figure 9A) resulting in an increased splenic weight (Figure 9B, +1.5g, p=0.02). This apparent accumulation of blood is consistent with reduced drainage through the splenic vein which was severed during the partial pancreatectomy. However, the reduced drainage observed at this time was not found to impact splenocyte viability (Figure 9C, n=3 vs n=5, p=0.744). In addition, no significant difference in TNFα secretion from CD8+ T cells stimulated with PMA/ionomycin was detected (Figure 9D, n=3 vs n=5, p=0.4), suggesting that the viability and function of CD8+ T cells within the spleen was unaltered following surgical resection.

A

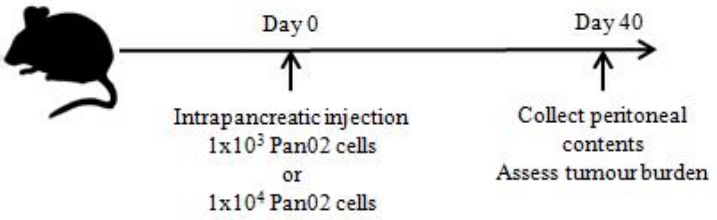
Day 0
Day 40
Intrapancreatic injection
1x10³ Pan02 cells
or
1x10⁴ Pan02 cells
Collect peritoneal
contents
Assess tumour burden

B


1x10³
1x10⁴
1x10⁵

C

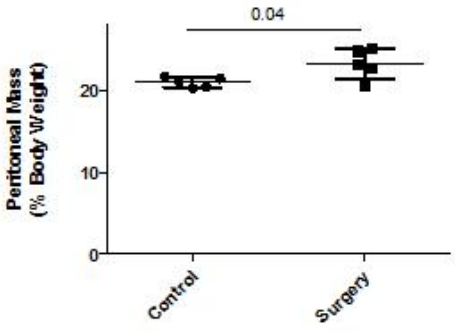
0.04
Peritoneal Mass
(% Body Weight)
20
10
0
Control
Surgery

Figure 8: Orthotopic model is amenable to tumour surgical resection. (A) Timeline for partial pancreatectomy to resect the primary pancreatic tumour. (B) Peritoneal metastases are visible 20 days post-surgery at all initial Pan02 cell concentrations (n=10 per group). Representative images peritoneal cavity at 20 days post resection. (C) Weight of the peritoneal cavity normalized to the total mass of the mouse 20 days post-surgery (n=10 per group).

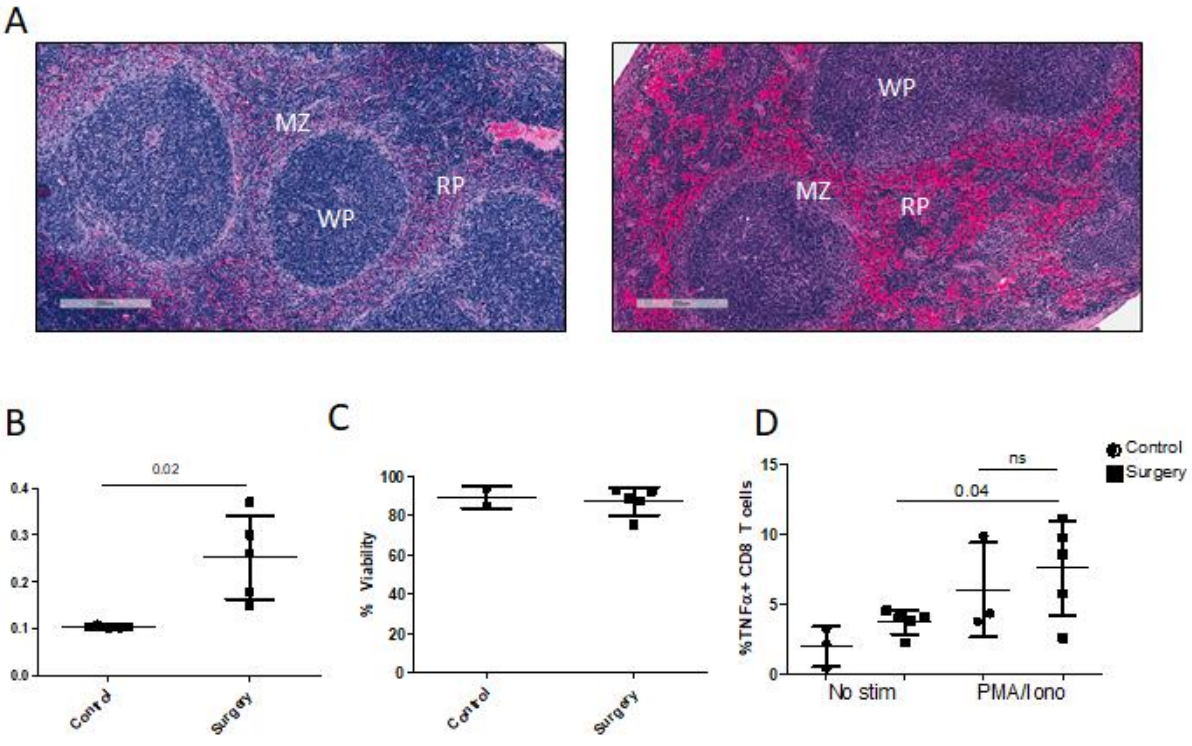
A
MZ
WP
RP
WP
MZ
RP
B
0.02
Weight (g)
0.4
0.3
0.2
0.1
0.0
Control
Surgery
C
% Viability
100
80
60
40
20
0
Control
Surgery
D
Control
Surgery
ns
0.04
%TNFα+ CD8 T cells
15
10
5
0
No stim
PMA/Iono

Figure 9: Splenic T cell function is preserved following partial pancreatectomy. (A) Histological examination of spleens from healthy mice (left), and mice 20 days following surgical resection of primary tumours(right). W=white pulp, R=red pulp, MZ = marginal zone. Scale bar = 200μm. (B) Splenic weight of collected spleens and (C) cell viability of collected splenocytes as measured by trypan blue exclusion. All splenic measurements were compared to age matched healthy controls. (D) TNFα secretion of CD8+ T cells was measured by flow cytometry of whole splenocytes that received no stimulation, or PMA/Ionomycin stimulation (N=6 per group). Error bars represent standard deviation. Significance measured by Student's t test.

3.1.5 Surgical resection of the primary tumour alone does not improve survival outcomes

To investigate the effect of surgical resection on survival and disease recurrence, established tumours were resected in accordance with the criteria for clinical surgical intervention outlined previously. In particular, there was no evidence of peritoneal disease at the time of surgery and the primary tumour was completely resected based on gross visual inspection. Surgical intervention was associated with a significant reduction in body weight during the immediate perioperative period however the rate of weight gain was comparable to non- surgically resected mice during the subsequent weeks (Figure 10A). Importantly, despite resection of the primary tumour, surgery did not provide any survival benefit in comparison to the non-surgery group (Figure 10B, n=13-20 per group, p=0.898 by log rank test). The two initial cell concentrations of $1x10^4$ and $1x10^5$ demonstrated slightly different models of PDAC, as outlined by survival observed in Table 3, with the lower cell concentration having slightly increased survival rates. At endpoint, examination of the peritoneal cavity revealed disease recurrence at the site of the primary tumour, as well as evidence of disseminated disease throughout the cavity, particularly marked by metastases in the spleen and liver (Figure 10C and D).

Table 3: Effects of surgery on long term survival in the surgical model

		Immediate Resection	$1x10^3$	$1x10^4$	$1x10^5$
Survival >100 days	Without Surgery	———	———	2/8	1/20
	With Surgery	4/5	———	7/21	1/13

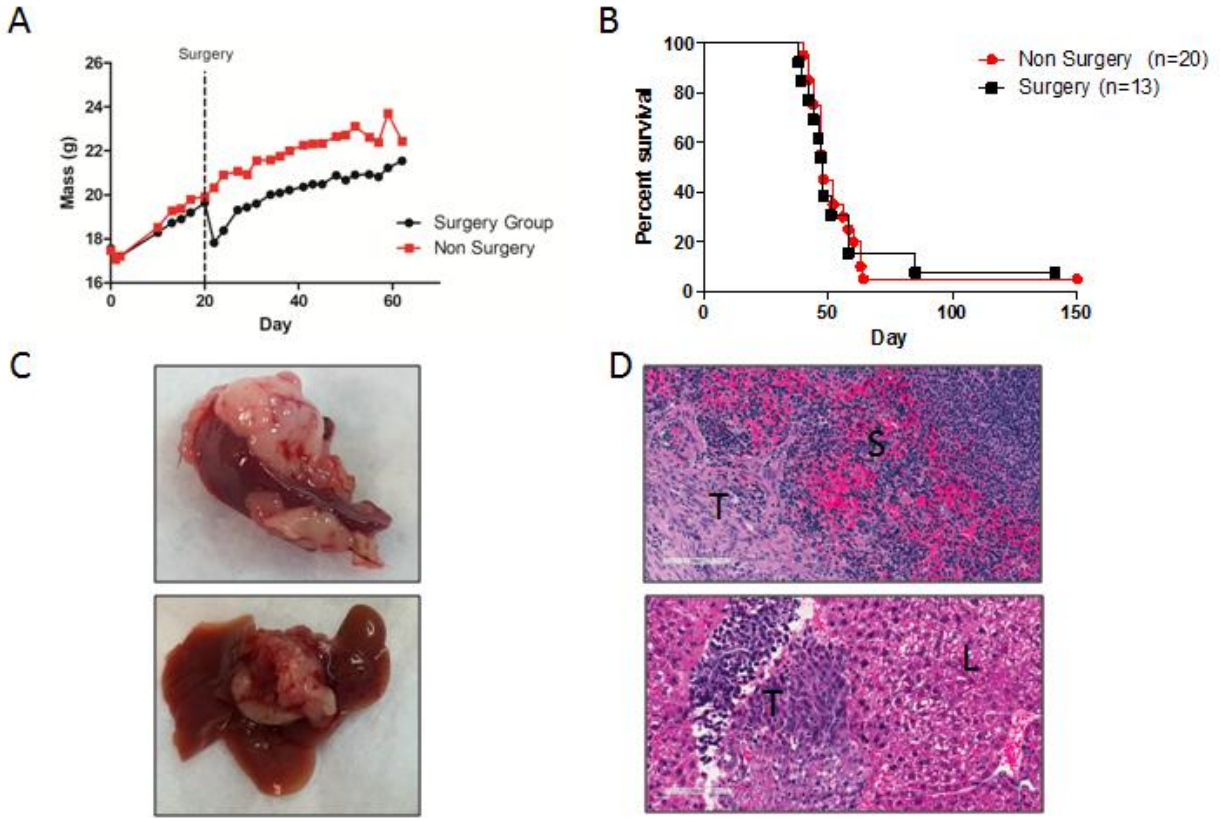
A
Surgery
Mass (g)
Day
Surgery Group
Non Surgery
B
Percent survival
Day
Non Surgery (n=20)
Surgery (n=13)
C
D
S
T
T
L

Figure 10: Surgical intervention has no effect on overall survival of mice. (A) Mice were weighed every day post-surgical resection of primary tumours ($1x10^4$) to monitor overall health (n=7 per group). (B) Survival of mice following surgical removal of the primary tumour ($1x10^5$) at day 15 (pooled data from 3 experiments, total mice indicated in figrue). (C) Tumours/metastases were specifically found to have spread to the spleen (top) and liver (bottom) of all mice at their respective endpoint (representative images), (D) which were confirmed by H&E (Inset magnification 200X) T= tumour, S = spleen, L = liver.

3.1.6 Therapeutics in the surgery model demonstrate the power of this model as an investigative tool

To investigate the potential of this model as a tool to determine the efficacy of therapeutic strategies during the perioperative period, mice were treated with GVAX combined with T_{reg} depletion and GVAX preoperatively. GVAX is currently being investigated for use with combination checkpoint blockade in PDAC surgery patients, however its effect in the context of surgery could not be explored pre-clinically in currently published murine models [160]. Mice implanted with orthotopic PDAC tumours received T_{reg} depletion and GVAX two days prior to partial pancreatic resection (Figure 11A). Survival of mice receiving therapy in addition to surgery was improved over surgery alone ($p=0.0005$), highlighting the importance of having models to investigate the impact of immunotherapeutics in the context of surgical resection (Figure 11B).

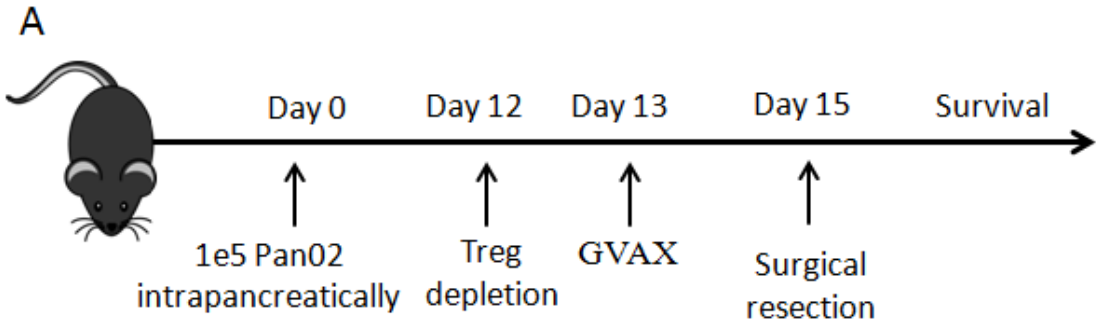
A
Day 0
Day 12
Day 13
Day 15
Survival
1e5 Pan02
intrapancreatically
Treg
depletion
GVAX
Surgical
resection

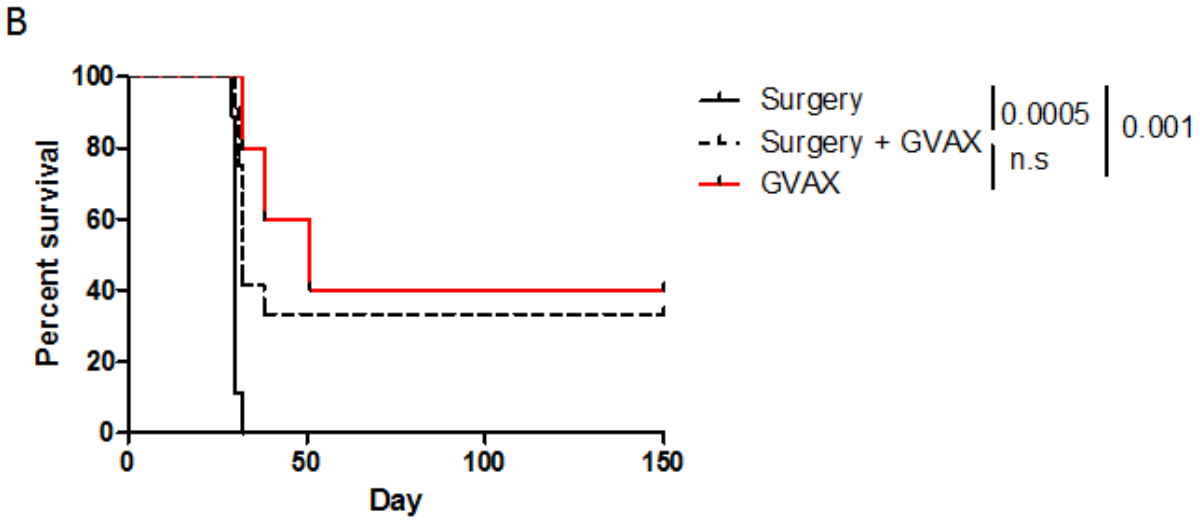
B
Percent survival
100
80
60
40
20
0
0
50
100
150
Day
Surgery
Surgery + GVAX
GVAX
0.0005
n.s
0.001

Figure 11: GVAX vaccination improves survival post surgery. (A) Timeline of surgical resection and GVAX treatment. Treg depletion was performed with 50µg anti-CD25(PC61.5) and 100mg/kg cyclophosphamide. A single GVAX injection was given in both hind limbs. (B) Survival of mice receiving surgery alone, GVAX or surgery and GVAX combined, n= 5-12 mice per group. Log rank test was utilized for significance of survival.

3.2 Characterization of a Maraba virus encoding the tumour associated antigen mesothelin.

Heterologous prime-boost vaccination strategies designed to present TAA to the immune system are recognized as an effective approach for inducing robust immune responses capable of providing protection from tumour outgrowth [123]. Although a number of vectors can be used the oncolytic Maraba variant MG1 has been shown to elicit curative immune responses against several antigens including hDCT when used as a boosting vector with an Adenovirus prime expressing hDCT fused to GFP[129]. However, the efficacy of this approach has not previously been investigated in PDAC. As a first step I aimed to engineer and characterize an MG1 virus expressing mesothelin, a TAA overexpressed in the majority of PDAC patients [140].

3.2.1 Creating a Maraba MG1 virus expressing mesothelin

The heterologous prime-boost platform used in my studies consists of an Adenovirus priming vector encoding a full length mesothelin protein fused to GFP (developed by Kyle Stephenson at McMaster) and a Maraba MG1 boosting vector encoding a codon optimized full length mesothelin protein which I cloned and rescued (Figure 12A, genetic sequences found in Appendix 8.3). MluI restriction sites were included at terminal ends of the mesothelin coding sequence to enable cloning into the plasmid encoding the Maraba viral backbone (Figure 12B). After restriction digest, ligation and transformation, bacterial colonies were screened by colony PCR (Figure 12C) and digestion of purified plasmid DNA (Figure 12D) before sequencing. The virus was subsequently rescued and purified as outlined in the methods section. This replication competent virus, MG1meso, replicated in the Pan02 target cells with similar kinetics as the parental Maraba MG1 virus (Figure 13A and B).The parental and MG1meso viruses displayed

A

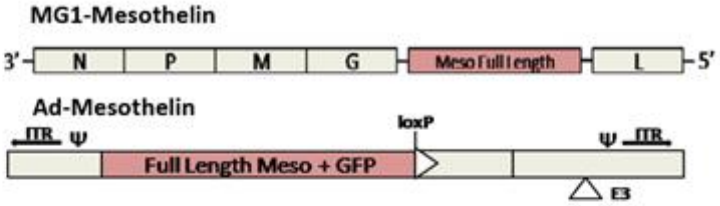
MG1-Mesothelin
3'
N
P
M
G
Meso Full Length
L
5'
Ad-Mesothelin
ITR
ψ
loxP
Full Length Meso + GFP
ψ
ITR
E3

B

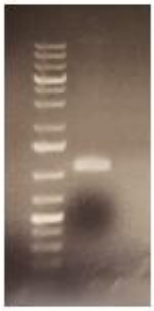

C

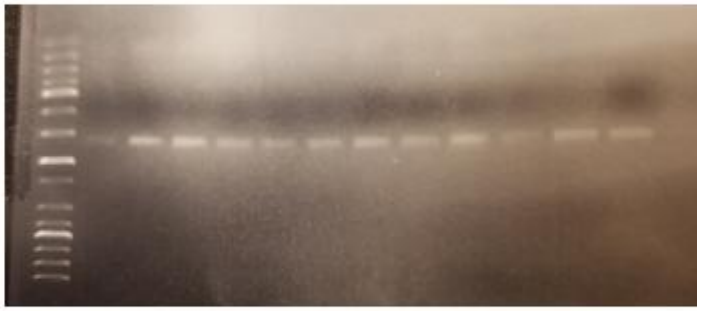

D

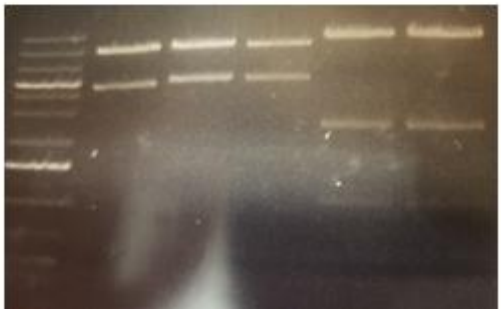

Figure 12: Inserting mesothelin into the Maraba backbone. (A) Schematic showing insertion sites of mesothelin and the mesothelin-GFP fusion protein into their respective viral backbones. (B) PCR expansion of mesothelin sequence. Confirmation of mesothelin insertion into the Maraba plasmid by (C) PCR expansion of clones and (D) restriction digest of the Maraba plasmid with Mlu1.

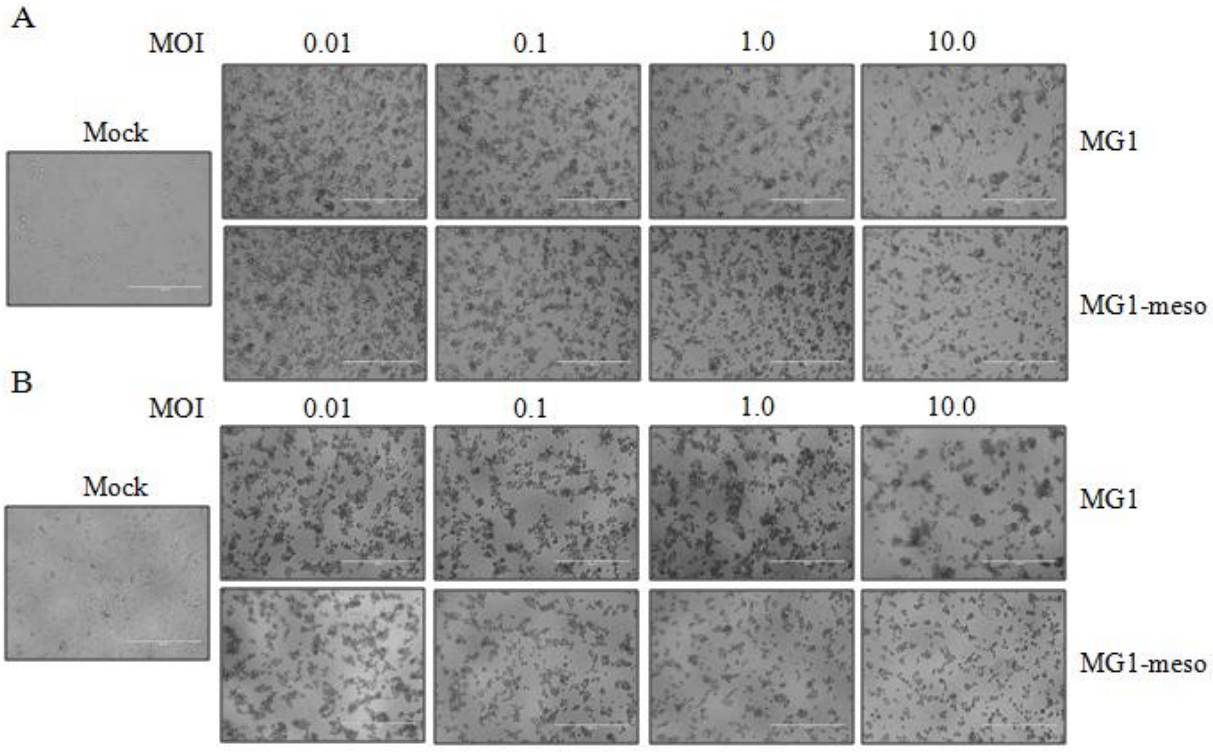
A
MOI
0.01
0.1
1.0
10.0
Mock
MG1
MG1-meso
B
MOI
0.01
0.1
1.0
10.0
Mock
MG1
MG1-meso

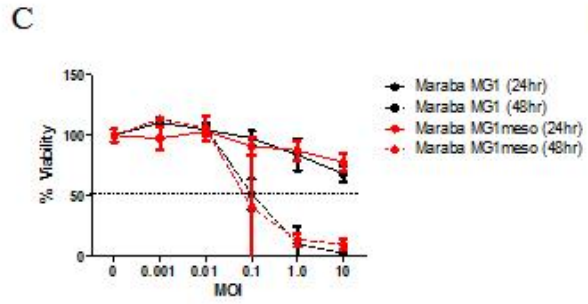
C
% Viability
MOI
Maraba MG1 (24hr)
Maraba MG1 (48hr)
Maraba MG1meso (24hr)
Maraba MG1meso (48hr)

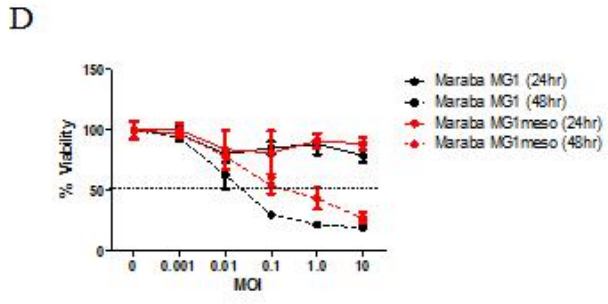
D
% Viability
MOI
Maraba MG1 (24hr)
Maraba MG1 (48hr)
Maraba MG1meso (24hr)
Maraba MG1meso (48hr)

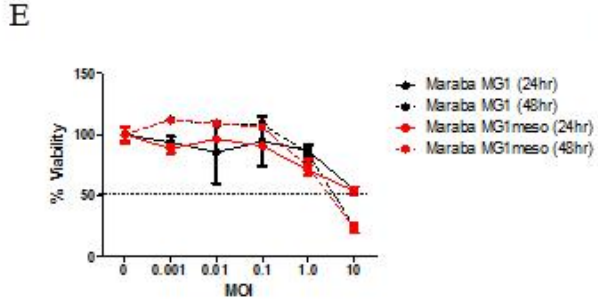
E
% Viability
MOI
Maraba MG1 (24hr)
Maraba MG1 (48hr)
Maraba MG1meso (24hr)
Maraba MG1meso (48hr)

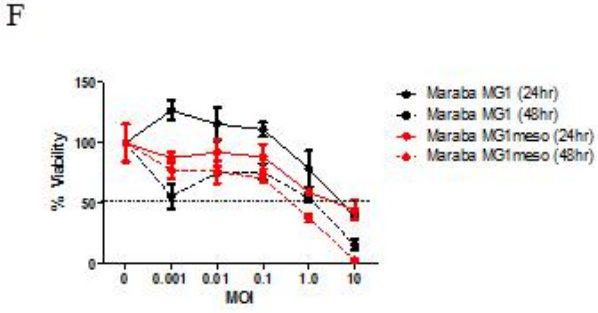
F
% Viability
MOI
Maraba MG1 (24hr)
Maraba MG1 (48hr)
Maraba MG1meso (24hr)
Maraba MG1meso (48hr)

Figure 13: Maraba MG1-meso displays similar cytotoxicity to its parent virus. Pan02 cells were infected with Maraba MG1(top) or Maraba MG1-meso(bottom) at the indicated MOI. Images were taken (A) 24hrs and (B) 48hrs post infection. At these time points, a resazurin-based viability assay was performed. Viability at both 24hrs and 48hrs was compared to mock infected cells. Cytotoxicity of the viruses was measured in cancerous (C) Pan02 cells, (D) Vero, (E) CT26 cells, and (F) non-cancerous GM38 cells.

similar cytotoxicity in both cells permissive to rhabdovirus infection (Pan02 and Vero) and cell lines found to be more resistant to infection(CT26 and GM38) (Figure 13C-E).

The viral fitness of the cloned MG1meso virus was compared to its parental Maraba MG1 virus in Vero cells. A single step growth curve to measure viral production revealed a similar kinetic to Maraba MG1, but a greater production of total virus (10^6 vs 10^8 by 24 hrs, Figure 14A). A multi step curve was then performed to measure the viral spreading capabilities of MG1meso, where no difference was observed between the cloned and parental virus (Figure 14B). Together these data indicate that MG1meso is comparable to the parental virus but may be able to produce more viruses on a single cell scale.

3.2.2 Mesothelin protein is expressed in MG1meso infected cells

Next, we sought to confirm that the viral vectors expressed mesothelin protein by immunoblotting using a commercially available antibody. Notably, with the exception of the brain, mesothelin was not detected in any tissues of a mouse bearing an orthotopic Pan02 tumour, including pancreatic tissue adjacent to orthotopic Pan02 tumours (Figure 15A). The bands observed in the brain tissue sample are unexpected based on the known expression of mesothelin and could indicate either metastases or background staining. Further confirmation of viral transgene expression was confirmed by collecting whole cell lysates of 293T and Pan02 cells infected with MG1, MG1meso or AdmesoGFP at 24 hpi. As expected, mesothelin was detected in Pan02 cells but was absent from 293T cells in the absence of infection with a mesothelin expressing virus, further establishing antibody specificity. However, a lower molecular weight band was detected in MG1meso infected cell lysates from both cell lines (Figure 15C). This smaller molecular weight may potentially represent an unglycosylated or differentially folded form.

A

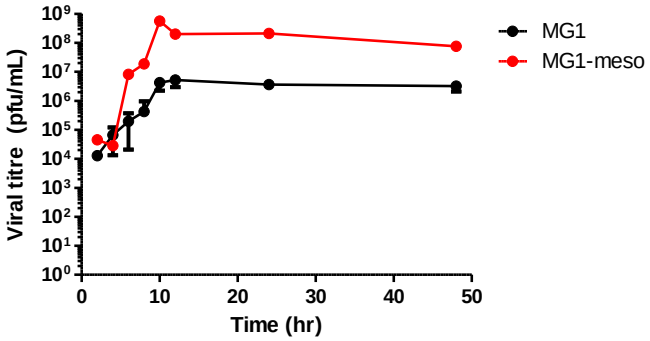
Viral titre (pfu/mL)
Time (hr)
MG1
MG1-meso

B

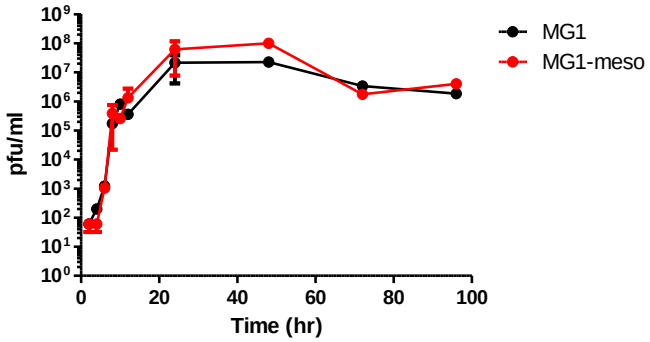
pfu/ml
Time (hr)
MG1
MG1-meso

Figure 14: Maraba MG1-meso has similar growth kinetics as its parent virus. (A) A single step growth curve was performed in Vero cells. Briefly, Vero were infected at an MOI of 10 with both viruses and supernatants were collected at the indicated time points, and titered. (B) A multi-step growth curve was performed on Vero cells that were infected at an MOI of 0.01. Supernatants were collected at the indicated time points, and titered. Growth curves were performed in technical replicates.

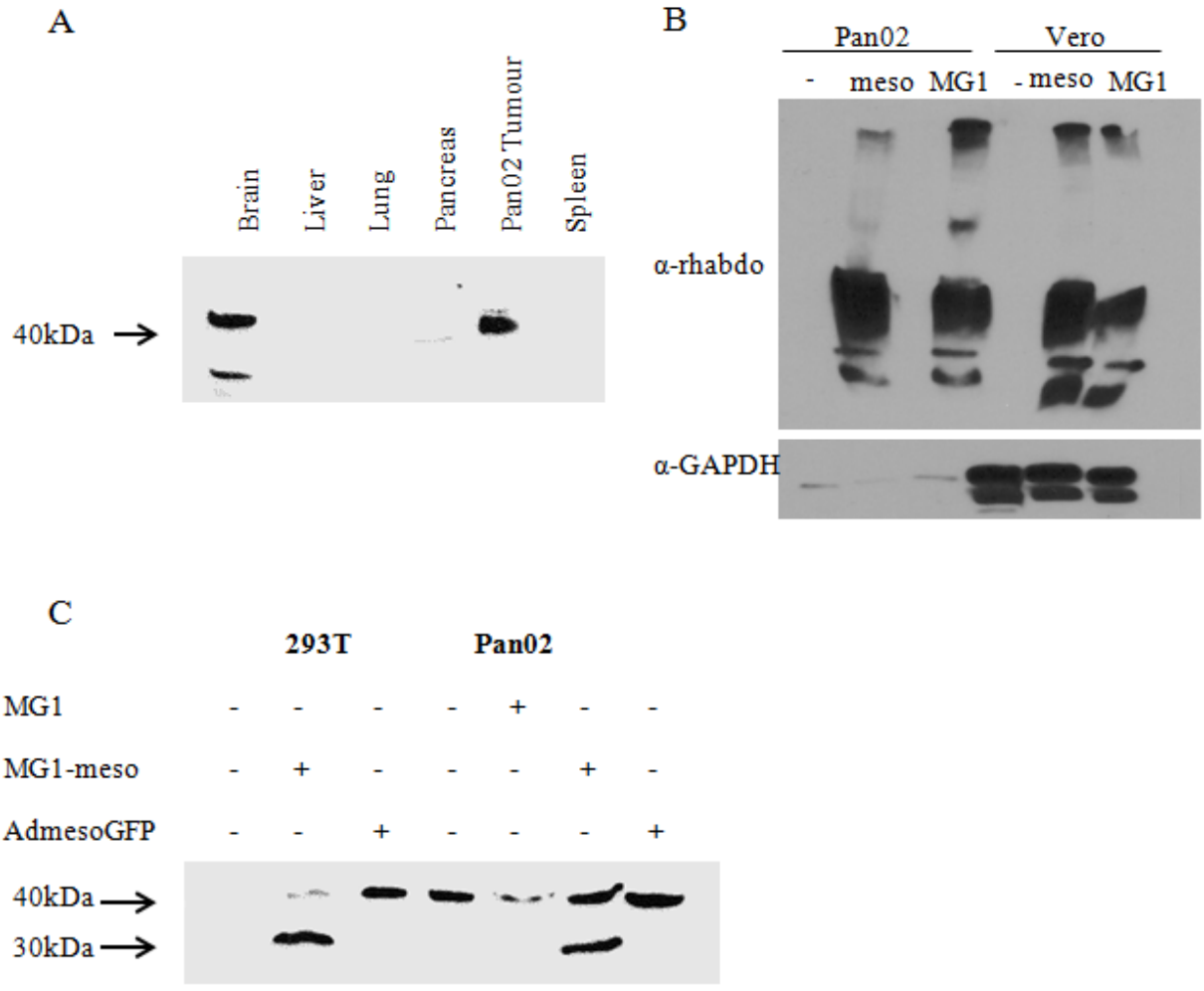
A
Brain
Liver
Lung
Pancreas
Pan02 Tumour
Spleen
40kDa
B
Pan02
Vero
-
meso
MG1
-
meso
MG1
α-rhabdo
α-GAPDH
C
293T
Pan02
MG1
MG1-meso
AdmesoGFP
40kDa
30kDa

Figure 15: MG1-meso virus expresses mesothelin protein. Pan02, 293T and Vero cells were infected with the indicated viruses at an MOI of 10. After 24hrs, total cell lysate was collected, and proteins were isolated and measured by BCA. (A) Mesothelin expression was measured in various murine tissues. (B) MG1-meso has similar expression of rhabdoviral proteins as its parent virus. 18ug protein loaded, human GAPDH was used as a loading control. (C) Mesothelin expression in meso-negative 293T cells and meso-positive Pan02 cells pre and post infection with MG1, MG1-meso and AdmesoGFP.

3.2.3 MG1meso can be safely administered in vivo

The efficacy of MG1 as a boosting vaccine has been previously examined following iv administration of doses up to 1e9 PFU [125]. To determine whether MG1meso was safe to administer at this dose both MG1meso and MG1 viruses were produced and Optiprep™ purified at high titre and injected i.v. into mice at concentrations of 1e9pfu/mouse. In contrast to previous reports, a dose of 1e9pfu was consistently associated with a drop in mass and 50% mortality rate within 7 days of injection. A necropsy revealed liver damage and loss of internal fat deposits (Figure 16A). In a cohort of animals receiving a lower dose(1e8pfu/mouse) no mortality was observed (Figure 16C) despite an initial reduction in weight (Figure 16B) indicating that a dose of 1e8pfu/mouse i.v. can be safely administered.

3.3 Depletion of regulatory T cells is necessary to induce an anti-mesothelin response

3.3.1 A heterologous prime-boost vaccination with AdmesoGFP and MG1meso alone is unable to induce an anti-mesothelin response

The route of delivery and schedule of vaccination used in my studies was based on the work of Brun et al and Bridle et al, demonstrating that robust T cell responses against an antigen are generated in mice receiving an i.m. injection of antigen-encoding Ad followed by a boost 7 days later with i.v. antigen-encoding MG1(Figure 17A)[124,129]. However, no mesothelin reactive T cells were detected in splenocytes harvested 7 days after boosting, a time when T cell responses should be at their peak (Figure 17B). This finding could not be attributed to general T cell dysfunction as IFNγ+ T cells were observed following stimulation with both PMA/ionomycin (a positive control of general stimulation) and peptide specific responses against VSVn (a peptide from the N protein that is presented to T cells when mice are vaccinated with either VSV or MG1 based rhabdoviruses).

A

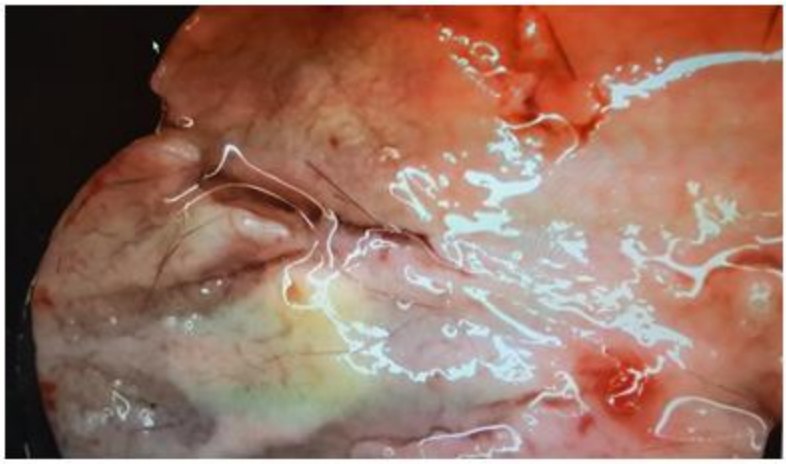

B

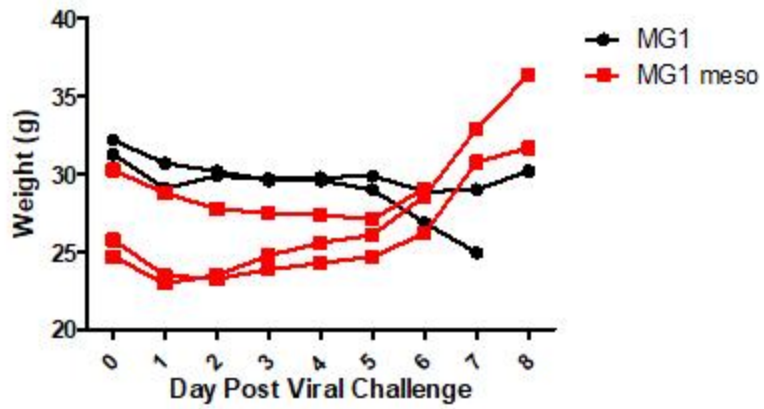
Weight (g)
40
35
30
25
20
0
1
2
3
4
5
6
7
8
Day Post Viral Challenge
MG1
MG1 meso

C

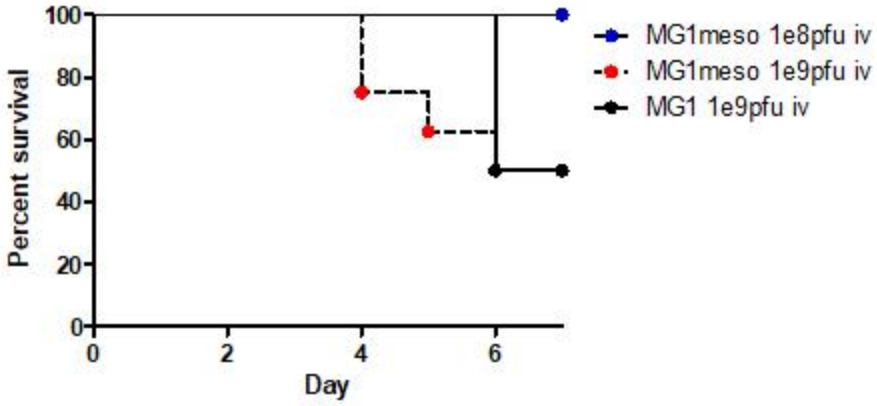
Percent survival
100
80
60
40
20
0
0
2
4
6
Day
MG1meso 1e8pfu iv
MG1meso 1e9pfu iv
MG1 1e9pfu iv

Figure 16: High dose Maraba virus shows toxicity *in vivo*. Mice were injected with 1e9 pfu of virus as previously described. Within 4-7 days of injection, 50% of mice would die with emaciation, and toxicity syndromes. (A) Toxicity within the liver of a mouse that died 4 days after receiving 1e9pfu *i.v.* (B) Weight was monitored in mice receiving 1e9pfu of purified Maraba MG1 virus or Maraba MG1meso virus. Mice that eventually recover regain weight within 7 days, those that die become emaciated and continue to lose weight. (MG1 n=2, 1/2 survival; MG1meso n=3, 2/3 survival). (C) Overall survival of mice receiving 1e9pfu of MG1 or MG1meso *i.v.* compared to mice receiving MG1meso 1e8pfu *i.v.* within 7 days of injection. Mice are declared to be at endpoint according to ACVS guidelines and are necropsied at death.

A

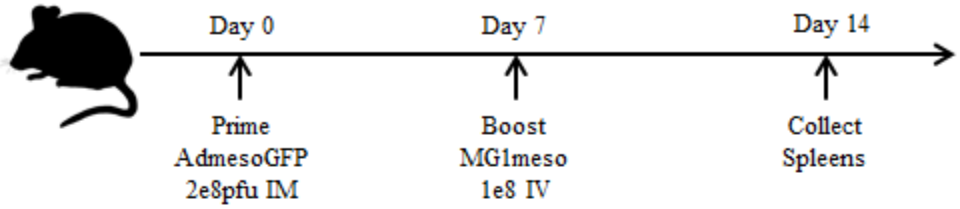
Day 0
Day 7
Day 14
Prime
AdmesoGFP
2e8pfu IM
Boost
MG1meso
1e8 IV
Collect
Spleens

B

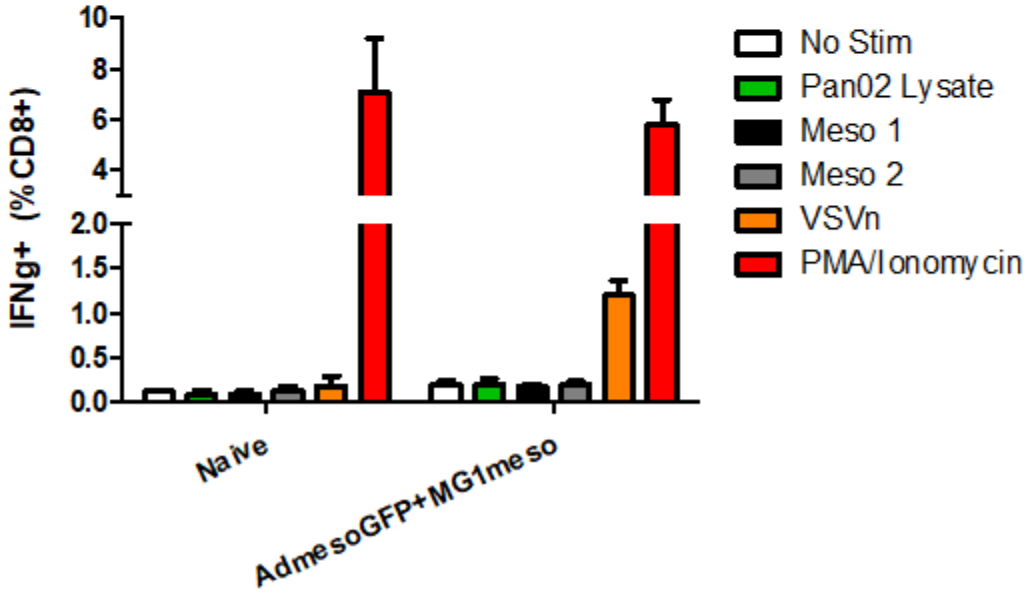
IFNg+ (%CD8+)
10
8
6
4
2.0
1.5
1.0
0.5
0.0
Naïve
AdmesoGFP+MG1meso
No Stim
Pan02 Lysate
Meso 1
Meso 2
VSVn
PMA/Ionomycin

Figure 17: Vaccination alone does not elicit an anti-mesothelin immune response. (A) Timeline showing the vaccination strategy. Briefly, mice received 2e8pfu AdmesoGFP *i.m.* followed 7 days later by 1e8 MG1meso *i.v.* Immune responses were measured in the spleen 7 days following the boost. (B) Proportion of IFNγ+ CD8+ T cells following 5-hour stimulation with the peptides indicated, with brefeldin A being added 1 hour into the incubation. N=3 in both groups.

3.3.2 Depletion of regulatory T cells at the time of vaccination is required for generating an anti-mesothelin CD8+ T cell response

The lack of a successful anti-mesothelin response as measured by intracellular staining for IFNγ in CD8+ T cells after meso peptide stimulation could be due to technical limitations or an inability of the vaccine to stimulate a measurable anti-mesothelin response. Unlike previously tested TAAs, mesothelin is a self antigen and therefore CD8+ T cells with strong affinity for it are likely eliminated through negative selection in the thymus [161], and those with a weaker affinity are limited by regulatory T cells in circulation[162]. Indeed, other groups have been able to successfully detect mesothelin-reactive T cells following vaccination with a GM-CSF expressing whole cell vaccine only when combined with regulatory T cell depletion through treatment with low dose cyclophosphamide and anti-CD25 depleting antibody[59]. To begin to investigate whether regulatory T cells prevent detection of mesothelin reactive CD8+ T cells in vaccinated mice I used the dosing schedule outlined by Leao et al to demonstrate that CD4+CD25+Foxp3+ cells can be successfully depleted by 7 days post injection without any effect on overall proportions of splenic T cell populations cells (Figure 18).

Next, the effects of T_{reg} depletion on T cell responses in mice receiving only a priming dose of either the established AdhDCT virus or AdmesoGFP. Notably, the priming dose could be delivered safely under these conditions and T_{reg} cells remained depleted while other T cell subsets were not significantly impacted despite a trend to increased proportions in T_{reg} depleted mice receiving virus (Figure 19A-C). Despite the total depletion of regulatory T cells (Figure 19D), no effect was observed on overall peptide specific CD8+IFNγ+ responses, either with AdhDCT or AdmesoGFP (Figure 19E). Interestingly the off-target reactivity of CD8+ T cells

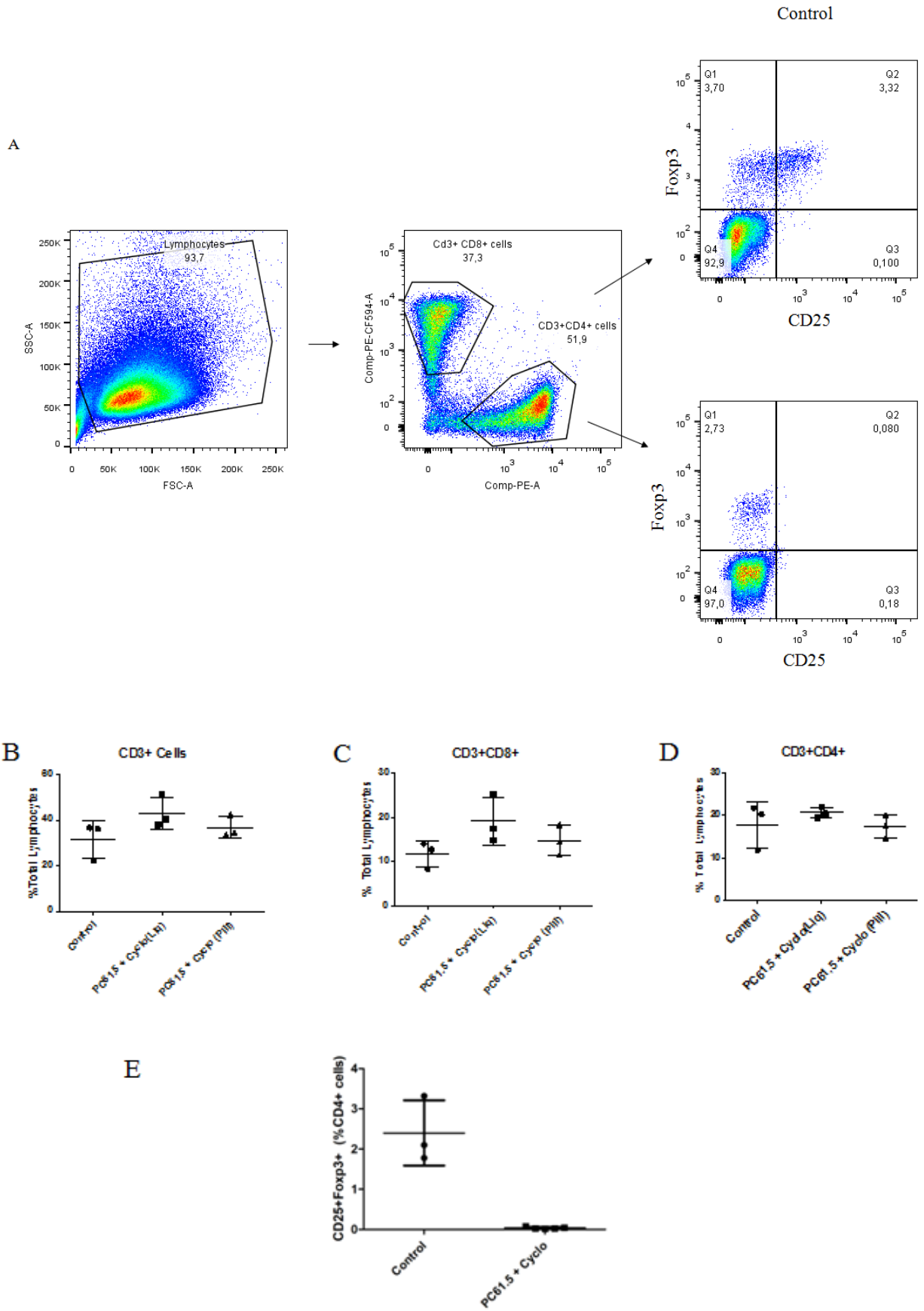
Control
A
Lymphocytes
93,7
SSC-A
FSC-A
Cd3+ CD8+ cells
37,3
CD3+CD4+ cells
51,9
Comp-PE-CF594-A
Comp-PE-A
Q1
3,70
Q2
3,32
Q4
92,9
Q3
0,100
Foxp3
CD25
Q1
2,73
Q2
0,080
Q4
97,0
Q3
0,18
Foxp3
CD25
B
CD3+ Cells
%Total Lymphocytes
Control
PC61,5 + Cyclo(Liq)
PC61,5 + Cyclo (Pill)
C
CD3+CD8+
% Total Lymphocytes
Control
PC61,5 + Cyclo(Liq)
PC61,5 + Cyclo (Pill)
D
CD3+CD4+
% Total Lymphocytes
Control
PC61,5 + Cyclo(Liq)
PC61,5 + Cyclo (Pill)
E
CD25+Foxp3+ (%CD4+ cells)
Control
PC61,5 + Cyclo

Figure 18: Low dose cyclophosphamide and antibodies against CD25 deplete regulatory T cells *in vivo*. (A) Gating strategy for regulatory T cells defined as CD3+CD4+CD25+FoxP3+ cells. Splenic levels of (B) total CD3+ cells, (C) CD3+CD8+ cells and (D) CD3+CD4+ cells. (E) Cyclophosphamide (100µg/kg) combined with anti-CD25 (clone PC61.5) at 50µg per mouse injected intraperitoneally depleted regulatory T cells from circulation as measured in spleens of mice 7 days post injection. N=3 mice per group.

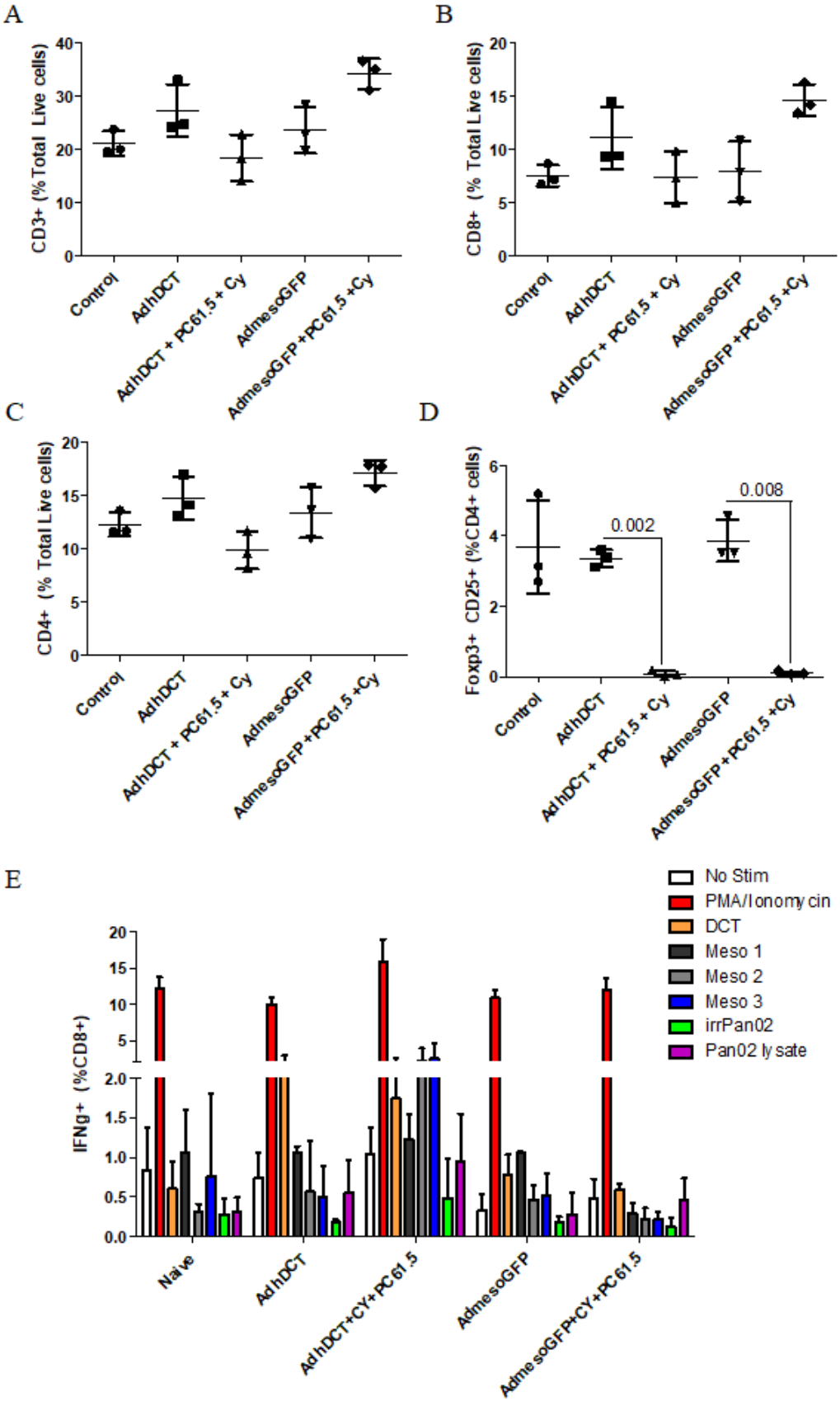
A
CD3+ (% Total Live cells)
0
10
20
30
40
Control
AdhDCT
AdhDCT + PC61.5 + Cy
AdmesoGFP
AdmesoGFP+PC61.5 +Cy
B
CD8+ (% Total Live cells)
0
5
10
15
20
Control
AdhDCT
AdhDCT+ PC61.5 + Cy
AdmesoGFP
AdmesoGFP +PC61.5 +Cy
C
CD4+ (% Total Live cells)
0
5
10
15
20
Control
AdhDCT
AdhDCT + PC61.5 + Cy
AdmesoGFP
AdmesoGFP+PC61.5 +Cy
D
Foxp3+ CD25+ (%CD4+ cells)
0
2
4
6
0.002
0.008
Control
AdhDCT
AdhDCT + PC61.5 + Cy
AdmesoGFP
AdmesoGFP+PC61.5 +Cy
E
IFNg+ (%CD8+)
0.0
0.5
1.0
1.5
2.0
5
10
15
20
No Stim
PMA/Ionomycin
DCT
Meso 1
Meso 2
Meso 3
irrPan02
Pan02 lysate
Naive
AdhDCT
AdhDCT+CY+PC61.5
AdmesoGFP
AdmesoGFP+CY+PC61.5

Figure 19: T_{reg} depletion does not reveal an anti-mesothelin response with AdmesoGFP alone. Mice were depleted of regulatory T cells with low dose cyclophosphamide (100mg/kg) and 50µg of anti-CD25 (PC61.5) and were vaccinated with AdmesoGFP or AdhDCT at 2e8pfu *i.m.* the following day. Splenocytes were collected and analyzed 7 days following vaccination. (A) CD3+, (B) CD8+, (C) CD4+, and (D) CD4+CD25+Foxp3+ cell levels were analyzed within the spleen. An unpaired t-test was performed, n=3 mice per group. (E) Splenocytes were incubated for 5 hours in the presence of brefeldin A with the indicated peptides/stimulation conditions and were stained for IFNγ+ on CD8+ T cells.

after T_{reg} depletion and AdhDCT vaccination was increased, with above background responses against meso 2 and meso 3 peptides being observed at this time point.

Finally, we incorporated a clinically used vaccination strategy known to stimulate mesothelin responses as a control to investigate whether T_{reg} depletion is limiting detection of CD8+ T cell responses. GVAX – a GM-CSF gene transduced tumour cell vaccine – employs the *in vivo* secretion of GM-CSF in the context of presenting irradiated tumour antigens to stimulate T cell responses and has been shown to stimulate mesothelin-specific responses both in humans and in mice[59,106,143,163]. Mice received prime and boost vaccination with AdmesoGFP and MG1meso or two doses of GVAX, with and without the addition of T_{reg} depletion performed one day prior to the first vaccination (Figure 20A). Seven days after receiving the boosting vaccination, mice were euthanized and both regulatory T cell levels and mesothelin-specific CD8+ T cells were measured in the spleen. As expected, the depletion of T_{regs} one day prior to vaccination led to 2-4% of CD8+ T cells responding to mesothelin peptide 2 and 3 in mice receiving GVAX. Similarly, the depletion of T_{regs} cells prior vaccinating with AdmesoGFP + MG1meso led to a significant increase (`2%) in CD8+ T cells secreting IFNγ in response to stimulation with mesothelin peptide 1 (Figure 20C). At this time point – a total of 15 days after the initial T_{reg} depletion – GVAX vaccinated mice were reduced by 60% from the levels observed in naïve mice($p=0.038$) and AdmesoGFP + MG1meso vaccinated mice were reduced by >98%($p=0.0001$) (Figure 20B).

A

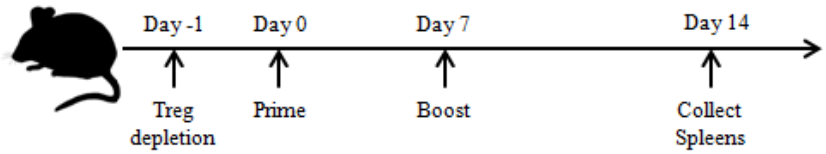
Day -1
Day 0
Day 7
Day 14
Treg depletion
Prime
Boost
Collect Spleens

B

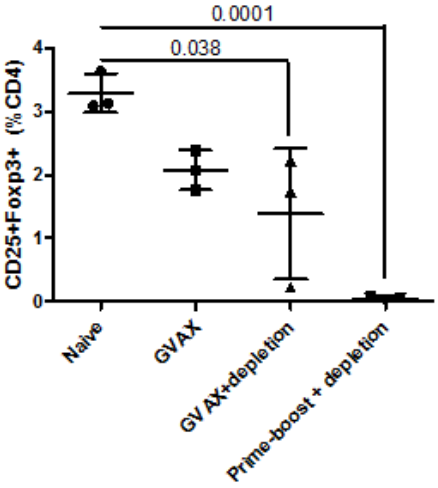
0.0001
0.038
CD25+Foxp3+ (%CD4)
Naive
GVAX
GVAX+depletion
Prime-boost + depletion

C

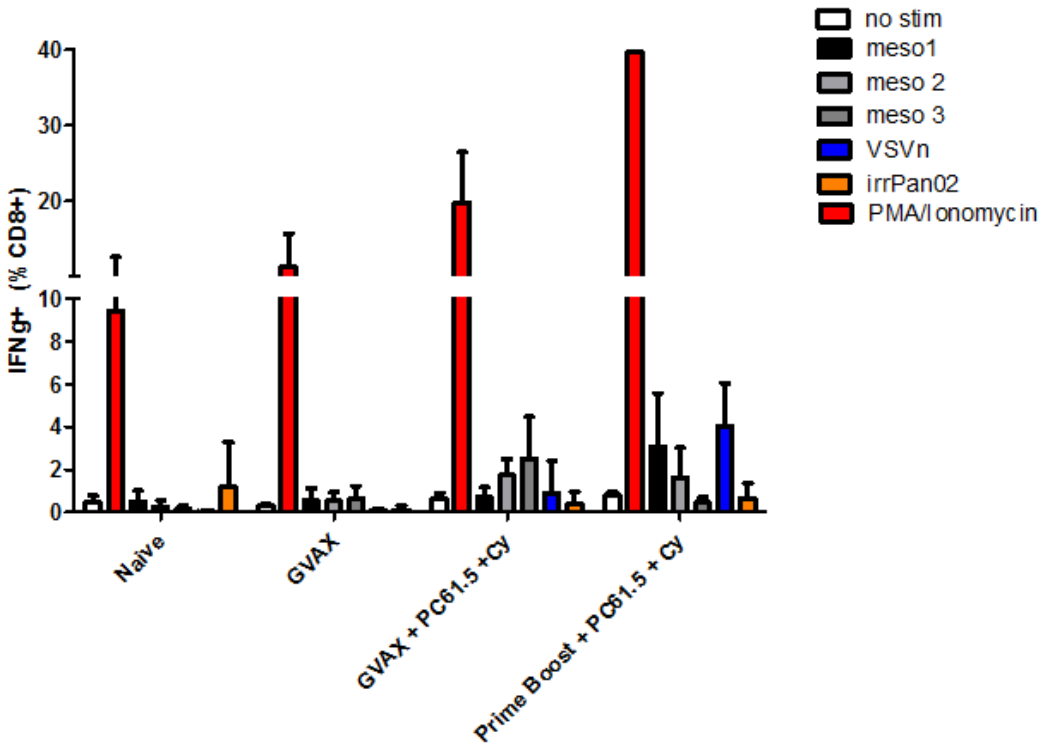
no stim
meso1
meso 2
meso 3
VSVn
irrPan02
PMA/Ionomycin
IFNg+ (% CD8+)
Naive
GVAX
GVAX + PC61.5 + Cy
Prime Boost + PC61.5 + Cy

Figure 20: T_{reg} depletion reveals an anti-mesothelin immune response. Using the established GVAX vaccine (kindly provided by the Jaffee group) as a control, the effects of T_{reg} depletion were investigated in the prime boost setting. (A) A representative timeline of the vaccination strategy. (B) Levels of regulatory T cells (CD3+CD4+CD25+Foxp3+) were measured in the spleen of every mouse at Day 14. (C) Intracellular staining of splenocytes was performed at day 14 after 5 hours of incubation (4hrs in the presence of brefeldin A). Percentage of IFNγ + CD8+ T cells is indicated for each stimulation condition using PMA/Ionomycin as a positive control, and no stimulation as the baseline for each mouse.

3.3.3 Heterologous vaccination promotes IFNγ producing mesothelin-specific CD8+ T cells

When measured at day 14 post T_{reg} depletion, the proportion of T_{regs} in the CD4 fraction was lowest in the AdmesoGFP and MGImeso vaccination group (Figure 21A, p= <0.0001). This led to a significant increase in the number of CD8+ T cells secreting IFNγ in response to stimulation with mesothelin peptide 1 from below 1% to 2% (Figure 21B, p=0.003). Interestingly, the heterologous prime-boost vaccination platforms resulted in the greatest increase in total splenocytes (Figure 21C). This increase in total splenocytes led to no difference between the whole cell and prime-boost vaccination approaches in the total number of mesothelin-specific CD8+ T cells despite the lower percentage of cells (Figure 21D, $1.2x10^5$ vs $2.2x10^5$, p= n.s.).

3.3.4 Mesothelin specific responses can be increased by priming with a GM-CSF secreting whole tumour cell vaccine.

Work by our group and others have demonstrated that cytokine producing whole tumour cell vaccines can elicit significant CD8+ T cell response to tumour antigens [155,164]. However, there have been no published reports investigated the use of this approach in a heterologous vaccination strategy when MG1 is used as a boosting vector. To determine whether this approach may result in stronger mesothelin specific CD8+ T cell responses with a broader antigen repertoire., a variety of possible priming vectors were investigated for the priming potential including: GVAX, AdmesoGFP, irradiated Pan02 cells alone and irradiated Pan02 cells infected with a vaccinia virus encoding murine GM-CSF (JX-594) (Figure 22A) . The overall GM-CSF produced from each prime *in vitro* was measured (Figure 22B), and the depletion of regulatory T cells was confirmed *in vivo* (Figure 22C). Notably, mesothelin specific responses were detected irrespective of the priming strategy used and since a GVAX prime did promote a greater

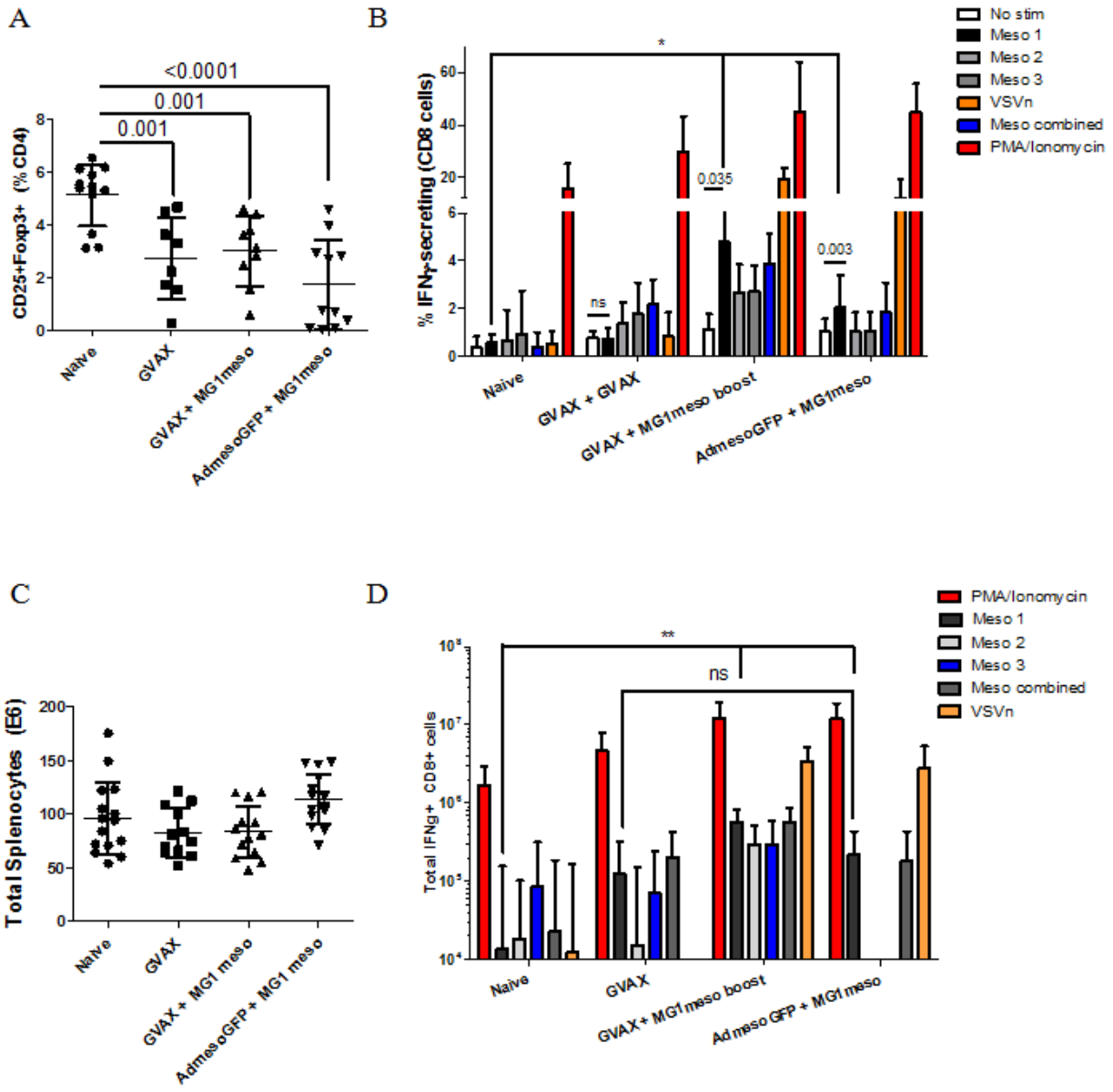
A
<0.0001
0.001
0.001
CD25+Foxp3+ (% CD4)
Naive
GVAX
GVAX + MG1meso
AdmesoGFP + MG1meso
B
No stim
Meso 1
Meso 2
Meso 3
VSVn
Meso combined
PMA/Ionomycin
% IFNγ-secreting (CD8 cells)
*
0.035
ns
0.003
Naive
GVAX + GVAX
GVAX + MG1meso boost
AdmesoGFP + MG1meso
C
Total Splenocytes (E6)
Naive
GVAX
GVAX + MG1 meso
AdmesoGFP + MG1 meso
D
PMA/Ionomycin
Meso 1
Meso 2
Meso 3
Meso combined
VSVn
Total IFNg+ CD8+ cells
**
ns
Naive
GVAX
GVAX + MG1meso boost
AdmesoGFP + MG1meso

Figure 21: Prime-boost vaccination leads to similar numbers of total anti-mesothelin CD8+ T cells as the standard vaccination strategy. Following the same vaccination strategy as previously used, mice were sacrificed at day 14 and spleens were collected. All treatment groups were T_{reg} depleted using anti-CD25 and low dose cyclophosphamide. (A) Total regulatory T cells present in mouse spleens at day 14. (B) Percent IFNγ+ CD8+ T cells after stimulation with mesothelin peptides. (C) Total live splenocytes present in each treatment group, as calculated by trypan blue exclusion on a VICELL cell counter. (D) Total number of anti-mesothelin CD8+ T cells in the spleen over baseline, calculated using the percentage of IFNγ+ cells and the toal number of splenocytes . All data is pooled data from 3 separate experiments, n=5 mice per group for each run.

A

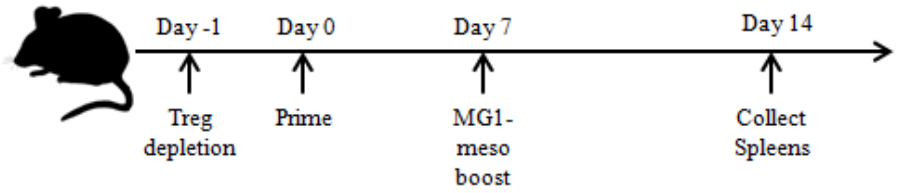
Day -1
Day 0
Day 7
Day 14
Treg depletion
Prime
MG1-meso boost
Collect Spleens

B

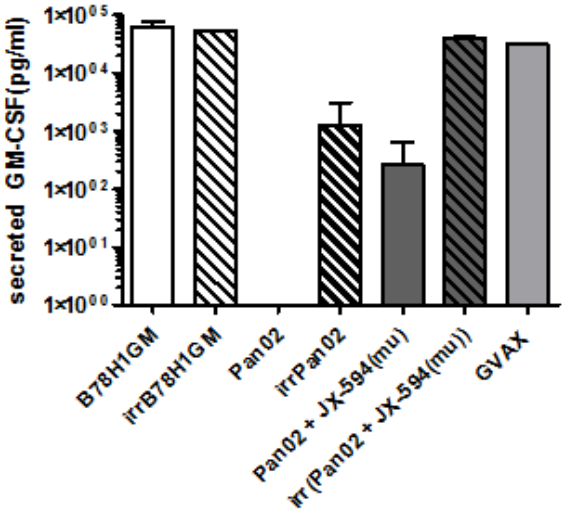
secreted GM-CSF(pg/ml)
1x10^05
1x10^04
1x10^03
1x10^02
1x10^01
1x10^00
B78H1GM
irrB78H1GM
Pan02
irrPan02
Pan02 + JX-594(mu)
irr(Pan02 + JX-594(mu))
GVAX

C

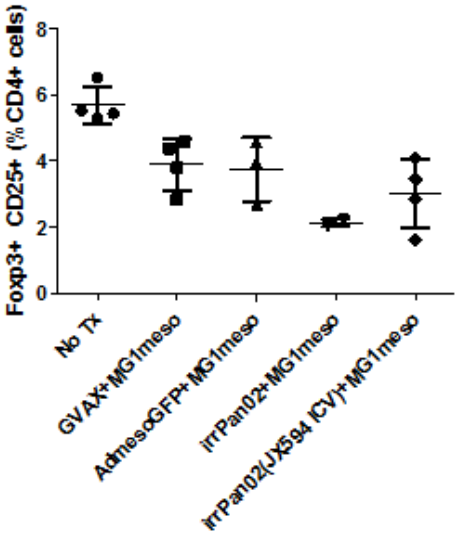
Foxp3+ CD25+ (% CD4+ cells)
8
6
4
2
0
No Tx
GVAX+MG1meso
AdmesoGFP+MG1meso
irrPan02+MG1meso
irrPan02(JX594 ICV)+MG1meso

D

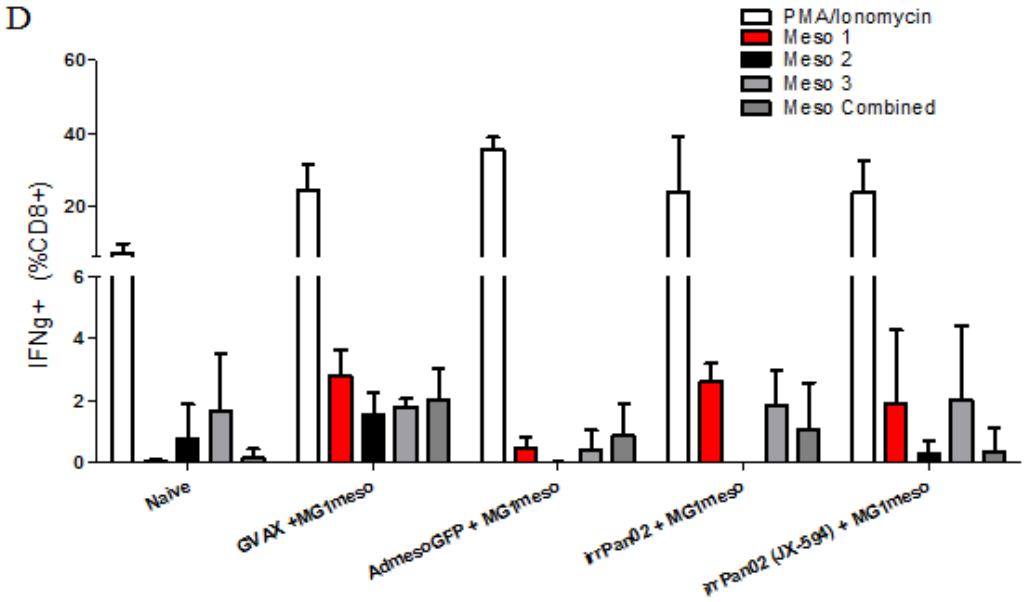
PMA/Ionomycin
Meso 1
Meso 2
Meso 3
Meso Combined
IFNg+ (%CD8+)
60
40
20
6
4
2
0
Naive
GVAX +MG1meso
AdmesoGFP + MG1meso
irrPan02 + MG1meso
irrPan02 (JX-594) + MG1meso

Figure 22: GM-CSF contributes to a better prime for an anti-mesothelin response *in vivo*. (A) Timeline of the vaccination strategy, where all groups are boosted with 1e8pfu of MG1meso at day 7. (B) Measuring secreted GM-CSF of various priming strategies. Cells were treated as indicated (irradiation performed at 60Gy, any infections performed at an MOI of 10 for 2 hours), and then plate at 1e6 cells per well in a 6 well dish for 18hrs. Supernatants were collected, and frozen at -20°C before being quantified by solid-phase sandwich ELISA. GVAX, JX594 ICV ad irrPan02 as a control were used as priming vectors in a vaccination experiment. At day 14, spleens were collected, dissociated and stained or stimulated and stained for intracellular cytokine production. (C) Regulatory T cells (CD3+CD4+CD25+Foxp3+ cells) were measured to confirm depletion in all the groups. (D) Percentage of IFNγ + CD8+ T cells is indicated for each stimulation condition after 5-hour stimulation with each indicated mesothelin peptide, or a pool of the three peptides. PMA/Ionomycin was used as a positive control, and no stimulation as the baseline for each mouse.

response to multiple mesothelin peptides, similarly to that achieved with AdmesoGFP priming this approach was used in subsequent studies as a secondary positive control (Figure 22D).

3.4 Heterologous prime-boost vaccination induces mesothelin reactive T cells with cytotoxic activity

3.4.1 Heterologous prime boost induces tumour reactive CD8+ T cells.

The previous work characterizing mesothelin reactive CD8+ T cells were performed using peptide pulsed splenocytes however it is necessary to determine whether CD8+ T cells are similarly reactive to the TAA processed and presented directly by the tumour cells themselves. Although Pan02 cells express mesothelin, the lack of MHCI expression *in vitro* prevents recognition and binding to CD8+ T cells (Figure 23A left). However, stimulation with IFNγ for 18hrs is sufficient to upregulate MHC I expression (Figure 23B). Culturing splenocytes with IFNγ-stimulated Pan02 cells resulted in a significant increase in the percentage of IFNγ+CD8+ T cells in AdmesoGFP+MG1meso compared to control mice (Figure 23C, $p=0.03$) indicating that this vaccination strategy is capable of inducing tumour reactive T cell responses.

3.4.2 CD8+ T cells generated from vaccination with AdmesoGFP and MG1meso are cytotoxic

IFNγ production from CD8+ T cells indicates specificity and activation in the presence of target peptide but does not always correspond to a cytotoxic response[165,166]. Therefore, to directly assess the functional activity *in vivo* cytotoxicity assay was performed as described in the methods (Figure 24A). Briefly, splenocytes were harvested 18 hr after animals received differentially labelled splenocytes pulsed with or without the indicated peptides (Figure 24B, left = naïve; middle = VSVn peptide; right = mesothelin peptide). Quantification of the fluorescently labelled splenocytes populations 18 hrs after iv injection revealed that nearly 100% of the VSVn peptide-pulsed splenocytes were killed in mice receiving a MG1meso boost which is consistent

A

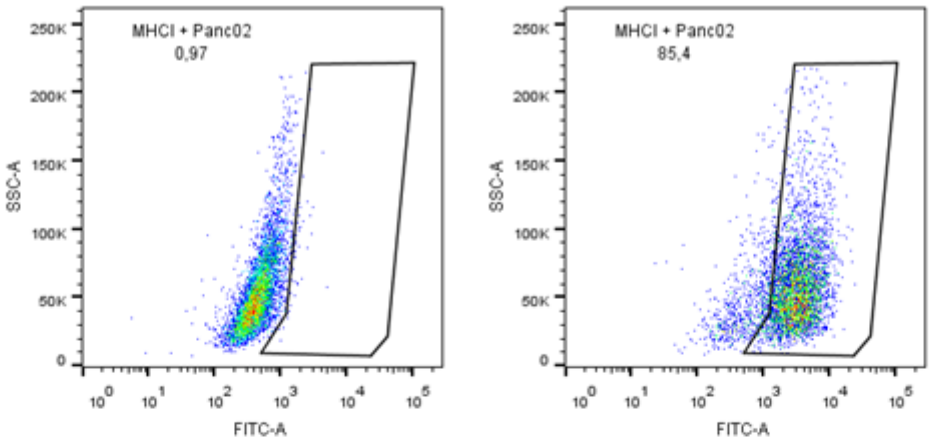
MHCI + Panc02
0,97
MHCI + Panc02
85,4
SSC-A
FITC-A

B

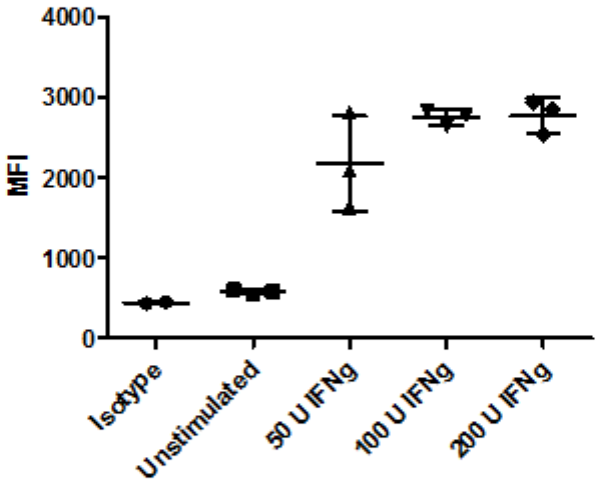
MFI
Isotype
Unstimulated
50 U IFNg
100 U IFNg
200 U IFNg

C

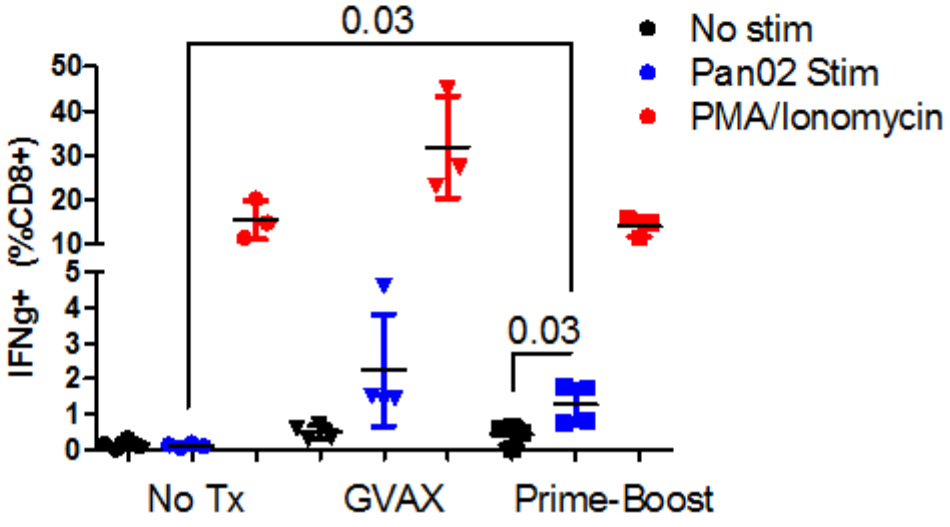
0.03
0.03
No stim
Pan02 Stim
PMA/Ionomycin
IFNg+ (%CD8+)
No Tx
GVAX
Prime-Boost

Figure 23: AdmesoGFP + MG1meso vaccination leads to tumour-specific immunity. (A**)** At baseline, Pan02 cells do not express MHC I (left), but IFNγ stimulation upregulates its expression (right). Representative flow plots. (B) Optimization of IFNγ stimulation dose on Pan02 cells. (C) Proportion of CD8+ cells secreting IFNγ in response to Pan02 stimulation. t-tests were used to calculate significance, with n=4 mice per group.

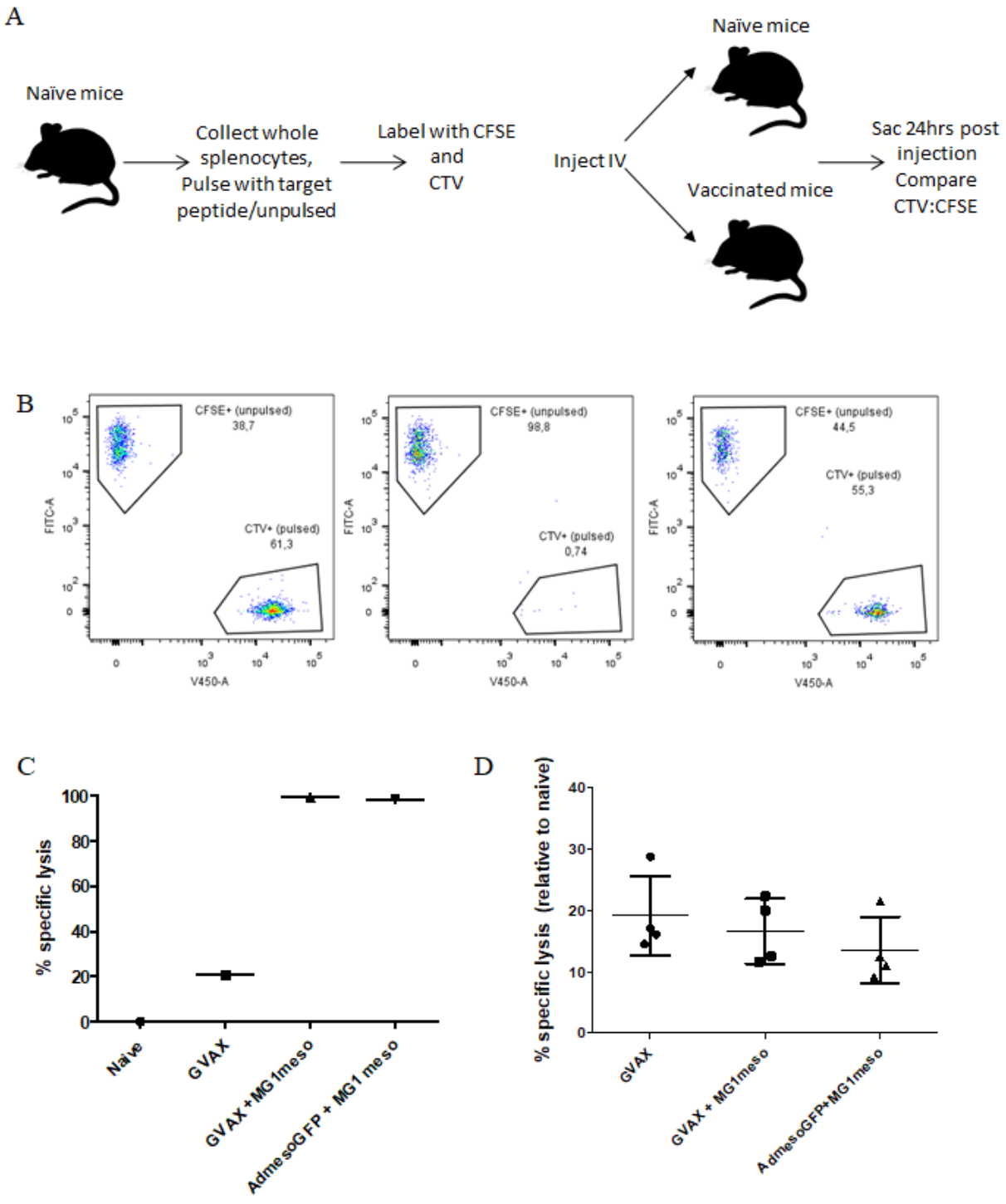
A
Naïve mice
Collect whole splenocytes, Pulse with target peptide/unpulsed
Label with CFSE and CTV
Inject IV
Naïve mice
Vaccinated mice
Sac 24hrs post injection Compare CTV:CFSE
B
CFSE+ (unpulsed) 38,7
CTV+ (pulsed) 61,3
CFSE+ (unpulsed) 98,8
CTV+ (pulsed) 0,74
CFSE+ (unpulsed) 44,5
CTV+ (pulsed) 55,3
FITC-A
V450-A
C
% specific lysis
Naïve
GVAX
GVAX+MG1meso
AdmesoGFP + MG1meso
D
% specific lysis (relative to naive)
GVAX
GVAX + MG1meso
AdmesoGFP+MG1meso

Figure 24: Prime-boost vaccination leads to *in vivo* cytotoxic CD8+ T cells. (A) Methodology of an *in vivo* CTL assay. (B) Representative flow plots gated on stained splenocytes. The proportion of peptide-pulsed CellTrace Violet stained splenocytes is compared to unpulsed CFSE stained splenocytes in naïve mice (left) vs vaccinated mice (middle and right). Almost complete elimination can be observed with the VSVn peptide (middle) as compared to partial killing of the mesothelin 1 peptide (right) after 18hrs *in vivo*. (C) The percent specific lysis was calculated against the VSVn peptide in vaccinated mice. (D) The percent specific lysis of vaccinated mice against the meso 1 peptide over that of naïve mice. N=4 per group.

with an anti-viral response (Figure 24C). In addition, specific lysis of mesothelin peptide-pulsed splenocytes ranged from 10-20% relative to naïve mice with all three vaccination strategies (Figure 24D).

3.4.3 Immune cells are recruited to the tumour microenvironment in vaccinated mice

Together these findings demonstrate that a prime boost vaccination strategy can induce mesothelin reactive CD8+ T cells capable of recognizing Pan02 tumour cells *in vitro*. Next, I sought to determine whether vaccination would result in the recruitment of tumour reactive cells to the tumour in vivo. To investigate this possibility Pan02 cells embedded within Cultrex™ were implanted subcutaneously. Three days following injection, the plugs were surgically excised, dissociated and analyzed by flow cytometry. Consistent with my previous findings in orthotopic Pan02 tumours CD45+ cells were recruited to the implanted plugs in all of the groups however distinct differences in the phenotype of these cells were observed between the groups. In particular, a large population of CD45+ cells with high side scatter were present in mice receiving GVAX compared to prime-boost vaccinated mice (Figure 25A, representative dot plots). Although the total number and relative proportion of CD3+ cells were increased in vaccinated mice, the GVAX response included a relatively larger CD4+ response in comparison to prime-boost mice which exhibited an increased CD8+ T cells (Figure 25B-F).

Finally, the recruitment of immune cells to two different tumours was compared in the same mouse. Mice received plugs embedded with MC38 cells – a colorectal cancer line- on one flank, and on the other they received the Pan02 plugs. Interestingly, vaccination with GVAX did lead to recruitment of a variety of immune cells in both MC38 and Pan02 plugs though the numbers of recruited lymphocytes and dendritic cells was increased in Pan02 plugs. Prime-boost

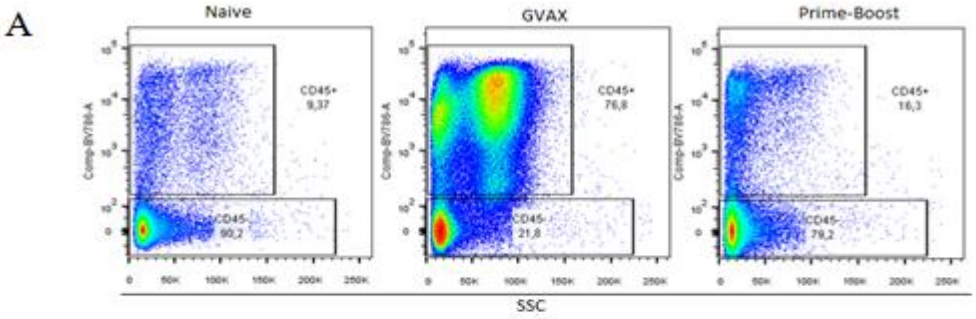
A
Naive
GVAX
Prime-Boost
CD45+
9,37
CD45-
90,2
CD45+
76,8
CD45-
21,8
CD45+
16,3
CD45-
79,2
SSC

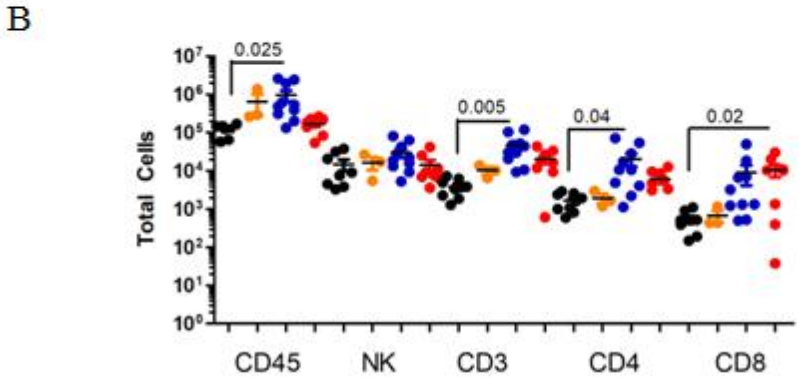
B
Total Cells
0.025
0.005
0.04
0.02
CD45
NK
CD3
CD4
CD8

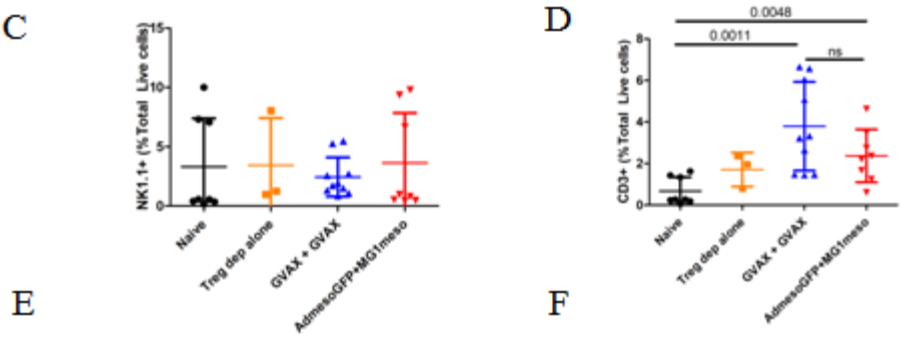
C
NK1.1+ (% Total Live cells)
D
CD3+ (% Total Live cells)
0.0048
0.0011
ns
Naive
Treg dep alone
GVAX + GVAX
AdmesoGFP+MG1meso

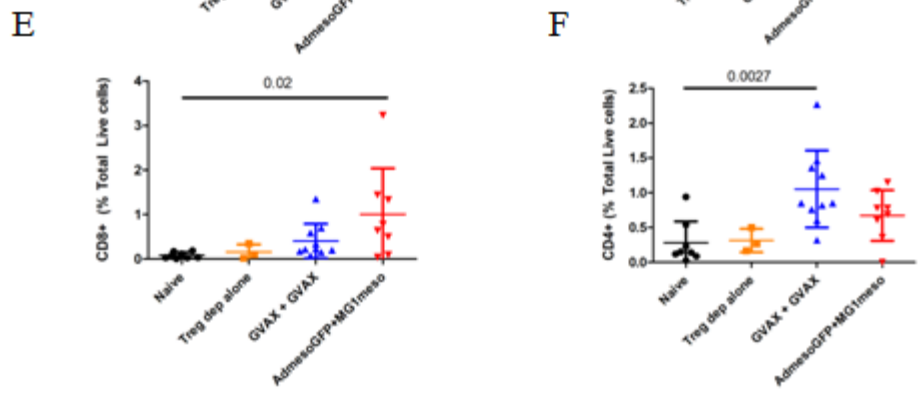
E
CD8+ (% Total Live cells)
0.02
F
CD4+ (% Total Live cells)
0.0027
Naive
Treg dep alone
GVAX + GVAX
AdmesoGFP+MG1meso

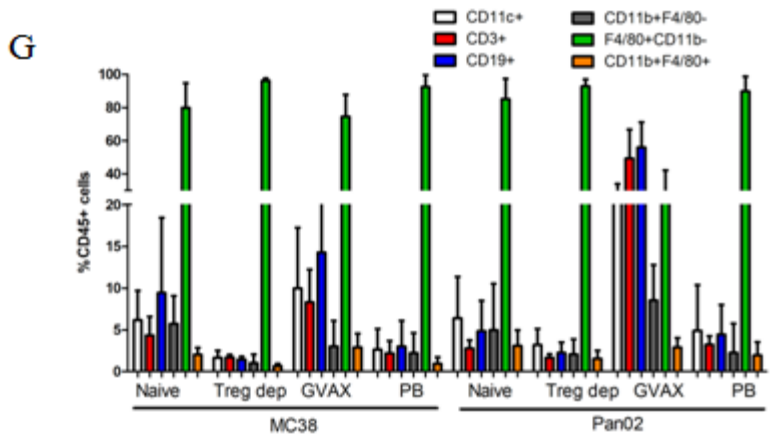
G
CD11c+
CD3+
CD19+
CD11b+F4/80-
F4/80+CD11b-
CD11b+F4/80+
%CD45+ cells
Naive
Treg dep
GVAX
PB
MC38
Pan02

Figure 25: Prime-boost vaccination leads to the recruitment of CD8+ T cells at the site of tumour challenge. (A) Total number of CD45+ cells and select lymphocyte populations to the Cultrex™ plug after three days in naïve (black), T_{reg} depleted alone (orange), GVAX (blue) and prime-boost (red) mice. The proportion of various CD45 positive subsets was characterized within the plugs including (B) NK1.1+CD3- cells, (C) NK1.1-CD3+ cells, (D) CD3+CD8+ cells and (E) CD3+CD4+ cells. (F) Vaccinated mice were injected with two plugs. On the right flank they received plugs embedded with MC38 cells, and on the left flank they received plugs embedded with the target Pan02 cells. After three days, plugs were excised and the CD45 immune infiltrate was investigated include both lymphocytic (CD3, CD19, NK1.1) and leukocytic populations.

vaccinated mice only did not show increased recruitment of CD45+ cells in the MC38 plug unlike the whole cell vaccine approach (Figure 25G) indicating that the anti-mesothelin immune response did not result in spreading to the colorectal cancer with this vaccination strategy.

Overall my investigations in Aim 2 led to the development of a viral backbone with a similar phenotype to its parental MG1 virus. Unlike with the published heterologous prime-boost model that employs the xenoantigen hDCT, targeting the self-antigen mesothelin requires the depletion of regulatory T cells prior to vaccination, and results in an attenuated 2-4% mesothelin specific population as opposed to the greater than 40% expansion observed against hDCT. The CD8+ T cells induced with this vaccination strategy are able to recognize and lyse splenocytes loaded with mesothelin peptide at similar levels as a whole cell vaccine, and furthermore recognize the target Pan02 cells *in vitro* and are recruited to Pan02 challenge.

3.5 The prime-boost vaccine does not provide protection from tumour challenge

3.5.1 Prime-boost vaccination with T_{reg} depletion performs similarly to T_{reg} depletion alone in protecting mice from Pan02 tumour challenge

Having established the efficacy of the prime-boost vaccination strategy in promoting mesothelin reactive CD8+ T cells I next sought to determine whether this response could control tumour growth *in vivo*. Importantly no efficacy beyond the effects of depleting T_{reg} cells alone was observed when vaccinated animals were challenged with $2.5x10^5$ Pan02 cells subcutaneously at the peak T cell response as outlined in Figure 26A. Tumours consistently grew in naïve mice (19/25) with the majority succumbing to tumour outgrowth within 100 days of challenge (Figure 26B). In contrast both GVAX and GVAX boosted with MG1meso afforded total protection from tumour challenge whereas the prime-boost vaccination protected only 53% of the challenged mice (Figure 26B). While this was encouraging, depletion of T_{regs} alone resulted in similar levels

A

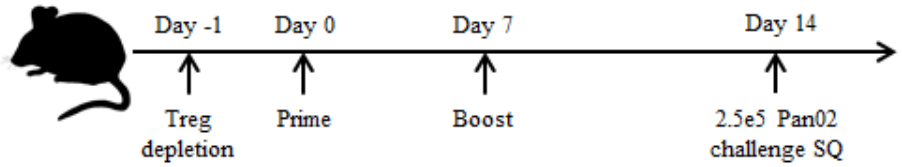
Day -1
Day 0
Day 7
Day 14
Treg depletion
Prime
Boost
2.5e5 Pan02 challenge SQ

B

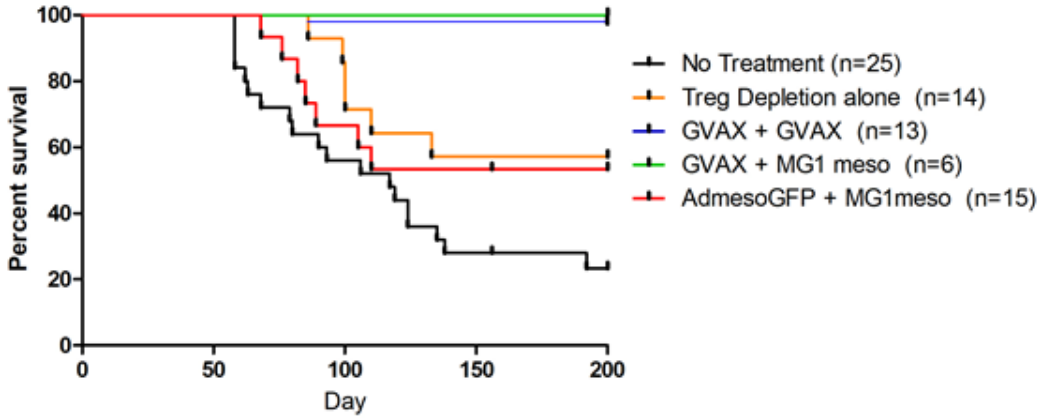
Percent survival
Day
No Treatment (n=25)
Treg Depletion alone (n=14)
GVAX + GVAX (n=13)
GVAX + MG1 meso (n=6)
AdmesoGFP + MG1meso (n=15)

C

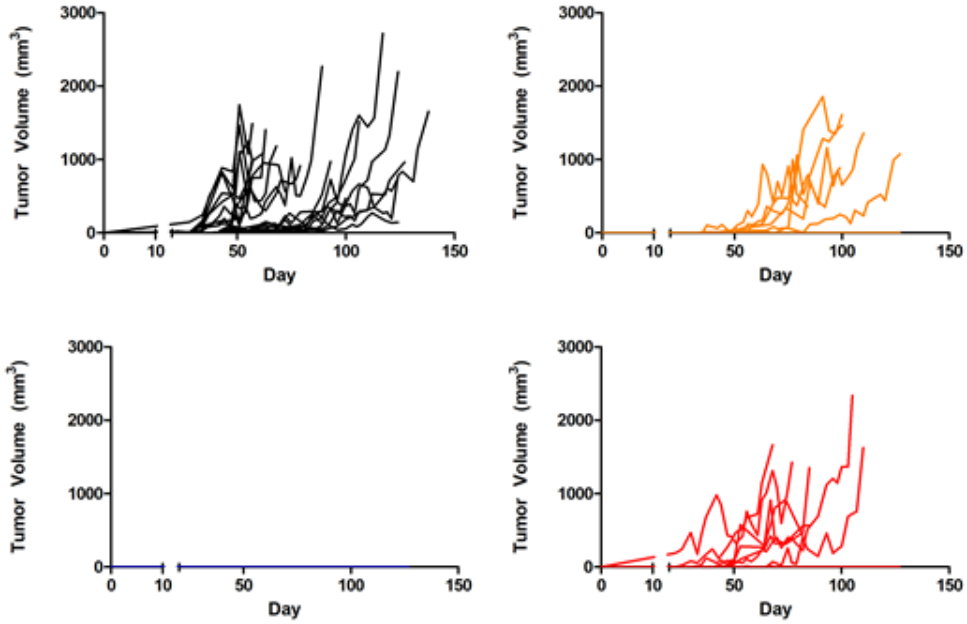
Tumor Volume (mm3)
Day

Figure 26: **Mesothelin vaccination demonstrates no efficacy in protecting mice from Pan02 challenge.** (A) Timeline of vaccination strategy. Briefly mice were depleted of regulatory T cells with 50µg anti-CD25 (PC61.5) and low dose cyclophosphamide followed by prime with either AdmesoGFP *i.m.* (2e8pfu) or GVAX *s.c.* in both hind limbs and a boost 7 days later of either MG1meso *i.v.* (1e8 pfu) or GVAX *s.c.* in both hind limbs. (B) Survival of mice challenged with 2.5e5 Pan02 cells *s.q.* Pooled data, n values as marked. (C) Tumour volume of mice was measured 3 times per week. All naïve mice (black), T_{reg} dep alone (orange), GVAX + GVAX (blue) and AdmesoGFP + MG1meso (red) are shown.

of protection (Figure 26C) indicating that the mesothelin specific immune responses observed in vaccinated animals are ineffective in preventing tumour growth.

However, the vaccinated animals that were protected from the initial tumour challenge were protected from a subsequent re-challenge with Pan02 cells whereas the naive mice were not (Figure 27). This continued rejection of re-challenge indicates that all three treatments provided long lasting memory T cell responses whereas in unvaccinated animals, spontaneous tumour rejection without generation of long-lasting immune memory occurred.

3.5.2 Tumour intrinsic escape mechanisms do not limit efficacy of the prime boost strategy.

Adaptive immune resistance, the mechanism by which cancer is recognized by the immune system but is able to protect itself to immune attack[19], could be a leading cause of the lack of efficacy observed after prime-boost vaccination. To investigate the role that tumour cell intrinsic mechanisms of primary and adaptive resistance to immunotherapy play in the anti-mesothelin vaccination platform, tumours were collected at endpoint and processed for analysis by flow cytometry, IHC, and RT-qPCR. MHC class I presentation of antigens is crucial for T cell recognition of antigens, and is a common escape mechanism of human tumours[167,168]. Although Pan02 cells do not express MHC class I *in vitro* (See Figure 23A) expression of MHCI in vivo was confirmed by flow cytometry (Figure 28A) and IHC (Figure 28B) with almost 50% of tumour cells staining positively at endpoint (Figure 28C, $p=0.0001$). Consistent with this finding MHCI expression is observed as early as 3 days following implantation *in vivo* as measured in Cultrex© was sufficient to upregulate MHC class I on tumour cells (Figure 28C).

In addition, RT-qPCR analysis of paraffin embedded tissue revealed that mesothelin is still expressed in the tumour tissue suggesting that the expression of the TAA was not down regulated to limit its presentation and recognition by CD8+ T cells following immunotherapy. (Figure 29).

A

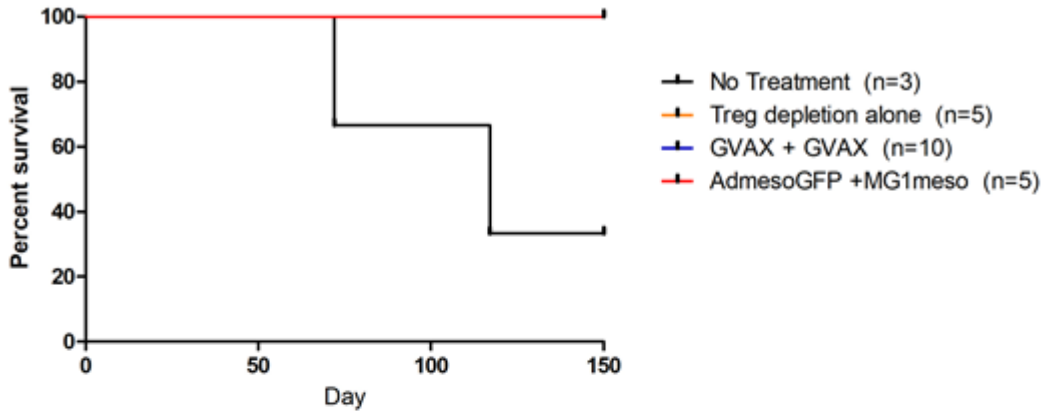
Percent survival
100
80
60
40
20
0
0
50
100
150
Day
No Treatment (n=3)
Treg depletion alone (n=5)
GVAX + GVAX (n=10)
AdmesoGFP +MG1meso (n=5)

B

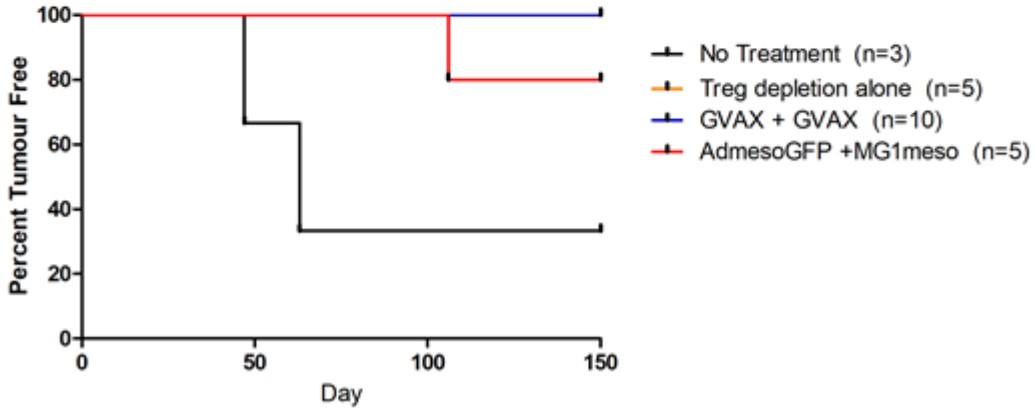
Percent Tumour Free
100
80
60
40
20
0
0
50
100
150
Day
No Treatment (n=3)
Treg depletion alone (n=5)
GVAX + GVAX (n=10)
AdmesoGFP +MG1meso (n=5)

Figure 27: Mice protected from an initial Pan02 challenge show long term protection from Pan02 challenge. Mice that were tumour free >200 days after an initial challenge of 2.5e5 Pan02 tumours were considered to have rejected an initial challenge. These mice were then re-challenged with 2.5e5 Pan02 cells in the flank and measured for continued protection from tumour challenge. (A) Survival and (B) Percent tumour rejection are shown.

A

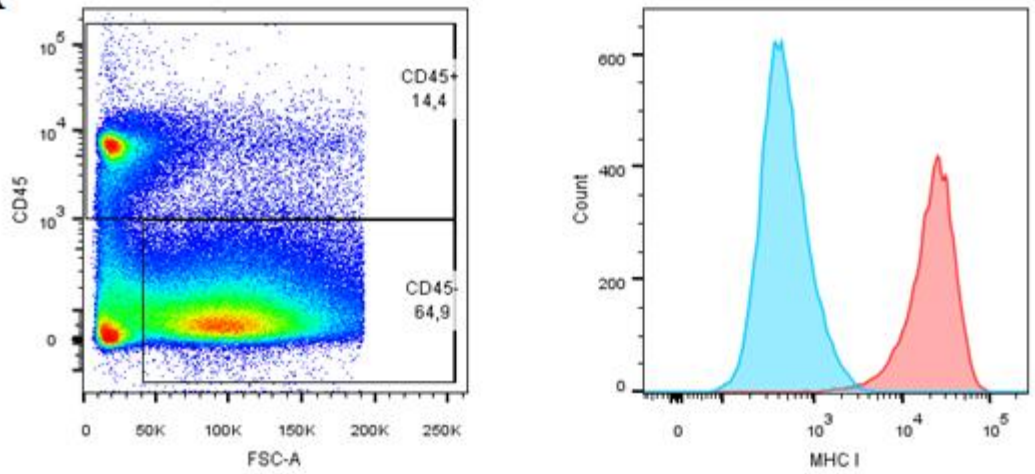
CD45+
14,4
CD45-
64,9
CD45
FSC-A
Count
MHC I

B

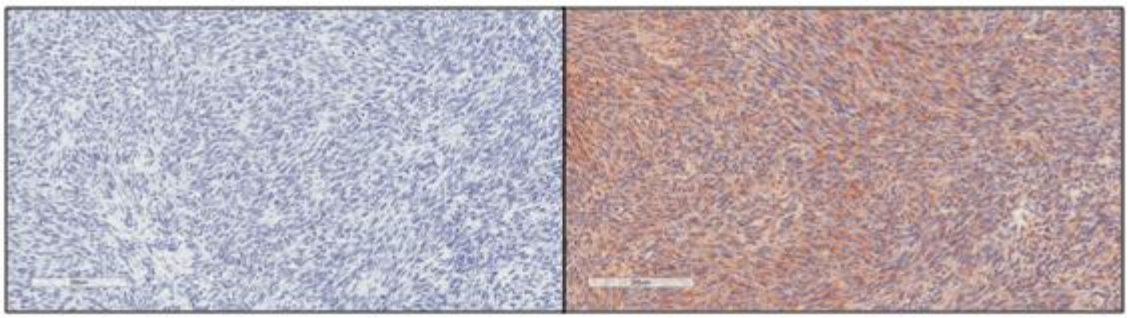

C

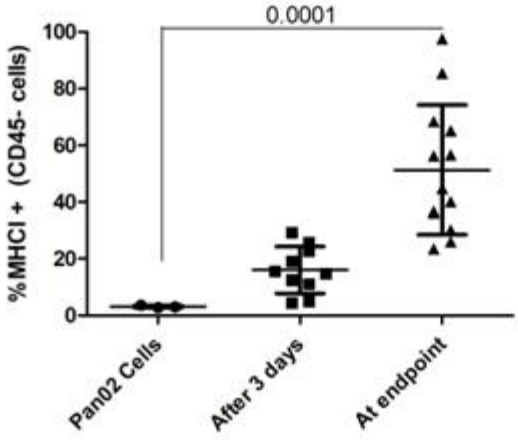
0.0001
% MHCI + (CD45- cells)
Pan02 Cells
After 3 days
At endpoint

Figure 28: Pan02 tumours upregulate MHC I expression *in vivo*. (A) Gating strategy for Pan02 tumours. Light blue = isotype, red = MHCI (B) IHC of MHCI expression in Pan02 tumours at endpoint. Left unstained uncontrol, right MHC I stain. Magnification 200X. (C) CD45- high granular cells were stained with isotype of MHC I antibody. The percentage of cells that are MHC I positive are indicated as measured *in vitro,* 3 days post injection and at endpoint. A one-way Anova with Dunnett's post hoc test compared to control was used for statistical analysis. P-value is stated.

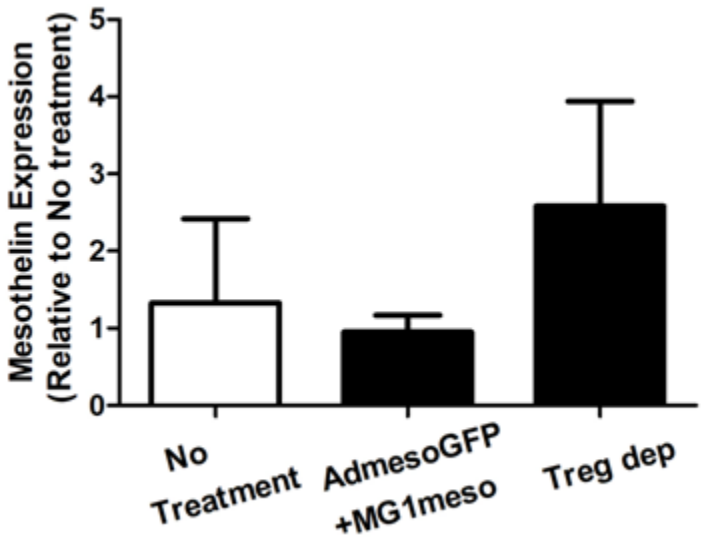
Mesothelin Expression
(Relative to No treatment)
5
4
3
2
1
0
No Treatment
AdmesoGFP +MG1meso
Treg dep

Figure 29: Mesothelin expression is not downregulated over time. mRNA was extracted from paraffin embedded tumour samples collected at endpoint. A qPCR was performed, and mesothelin levels were normalized to GAPDH and β-Actin internal housekeeping genes. Fold change over an untreated Pan02 tumour is indicated.

Together these findings suggest that tumour outgrowth is not due to tumour intrinsic factors which limit immune recognition indicating that adaptive resistance may be a contributing factor[19] or the immune response stimulated was not sufficient to fully protect against Pan02 challenge.

3.5.3 Depletion of regulatory populations cannot rescue the efficacy of the prime-boost vaccination

A second key mechanism of adaptive resistance to immunotherapy involves tumour cell extrinsic factors, such as the recruitment of immunosuppressive cells to the TME[19]. As T_{regs} are depleted in this model, other immunosuppressive subsets were investigated. In Aim 1 I established that both B cells and MDSCs were recruited to the Pan02 TME, so these two subsets were identified as potentially responsible for limiting the effects of the vaccine on tumour outgrowth. However, a combined depletion of both B and MDSC cells with (Figure 30A and B) did not impact overall survival or the rate of tumour outgrowth in each vaccination group (Figure 30C and D).

3.5.4 CD8+ T cells do not contribute to tumour control in mice receiving the prime-boost vaccine

Although vaccination with AdmesoGFP + MG1meso leads to the development of CD8+ T cells that can recognize tumour cells which are recruited to the site of tumour challenge there is no impact on survival over T_{reg} depletion alone. To confirm that CD8+ T cells are unable to provide protection against Pan02 tumour challenge CD8+ T cells were depleted prior to tumour challenge. The complete depletion of circulating CD8+ T cells (Figure 31A) had no overall effect on survival rates of mice receiving either the prime-boost or GVAX (Figure 31B). However, differences in the tumour outgrowth were observed in the absence of CD8+ T cells

A

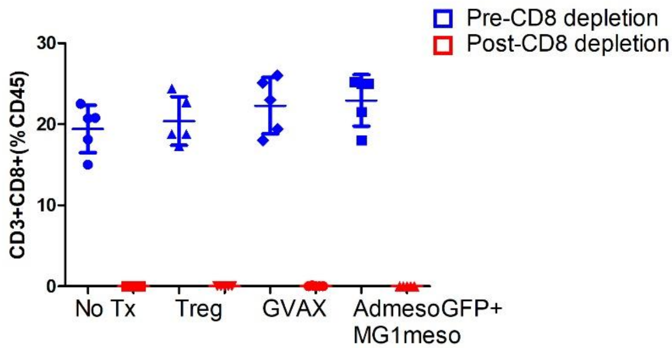
Pre-CD8 depletion
Post-CD8 depletion
CD3+CD8+(%CD45)
30
20
10
0
No Tx
Treg
GVAX
AdmesoGFP+
MG1meso

B

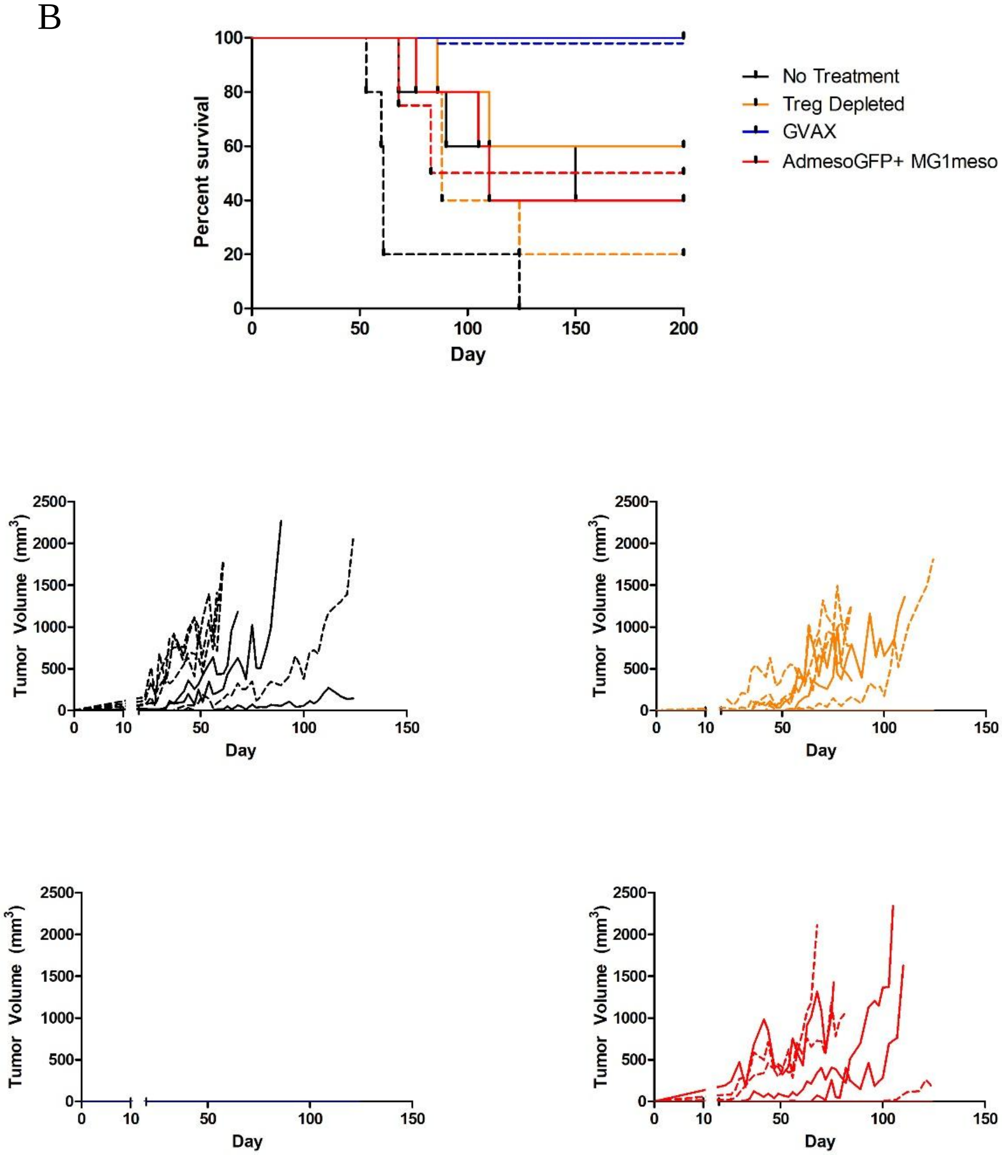
Percent survival
100
80
60
40
20
0
0
50
100
150
200
Day
No Treatment
Treg Depleted
GVAX
AdmesoGFP+ MG1meso
Tumor Volume (mm3)
2500
2000
1500
1000
500
0
0
10
50
100
150
Day

Figure 30: Depletion of regulatory populations does not increase efficacy of vaccination. Following vaccination, mice were depleted of B cells and MDSCs through the *i.v.* injection of anti-CD20 (200µg, clone SA271G2) and the *i.p.* injection of anti-GR1 (100µg, clone RB6-8C5) one day prior to tumour challenge. Depletion was maintained throughout the experiment following tumour challenge with twice weekly injections of anti-GR1, and injections of anti-CD20 every 20 days. (A) The depletion of CD19+ cells was confirmed 1 day and 1 week post depletion in blood. (B) The depletion of Ly6GhiLy6Clo cells was observed one day and one week following initial depletion of GR1+ cells. (C) Survival of mice is indicated, with dash lines indicating depleted mice as compared to non-depleted controls. (D) Tumour outgrowth of individual mice is indicated. N=5 per group.

A

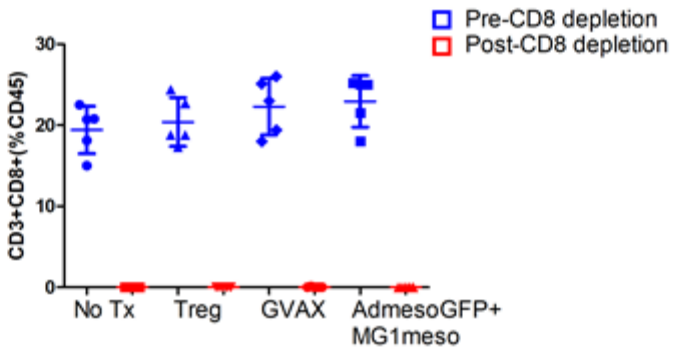
Pre-CD8 depletion
Post-CD8 depletion
CD3+CD8+(%CD45)
30
20
10
0
No Tx
Treg
GVAX
AdmesoGFP+ MG1meso

B

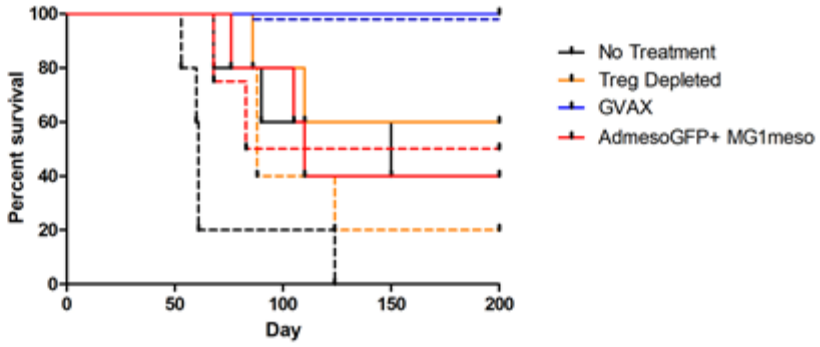
Percent survival
100
80
60
40
20
0
0
50
100
150
200
Day
No Treatment
Treg Depleted
GVAX
AdmesoGFP+ MG1meso

C

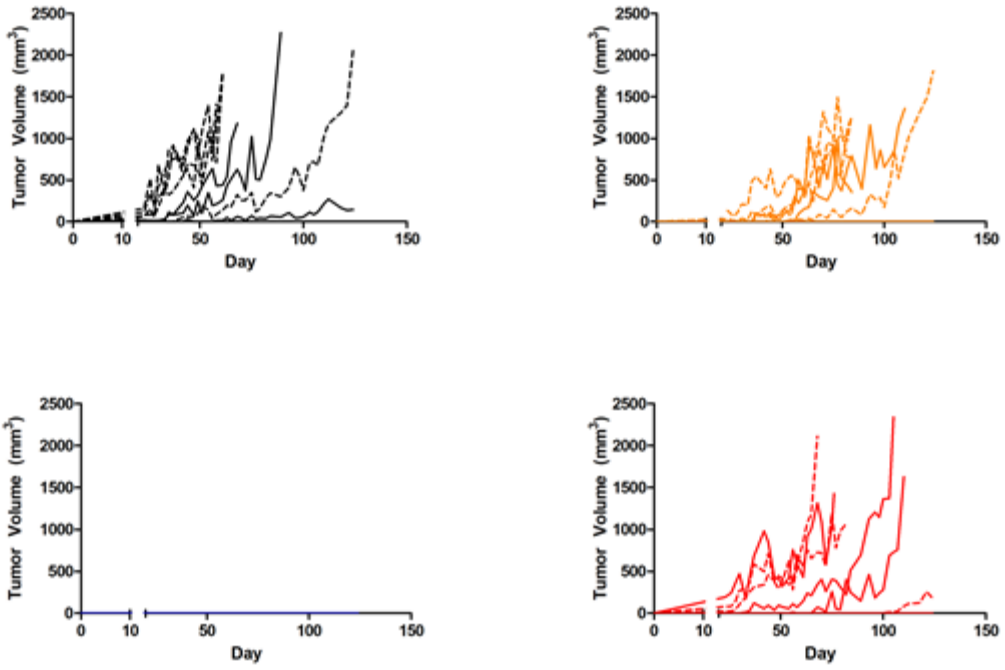
Tumor Volume (mm3)
2500
2000
1500
1000
500
0
0
10
50
100
150
Day

Figure 31: CD8 depletion does not decrease the efficacy of AdmesoGFP+MG1meso vaccination at protecting mice from tumour challenge. Following vaccination, mice were depleted of CD8+ T cells through the *i.p.* injection of anti-CD8α (100ug, clone 2.43) at days -1, -2 and +1 surrounding tumour challenge. Depletion was maintained throughout the experiment following tumour challenge with weekly injections of antibody. (A) The depletion of CD8+ T cells was confirmed by examining the CD8+ cells in circulating blood. (B) Survival of mice is indicated, with dash lines indicating CD8 depleted mice as compared to non-depleted controls. (C) Tumour outgrowth of individual mice is indicated.

with naïve mice depleted of CD8+ T cells developing tumours sooner (Figure 32A and B). In contrast, while there were differences in the timeline for tumour outgrowth based on the presence or absence of CD8+ T cells, there was still no observable difference between T_{reg} depletion alone, or T_{reg} depletion with AdmesoGFP+MG1meso, in which mean tumour outgrowth in the absence of effector T cells was similar over time (Figure 32C), lending further evidence to the essential role of T_{regs} during tumour seeding but no efficacy from the anti-mesothelin T cells.

3.6 Vaccination with an oncolytic prime boost targeting mesothelin shows no efficacy against other mesothelin expressing cancers

3.6.1 Colorectal and pancreatic cancers express mesothelin

To determine whether the ineffective response was restricted to Pan02 tumours or is reflective of a broader defect in mesothelin reactive CD8+ T cells in controlling tumour growth I attempted to identify other mesothelin expressing cell lines. Although neither of the two melanoma lines – B16 and B78H1GM – were found to express mesothelin, all peritoneal cancers including a colorectal cancer line (MC38), a second pancreatic cancer (TH04) and two ovarian cancers (ID8 and STOSE) expressed high levels of mesothelin *in vitro,* with both MC38 and TH04 expressing mesothelin at higher levels than Pan02 cells (Figure 33).

3.6.2 No efficacy is observed against the aggressive, fast-growing PDAC line TH04

The vaccination protocol was repeated in the second PDAC murine model – TH04 – that also expressed mesothelin. The mice were vaccinated as previously described except GVAX was prepared using irrB78H1GM cells in a 1:1 ratio with irrTH04 cells. In contrast to the Pan02 model, TH04 tumours grow quickly and no protection from tumour challenge was observed with any vaccination strategy, including GVAX (Figure 34A and B).

A

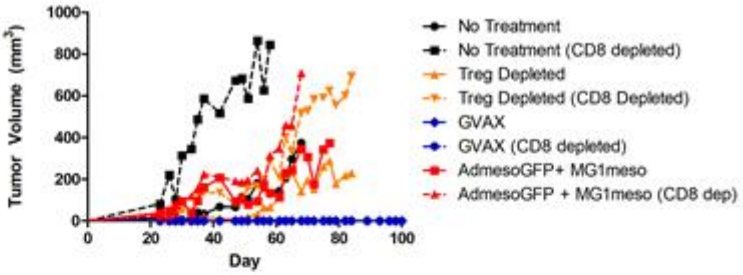
Tumor Volume (mm³)
1000
800
600
400
200
0
0
20
40
60
80
100
Day
No Treatment
No Treatment (CD8 depleted)
Treg Depleted
Treg Depleted (CD8 Depleted)
GVAX
GVAX (CD8 depleted)
AdmesoGFP+ MG1meso
AdmesoGFP + MG1meso (CD8 dep)

B

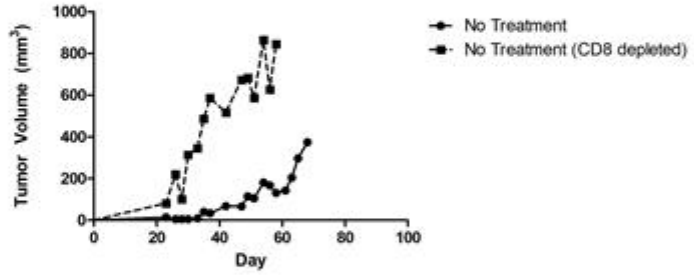
Tumor Volume (mm³)
1000
800
600
400
200
0
0
20
40
60
80
100
Day
No Treatment
No Treatment (CD8 depleted)

C

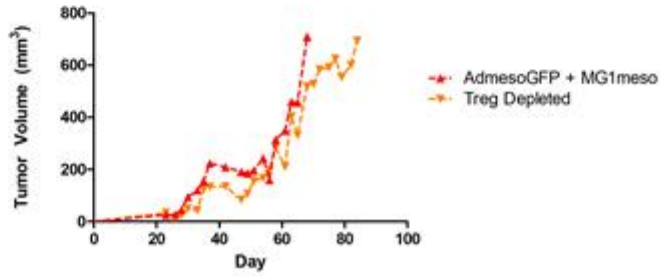
Tumor Volume (mm³)
800
600
400
200
0
0
20
40
60
80
100
Day
AdmesoGFP + MG1meso
Treg Depleted

Figure 32: Tumour outgrowth rates are dependent on the presence of CD8 T cells. (A) Mean tumour volumes of mice depleted of CD8 T cells prior to tumour challenge are indicated. Comparison of (B) non-treated mice with or without CD8 depletion, as indicated by dashed lines and (C) CD8 depleted AdmesoGFP+MG1meso or Treg depleted mice from Figure A.

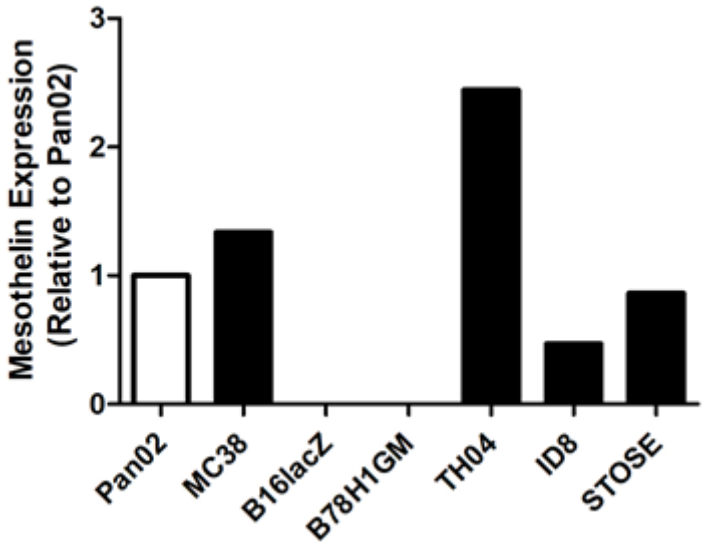
Mesothelin Expression
(Relative to Pan02)
3
2
1
0
Pan02
MC38
B16lacZ
B78H1GM
TH04
ID8
STOSE

Figure 33: Murine peritoneal cancer models express mesothelin. RNA was collected from various murine cancer lines, and the presence of mesothelin mRNA was investigated by RT-qPCR. Fold change over levels observed in Pan02 cells is indicated. Fold change was calculated by ΔΔCT and was normalized to both β-Actin and GAPDH.

A

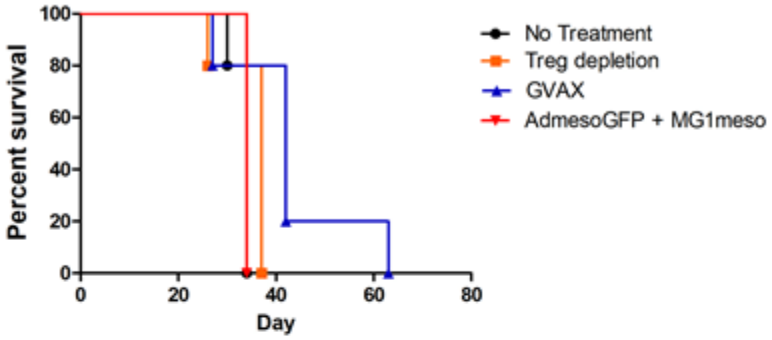
Percent survival
Day
No Treatment
Treg depletion
GVAX
AdmesoGFP + MG1meso

B

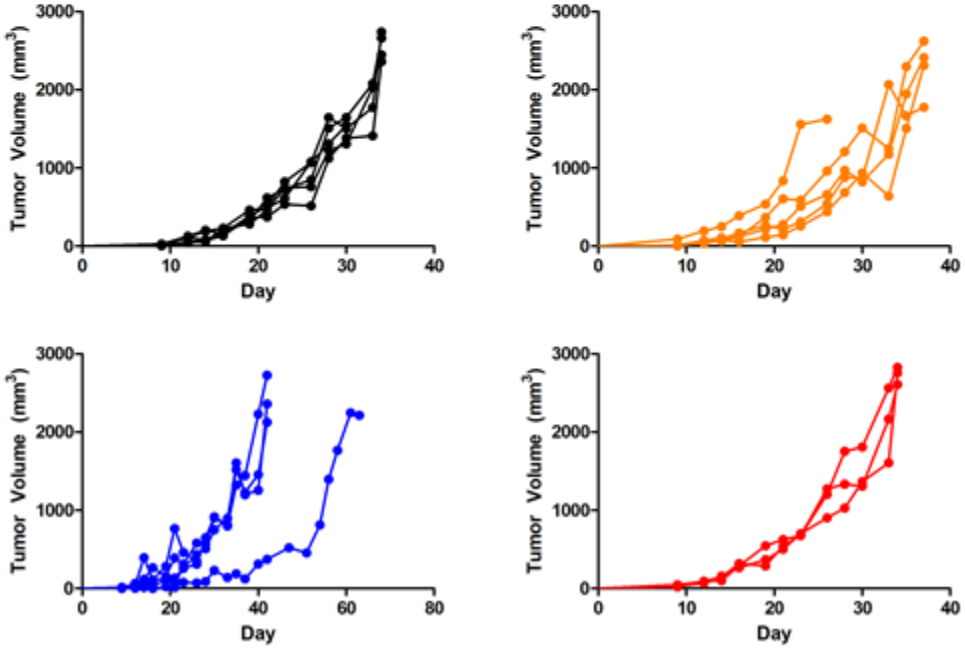
Tumor Volume (mm3)
Day

Figure 34: AdmesoGFP + MG1meso does not protect mice from TH04 tumour challenge. (A) Survival of mice challenged with $1x10^5$ TH04 cells subcutaneously. (B) Individual tumour outgrowth of naïve, T_{reg} depleted, GVAX vaccinated and AdmesoGFP + MG1meso vaccinated mice. N=5 mice per group.

3.6.3 Mice protected from Pan02 challenge are not protected from mesothelin-expressing MC38 challenge

Next, long term surviving mice from Pan02 challenge and re-challenge were subsequently challenged with $1x10^5$ MC38 cells subcutaneously. Both mice who had received T_{reg} depletion alone initially and mice who had received T_{reg} depletion followed by AdmesoGFP prime and MG1meso boost succumbed to MC38 challenge (Figure 35A). In fact, only mice who had originally received GVAX vaccination, prepared with Pan02 cells, demonstrated an immune response against MC38 cells with 2/3 mice resisting re-challenge (Figure 35B). Therefore, initial vaccination and survival post anti-mesothelin vaccination did not translate to survival against a second mesothelin-expressing tumour line.

3.7 Mesothelin is not an effective target for therapeutic treatment of orthotopic Pan02

3.7.1 Therapeutic vaccination of orthotopic Pan02 tumours with AdmesoGFP + MG1meso leads to stronger mesothelin and anti-tumour responses

Pre-existing anti-tumour immune responses are found within tumour-bearing mice and patients due to the presence of TAA, and may lead to stronger anti-tumour immune responses when combined with vaccination [169,170]. To investigate whether the prime-boost platform can potentiate pre-existing anti-tumour response, mice bearing orthotopic Pan02 tumours were treated as previously described with the addition of a group receiving an off target prime-boost vaccination platform (AdhdCT + MG1) to control for the oncolytic effect of the prime-boost platform. Saphenous blood collected on days -1, 7 and 12 surrounding vaccination to measure changes in the immune response. Prior to vaccination there was no measurable response to mesothelin peptide or to tumour cells in the blood of any animals (Figure 36A).

A

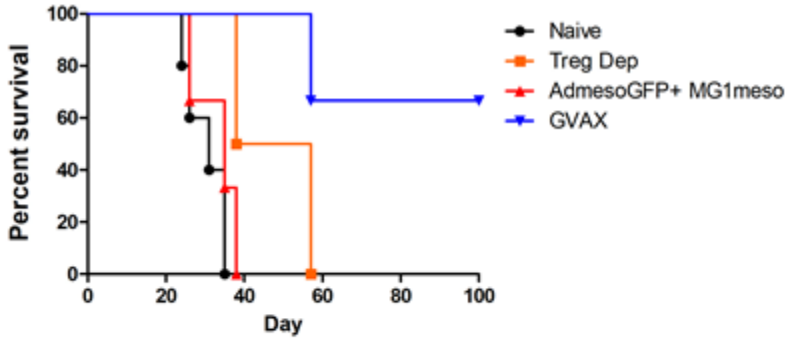
Percent survival
Day
Naive
Treg Dep
AdmesoGFP+ MG1meso
GVAX

B

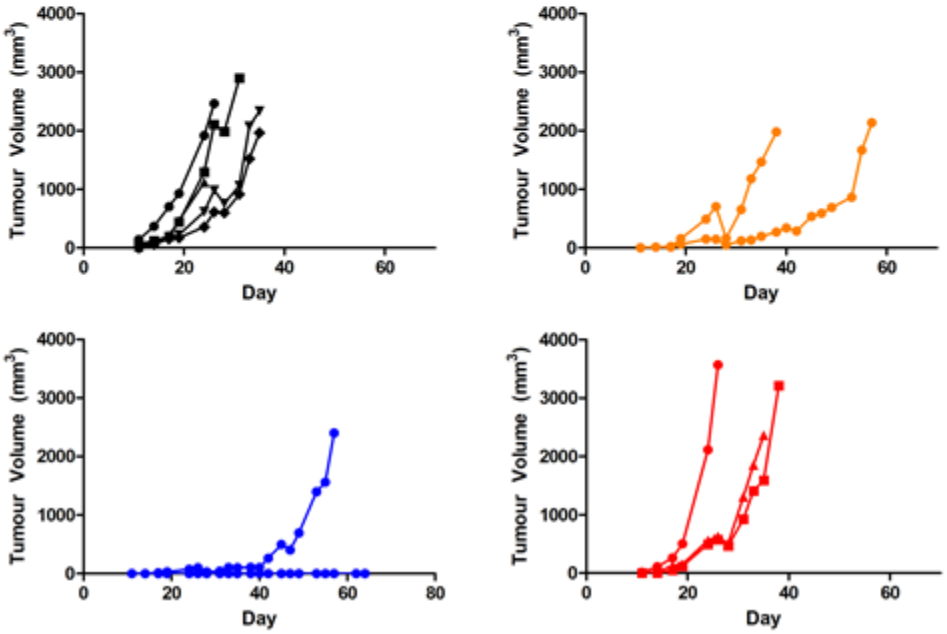
Tumour Volume (mm3)
Day

Figure 35: Mice protected from Pan02 challenge were not protected from MC38 challenge. Long term surviving mice from Pan02 challenge and re-challenge were subsequently challenged with mesothelin-expressing MC38 at $1x10^5$ cells subcutaneously. (A) Survival post MC38 challenge is indicated. (B)Tumour outgrowth in naïve mice as well as re-challenged T_{reg} depleted, GVAX and AdmesoGFP + MG1meso in individual mice is indicated.

A

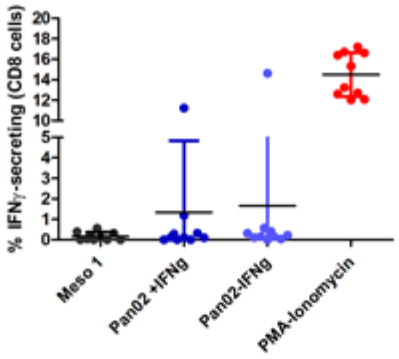
% IFNγ-secreting (CD8 cells)
20
18
16
14
12
10
5
4
3
2
1
0
Meso 1
Pan02 +IFNg
Pan02-IFNg
PMA-Ionomycin

B

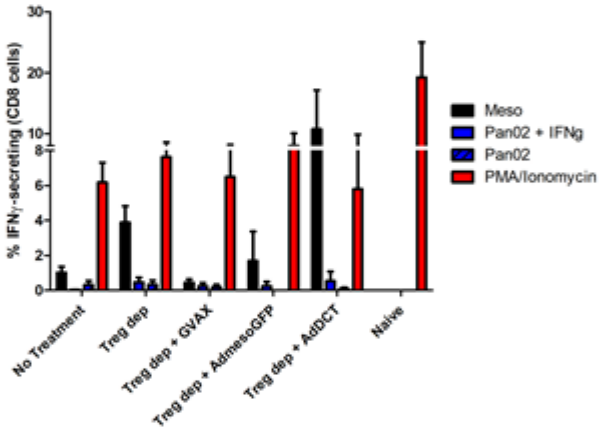
% IFNγ-secreting (CD8 cells)
30
20
10
8
6
4
2
0
Meso
Pan02 + IFNg
Pan02
PMA/Ionomycin
No Treatment
Treg dep
Treg dep + GVAX
Treg dep + AdmesoGFP
Treg dep + AdDCT
Naive

C

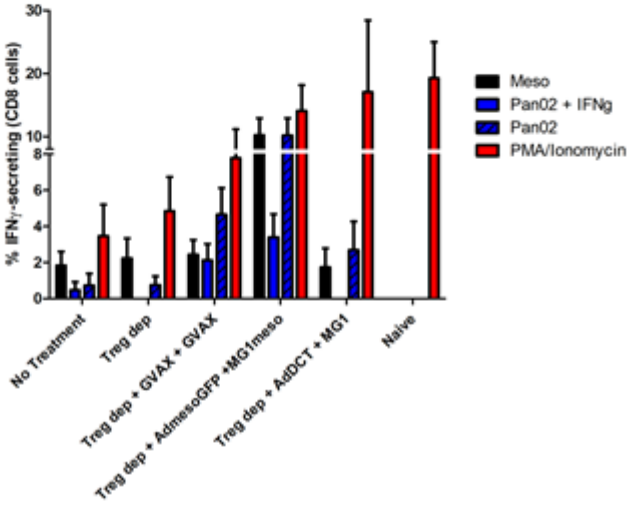
% IFNγ-secreting (CD8 cells)
30
20
10
8
6
4
2
0
Meso
Pan02 + IFNg
Pan02
PMA/Ionomycin
No Treatment
Treg dep
Treg dep + GVAX + GVAX
Treg dep + AdmesoGFP +MG1meso
Treg dep + AdDCT + MG1
Naive

Figure 36: Therapeutic vaccination with AdmesoGFP and MG1meso leads to a strong anti-mesothelin immune response. Mice received intrapancreatic injections of $1x10^5$ Pan02 cells at day -15, followed by T_{reg} depletion at day -1, and prime-boost vaccination at days 0 and 7 respectively. Levels of IFNγ+CD8+ T cells in circulation after stimulation with meso peptide 1 and Pan02 cells (+/- IFNγ) are indicated (A) at day -1 pre vaccination or depletion, (B) at day 7 prior to the boost, and (C) at day 12.

However, circulating mesothelin reactive CD8+ T cells were observed following the priming vaccine alone, (Figure 36B). Unexpectedly, a priming dose of an adenovirus encoding the xenoantigen hDCT was associated with the greatest response to mesothelin peptide stimulation despite the lack of mesothelin in the vaccine and may potentially represent antigen spreading due to the simultaneous release of TAA as tumour cells die in this now active immune environment[171]. The anti-mesothelin response in AdmesoGFP primed mice was further enhanced with following the boost with MG1meso resulting in 10.2% of circulating CD8+ T cells reactive to mesothelin peptide stimulation (Figure 36C). As previously shown, the anti-mesothelin CD8+ T cells could also be stimulated to produce IFNγ in response to incubation with Pan02 cells. Notably, these responses exceeded those achieved with an irrelevant oncolytic platform (Ad-DCT and Meso) suggesting these results were not strictly dependent on tumour antigen presentation following oncolysis of the primary tumour. Furthermore, GVAX vaccination led to comparably lower mesothelin reactive CD8+ T cells. Interestingly the non-specific reactivity of T cells as measured by IFNγ production after stimulation with PMA/Ionomycin decreased over time with initially 14.5% of T cells responding at day 14, down to 3.5% in non treated mice by day 27 (Figure 36A-C) potentially indicating exhaustion or suppression.

3.7.2 No survival benefit is observed with therapeutic vaccination of orthotopic tumours

Therapeutically vaccinated mice were followed over time to correlate the survival benefit with the immune responses observed in circulation (Figure 37A). Despite the larger proportion of mesothelin-specific CD8+ T cells in circulation of AdmesoGFP + MG1meso vaccinated mice, no survival benefit was observed over non treated mice which is consistent with my previous findings suggesting mesothelin reactive CD8+ T cells are ineffective in tumour control (Figure 37B).

A

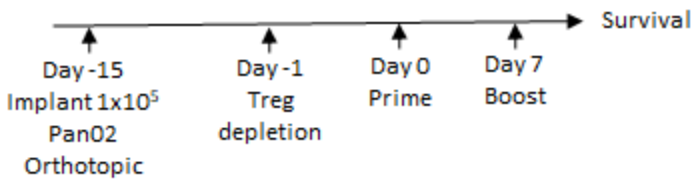
Survival
Day -15
Implant 1x10^5
Pan02
Orthotopic
Day -1
Treg
depletion
Day 0
Prime
Day 7
Boost

B

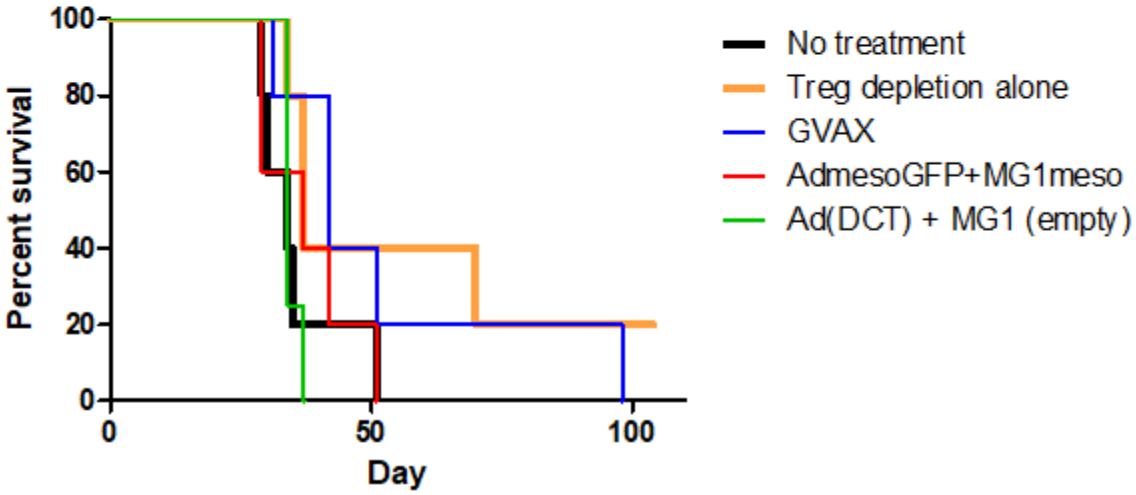
Percent survival
100
80
60
40
20
0
0
50
100
Day
No treatment
Treg depletion alone
GVAX
AdmesoGFP+MG1meso
Ad(DCT) + MG1 (empty)

Figure 37: Vaccination with AdmesoGFP followed by MG1meso provides no therapeutic benefit in an orthotopic model of Pan02. (A) A timeline of tumour challenge and vaccination. (B) Kaplan-Meier survival plot of therapeutic vaccination in an orthotopic Pan02 model. N=4-5 mice per group. Survival post tumour challenge.

4 Discussion

Pancreatic cancer is one of the deadliest cancers worldwide with no effective therapies currently available. The relatively recent improvement in the treatment of other malignancies with immunotherapeutics suggests that approaches which can effectively stimulate engagement of the immune response will be necessary for improving outcomes for patients with PDAC [19,22,26], As such my thesis focused on developing (i) a surgically resectable model of PDAC which is currently a major limitation in testing new therapies and (ii) an oncolytic vaccine targeting a PDAC antigen.

4.1 Developing a surgically resectable model of PDAC

Surgery, a mainstay of PDAC therapy, is typically only performed in early stage cancers[30,31], but does represent the best therapeutic option with 5 year survival rates of 26%[1,2,21,172]. However, despite aggressive surgical intervention and chemotherapy most patients will recur highlighting the urgent need for adjuvant therapies that can be combined with surgical resection for improved patient outcomes. Several groups have reported murine models of surgical resection which enable the investigation of potential therapies. However, a number of these implant either human primary xenografts or established cell lines into immunodeficient animals[37,60,61] - thereby limiting any investigations of potential immunotherapies. Importantly, work in our lab has clearly established that surgical resection of primary tumours can have profound effects on immune function and cancer growth[116,151,152], suggesting immunocompetent murine models are more likely to reflect disease pathogenesis. Furthermore, while the benefit of spleen saving pancreatectomies is debated in the clinic as in many cases the spleen must be resected to achieve negative margin resection[39,40] and provides no long term survival benefit[44], the short term effect on mortality, morbidity and recovery in the hospital is

undeniable[45]. Our understanding of the factors which contribute to the improved outcomes in spleen preserving procedures or the potential impact of promising new treatment modalities such as checkpoint inhibitors and other immunotherapies in this context are limited by the absence of an easily adopted immunocompetent murine model of surgically resectable PDAC, that permits spleen preservation. These facts constitute the rationale for developing a syngeneic spleen-saving resectable model of PDAC, wherein various therapies could be tested, and the direct effects of surgery could be investigated.

4.1.1 Orthotopic Pan02 injection into the tail of the pancreas represents a clinically-relevant resectable model of PDAC

In our current model we decided to proceed with using the syngeneic line of Pan02 cells as they offered us the ability to use immunocompetent mice and develop predictable timelines, with the possibility of measuring metastases. Similar to the results described by Partecke, our Pan02 tumours did lack some of the differentiation associated with clinical PDAC[20,53], but they did demonstrate 5 of 9 of the established histopathological associated with an invasive carcinoma (Figure 3). We determined that this model faithfully recapitulated a human PDAC tumour and could therefore be used to model a surgical resection. While murine models do exist that more accurately model PDAC, including the recent development of murine models with KRAS-mutations - present in 100% of PDAC tumours - that exhibit hallmarks of pancreatic cancer [48,173–176], unfortunately the variability of tumour development and progression make this model challenging for use in surgical studies. Some groups have attempted to develop cell lines from these mice, but the resulting tumours are either poorly differentiated, or demonstrate no ability to develop metastases and peritoneal carcinomatosis, which is frequent in late stage PDAC[174]. Syngeneic models of PDAC allow for predictable timelines, high reproducibility

and allow for the investigation of the immune system with tumours and therapeutics[53], which we found was true with Pan02 cells. These cells have been used in subcutaneous models, orthotopic injection as well as the use of a hemi-splenic metastasis model[58,59]. In our experimental model, direct injection of $1x10^4$ and $1x10^5$ Pan02 cells into the tail of the pancreas reliably resulted in the development of tumours 15-20 days post injection.

The significant immune infiltrate observed in our orthotopic Pan02 models is reflective of the essential role the immune component of the PDAC TME plays in tumour progression[174]. While PDAC tumours tend to lack the high rate of effector infiltration characteristic of "hot" tumours, the role of the ratio of effector CD8+ T cells to T_{reg} cells has prognostic value[69,83,84] . Unlike what is known from human patients[70], the large T cell proportion of the tumour tissue was highly infiltrated by both CD8+ and CD4+ subsets in equal proportions (Figure 6A). A closer examination of the CD4+ subset identified a large increase in T_{reg} cells(Figure 6B), both in circulation and within the tumour itself is highly representative of the immunosuppressive environment stimulated by PDAC, which is a signature of the immune defects characteristic of tumour progression[177,178]. Taken together, where high CD8+ infiltration into the tumour is matched by an increase in regulatory T cells is indicative of a resident effector population capable of targeting the pancreatic tumour that has become exhausted and suppressed. Furthermore, upon further characterization of the CD8+ T cells infiltrating into the tumour, they demonstrate no increase in activation as measured by CD69 expression but have nearly doubled in the percent PD-1+ expression (Figure 6C). This increase PD-1 expression, normally a marker of early activation in anti-viral responses[179], is a marker of tumour-antigen specific CD8+ T cells with an impaired phenotype[180], and has been linked to lower responses to checkpoint

blockade[181], especially when combined with the increased T_{reg} levels. This data indicates a suppressed and exhausted phenotype present in the TME and spreading systemically.

To further emphasize the suppressive phenotype of our orthotopic tumour immune microenvironment was the presence of infiltrating GR-1+ cells and macrophages (Figure 6E and F respectively). While markers alone cannot establish suppressive functionality, they are indicative of both MDSCs and TAM infiltration, which correlates to patient levels [62,178]. Unexpectedly these studies identified a large B cell infiltrate which although not yet characterized in PDAC tumours is correlated with metastases in murine models of breast cancer[81]. Notably, tumour infiltrating B cells are characterized by the increased surface expression of PD-L1 and CD86[182,183] which was observed in our model (Figure 6G) provides a interesting opportunity to investigate the potential role of B_{regs} in PDAC tumour progression and metastases.

4.1.2 Surgical resection offers no survival benefit in a murine model of PDAC

Unlike previous models of surgical resection of Pan02 tumours which do not enable the investigation of the immune component of PDAC[37,38], or employs the suturing of subcutaneous tumours to the tail of the pancreas which leads to an altered TME[36,53], we sought to determine the direct injection of syngeneic Pan02 cells into the tail of the pancreas could be surgically resected to recapitulate the state of PDAC being seen in the clinic. Our model of directly injecting tumour cells into the tail of the pancreas represents is well suited for investigating surgical intervention as it represents both pathological characteristics of disease and represents the immune TME. Our two cell volumes, 1x104 and 1x105 represent two different aspects of surgery - with 1x104 representing earlier stage PDAC and 1x105 representing later stage PDAC including borderline and locally advanced adenocarcinoma[184]. An important, unresolved debate is whether a splenectomy should be performed at the time of pancreatectomy,

or if splenic preservation should be preferred whenever possible. While certain groups indicate that en bloc procedures removing everything should always be performed to ensure negative margin resection and due to the proximity of the splenic vein and artery to the pancreas[185,186], other groups argue for spleen saving procedures when possible[46,72,187,188]. This recommendation is based on the improved post-operative outcomes due to the maintenance of immune surveillance and the limited blood loss during the procedure[39,72]. Limitations on the ability to save the spleen include metastasis, local spread, involvement of the vein and proximity of the tumour to the ilium. A direct investigation of this question in our model revealed that minimal residual disease outgrowth and metastases were found despite surgical resection (Figure 7) which correlates with clinical data wherein the 80% of patients that recur within two years of the operation are divided between local-only (27%), liver or lung only (24%) and multiple site recurrence (46%)[184]. Furthermore despite surgical resection of the primary tumour eventual outgrowth in both the pancreatic remnant and distant metastatic niches was evident at later time points in the majority of animals despite the absence of visible peritoneal disease at the time of resection(Figure 10), though no metastases was observed in the lungs of our mice. Although histopathological examination of the spleen suggested impaired draining of the spleen the viability and basic functionality of the spleen was maintained suggesting the inability of surgical resection to improve survival or prevent tumour outgrowth is not due to impaired splenic function (Figure 9). This eventual relapse likely reflects early dissemination of tumour cells throughout the pancreatic remnant as has been previously noted in preclinical animal studies and the clinical setting. This model presents precisely the disease that we would want to target with therapies, the cases where surgical resection fails to provide a curative option.

To provide a proof-of-concept validation of the ability to use this model to investigate the use of therapeutics in combination with surgical resection we employed the whole cell vaccine GVAX, which is currently being explored in clinical trials[146]. While the addition of GVAX improved survival over surgery alone, there was still a non-significant decrease in the efficacy of surgery plus GVAX over GVAX therapeutics alone (Figure 11). This result is not unexpected as while surgery remains a necessary component of the treatment of solid tumours, it is known to create an immunosuppressive environment which allows for increased metastasis[116,150,152]. This result further emphasizes the need for models that accurately depict surgical resection of PDAC so that the timing, dose and full efficacy of combination therapies can be fully explored.

4.2 Oncolytic vaccines are an ideal platform for treating PDAC

A number of strategies aimed at harnessing the immune system are currently be explored for the potential treatment of pancreatic cancer including CAR-T therapies, checkpoint blockade and vaccines [26,97,140]. Oncolytic viruses present an interesting and relatively unexplored option for pancreatic cancer due to their ability to both selectively infect and replicate in cancer cells[189] and immune stimulating properties[109,190,191]. Encoding a TAA into the viral backbone can allow oncolytic viruses to act as cancer vaccines and are able to stimulate strong T cell responses against the antigen[109]. The heterologous prime boost approach utilizing an adenovirus prime and a Maraba MG1 boost promotes an immune response against the antigen rather than against the viral vectors[109,190]. PDAC tumours are known for having a thick stroma and highly suppressive immune component which makes many therapeutic agents. The OVax platform has the advantage over other oncolytics in that it does not require direct injection or infiltration into the TME, but instead relies on the activation of the immune system. When this platform was used against murine melanoma tumours, over 30% of T cells were found to be

stimulated against the xenoantigen DCT[123], and the platform has been used to target the privileged testis TAA MAGE-A3 in first-in-human clinical trials after demonstrating success and safety in non-human primates[125]. This platform represents an ideal immunotherapeutic that could be utilized in PDAC therapy, potentially in combination with other therapies including surgery. The TAA mesothelin was identified as a target for the platform due to its increased expression in most PDAC patient tumours and its limited expression in healthy tissues, as well as for the early clinical data seen with CAR-T cells and whole cell vaccinations.

4.2.1 Immune tolerance against the self antigen mesothelin can be broken, resulting in measurable CD8+ T cell specific immunity

4.2.1.1 Identifying mesothelin as a candidate TAA for the treatment of PDAC

The heterologous prime-boost platform is well established oncolytic vaccine strategy capable of inducing strong anti-tumour responses[123,124]. However, these studies in mice and monkeys have thus far focused on the use of xenoantigens[123,124] or cancer testis antigens[125]. They also do not always translate to viable targets in PDAC, and thus a different antigen had to be selected. Tumour associated antigens are divided into 3 main types: (1) tumour specific antigens or neoantigens that arise from somatic mutations occurring within the cancer (2) cancer testis antigens like MAGE-A3 and NY-ESO-1 and finally (3) differentiation and/or overexpressed antigens[192]. Mesothelin has been identified as a potential target for vaccine therapy in PDAC, with whole cell vaccines, immunotoxins and Car-T therapies all being designed to target this antigen[140]. Following the work of Collela et al who targeted the self antigen tyrosinase related protein (Trp2) in mice and found that the self tolerance in place prevented the development of an effective anti-tyrosinase immune response[193], we decided that we would need to include a method for breaking immune tolerance to mesothelin. Steitz et al found that the fusion of Trp2 to the foreign antigen GFP in a viral backbone was found to be sufficient to break self tolerance and

induce an effective anti-tumour immune response likely through the engagement of CD4+ helper T cell responses[132] and through the induction of more efficient presentation on MHC molecules[131]. Therefore, GFP was fused to the full-length mesothelin in the priming vector of the prime-boost platform to break immune tolerance to the self antigen.

The viruses and target cells were both found to express high levels of the TAA (Figure 15), and thus *in vitro* and *in vivo* characterization of the virus was performed. Interestingly, despite performing similarly with *in vitro* assays as the parental MG1 virus, MG1meso was found to be toxic at the published dose of 1e9pfu (Figure 16) and it was found that they could only tolerate a log fold lower dose of 1e8pfu. While the MTD has been established for MG1[129], the differences observed may be due to the age of the mice, and therefore the MTD may be lower for younger mice.

4.2.1.2 Depletion of regulatory T cells is necessary to break immune tolerance

The inclusion of GFP in the priming vector was not sufficient to break tolerance to mesothelin (Figure 17), and resulted in no observable T cell responses to published peptides[59,134]. The presence of T_{regs} is well known to limit the expansion and effector function of tumour-reactive/self-reactive CD8+ T cells[194], and is therefore presented a likely target to uncover the response to mesothelin. Furthermore, other groups working with mesothelin have similarly had problems measuring T cell responses to the self antigen and have found that depleting regulatory T cells prior to vaccination broke immune tolerance and revealed CD8+ specific responses[59].

A similar regimen as proposed by Leao et al was performed to deplete regulatory T cells prior to vaccination and was found to be highly effective (Figure 18). Despite the depletion of regulatory T cells, vaccination with AdmesoGFP was still not enough to stimulate mesothelin specific CD8+ T cells (Figure 19). Therefore a positive control for the assay was sought, and was found in the GVAX vaccine – which relies on the secretion of GM-CSF in the presence of irradiated

tumour cells to stimulate an anti-tumour immune response[105]. With the addition of this positive control, we were fully able to investigate the validity of the peptides in the ICS experiments. Interestingly while AdmesoGFP-MG1meso vaccination produced an immune response that was limited to a single peptide, and produced a smaller proportion of mesothelin specific CD8+ T cells (2% vs 4%), the overall expansion of T cells in the presence of an oncolytic virus led to a similar total number of antigen reactive T cells (Figure 21). Furthermore, this response was characterized by 20% cytotoxicity at 18hrs post challenge (Figure 24), which was similar to the levels achieved by the established GVAX vaccine.

4.2.1.3 Mesothelin specific T cells recognize target Pan02 cells

Many immunotherapies focus on activating an immune response against cancer, and monitor the systemic immune levels[195]. An effective immunotherapy requires the direct recruitment of tumour-targeting immune cells into the tumour[195,196]. Tumours can avoid the recruitment of antigen-specific T cells through the downregulation of MHC presentation molecules, something that is observed in Pan02 cells at baseline (Figure 23A). The AdmesoGFP + MG1meso platform was able to elicit tumour specific CD8+ T cells responses (Figure 23C) and was able to recruit CD8+ T cells to the site of tumour challenge (Figure 25). The CD8+ T cells found to be infiltrating the site of tumour challenge could not be confirmed to be mesothelin- or tumour-specific due to limitations in the total number of cells and current measurement techniques. However, the significantly increased number of CD8+ cells over either other treatment indicates that this recruitment was treatment specific.

Vaccination with the heterologous prime-boost platform targeting the self-antigen mesothelin was able to induce an antigen specific CD8+ T cell response characterized by IFNγ secretion and cytotoxicity once the immune tolerance had been broken. While this response was lower than those elicited by OVax encoding the xenoantigen hDCT[123], the mesothelin response translated

to an anti-tumour immune response that was defined by the increased recruitment of CD45+ cells to the site of tumour challenge, specifically with an increase in CD8+ T cells over the clinically used GVAX platform.

4.2.2 Mesothelin does not represent an ideal target for the heterologous oncolytic vaccine platform

4.2.2.1 The immune response stimulated by AdmesoGFP+MG1meso is not sufficient to provide protection from a tumour challenge

Despite similar levels of mesothelin reactive T cells (Figure 21B), and a similar cytotoxicity to the whole cell GVAX platform, the AdmesoGFP-MG1meso platform did not provide protection beyond that achieved through T_{reg} depletion alone (Figure 26B). The protective effects of T_{reg} depletion alone is well documented[197–201]. Furthermore, TGF-β secretion by Pan02 tumours converts CD4+ helper T cells into T_{regs} which is essential to their growth[202]. Leao et al performed an early treatment model of subcutaneous Pan02 and found that vaccination with GVAX alone was not enough to cure tumours but the addition of T_{reg} depletion increased tumour free incidence to 60%, and therapeutic T_{reg} depletion starting two days post tumour challenge was sufficient to reduce tumour incidence to 30% [59]. So, while the positive effect of T_{reg} depletion on preventing tumour occurrence in 50% of mice was expected, the lack of increased efficacy of the prime-boost platform was unexpected. Of note, the expansion of the population of target-reactive CD8+ T cells observed in response to the platform targeting hDCT was in excess of 30% of all CD8+ T cells[123] whereas the numbers observed in our mesothelin experiments were below 5% (Figure 21B). Nevertheless, the levels of mesothelin-specific CD8+ T cells were still similar to those of the whole cell vaccine which is being used in the clinic. This result was not cell line specific, and when two other mesothelin expressing cell lines were used (TH04 and MC38), no increase in efficacy was observed. Furthermore, T_{reg} depletion alone was

sufficient to produce long lasting memory responses, attributed to the development of tumour-specific CD8+ T cell responses (Figure 27). Further evidence that this memory response could not be attributed to an anti-mesothelin response was demonstrated through the re-challenge of long-term surviving mice with a different mesothelin-expressing cell line, where only whole cell vaccinated mice were able to resist re-challenge (Figure 35).

To further demonstrate that the mesothelin specific CD8+ T cells stimulated through AdmesoGFP-MG1meso vaccination were not contributing to the 50% tumour rejection observed, a CD8+ depletion was performed post vaccination, but prior to tumour challenge. No difference in total mice protected from tumour challenge was observed in this treatment group (Figure 31B), though the importance of CD8+ cells in the speed of tumour development was noticeable (Figure 32). Interestingly while both CD4+ and CD8+ cells were found to be indispensable to earlier forms of the GVAX vaccine [203], in this model GVAX vaccinated mice were fully protected regardless of the status of CD8+ T cells, indicating an important role for either CD4+ T cells, B cells or NK cells in the observed protection.

4.2.2.2 Primary and adaptive resistance in the Pan02 model

Our search to understand why the prime-boost platform was ineffective initially settled on the immune escape through primary or adaptive resistance in the model [19]. Efforts to overcome this resistance has led to a new branch of immunotherapy – specifically that of checkpoint blockade which enhances pre-existing tumour immunity [19,204]. However, the upregulation of immune checkpoint molecules is by no means the only method of acquired tumour resistance and would not play a major role in the prophylactic setting. These include factors that make the tumour cells unrecognizable to T cells such as downregulation or lack of expression of MHC or B2M [167,168], lack of antigen, or loss of antigen expression[19]. Pan02 cells are known to be weakly immunogenic and have low expression of T cell and NK cell ligands[205], and we had

previously demonstrated that or tumours had a large immunosuppressive infiltrate and low expression of MHC class I on tumour cells *in vitro* (Figure 23A), which could be induced through activation using IFNγ. Without presentation of peptide on MHC I, T cells cannot recognize and kill tumour cells which could explain how the mesothelin-specific CD8+ T cells stimulated through AdmesoGFP-MG1meso vaccination were not effective in protecting mice from Pan02 challenge, despite their early recruitment to the site of tumour challenge. GVAX treatment, which proved effective was shown to not rely on CD8+ T cells, so the MHC I expression would not be relevant for that treatment. Contrary to what was seen *in vitro*, and what is observed in acquired resistance [19], MHC I expression increased over time *in vivo*, with a small increase observed after 3 days, and high levels observed at endpoint in all mice regardless of treatment group (Figure 28). This led to investigation of the other intrinsic method of avoiding T cell detection – loss of the targeted tumour antigen [19]. Whole cell vaccines, like GVAX or infected cell vaccines do not rely on previous knowledge of a targeted antigen or on a single antigen [59,155,164]. While targeted vaccine strategies require previous knowledge of an immunogenic antigen such as DCT in melanoma, they can result in very strong responses and antigen spreading [123]. They also leave themselves open to this form of acquired resistance. However, in the case of mesothelin the levels of mRNA expression of the antigen remained high at endpoint indicating that likely this was not the reason for the observed lack of efficacy. There is a limitation to this data in that while transcription levels can remain high there may be a deficiency in translation of the protein but without a working antibody this could not be explored.

A second cause of primary and adaptive resistance comes from tumour extrinsic factors[19] including secreted factors and other cells within the TME. As we observed, the Pan02 tumours

were highly infiltrated with T_{regs}, MDSCs and a high proportion of B cells that may be immunosuppressive in nature (Figure 6). In PDAC patients these cells are associated with a poor prognosis[62,83,84] due to the secretion of inhibitory cytokines and the expression of regulatory biomarkers. Furthermore, these regulatory cell subsets are known to directly limit CD8+ T cell expansion, differentiation[206], and effector function[207]. In recent years these cells have become the target of a number of therapeutics to block their suppressive activity and deplete them from circulation. Their importance in patient disease progression is undeniable. The efficacy of many immunotherapeutics can be dimmed or completely hidden by the presence of T_{regs} and MDSCs, which could be a contributing factor to the lack of efficacy observed in the mesothelin-specific T cells targeting of Pan02 tumours. In our model T_{regs} are depleted prior to vaccination, and the result of this depletion is undeniable in the 50% protection that it provides. However, both MDSCs and the high B cell infiltration observed in naive tumours are still present at the time of tumour challenge. The *in vivo* depletion of both these populations in conjunction with the absence of T_{regs} at the time of tumour challenge did not unleash the anti-mesothelin specific immune response and no increase in efficacy was observed (Figure 30), so while they may be playing a role in tumour progression these cells are not contributing to resistance towards the AdmesoGFP-MG1meso platform.

4.2.2.3 Increasing the proportion of mesothelin reactive T cells does not increase efficacy

Boosting pre-existing mesothelin reactive CD8+ T cells resulted in a much larger proportion of TAA specific T cells up to nearly 11% of the total population (Figure 36C). In addition, while the proportion of CD8+ T cells capable of reacting to general PMA/Ionomycin in naive mice decreased over the three week period from 15% reactivity to below 4% indicating general and progressive dysfunction the mice receiving an oncolytic virus treatment maintained the ability to secrete IFNγ (Figure 36 A-C). This correlates with the known ability to OVs to reactivate

suppressed immune cells as they respond to the PAMPs associated with a viral infection [190,208], however the established Pan02 tumour proved too difficult even for the GVAX platform which is fully capable of protecting mice from tumour challenge (Figure 37). Many therapeutics are unable to overcome the immunosuppressive TME present in established tumours. Furthermore, while anti-CD25 antibody is capable of depleting T_{regs} in circulation, it has been shown to be unable to deplete T_{regs} from within the TME[74].

4.2.2.4 Mesothelin is not an ideal TAA for immunotherapeutic strategies

The data presented in this thesis suggests that external factors are not the cause of the lack of efficacy of the prime-boost OVax platform targeting mesothelin. This leaves the possibility that the immune response itself - the 2% of CD8+ T cells targeting mesothelin - are not effective at protecting mice from challenge with tumours expressing mesothelin, which brings the selected antigen into question. Developing vaccines for effective anti-tumour immune responses requires the identification of an ideal TAA. Though highly mutated tumours, such as melanoma and lung cancer have many neoantigens, most TAAs on cancer derive from overexpressed self-antigens. The inherent problem that must be overcome when activating these immune responses is that of self tolerance - a natural and extremely important mechanism in our bodies. During early development, T cells that have successfully passed through positive selection in the thymus enter the thymic medulla and begin the process of negative selection[161]. This process involves the presentation of many self antigens on APCs, primarily medullary thymic epithelial cells, to the T cells and results in the deletion of strongly autoreactive T cells[161]. While this process is highly efficient and results in the elimination of over 90% of autoreactive T cells[209], the process is limited by the absence of privileged antigens - such as the testis cancer antigens - within the thymus, and also fails to eliminate T cells with a low affinity for self antigens[161,210]. This escape from the negative selection process is the reason that autoreactive T cells can be found in

the periphery of patients bearing tumours[210] and presents the possibility that these weakly reactive T cells could be activated to have anti-tumour activity. However the caveat is that despite their presence, these tumour-reactive T cells tend to because they have entered into an anergic state - which is a state of permanent T cell exhaustion - or ignore antigen positive cells present on the tumour due to inadequate affinity of self peptide for MHC class I molecules[210]. Anergic, or tolerant, CD8+ T cells lack distinct biomarkers making them currently difficult to identify *in vivo*. While they can be present in quite high numbers in many cancer types, due to their low-avidity TCRs these TAA-specific CD8+ T cells are unable to mount an effective adaptive immune response against TAA-expressing tumour cells[211]. The notable exception to this rule is that of MART-1, which has provided an effective target for many melanomas but also remains one of the few antigens that escapes negative selection in certain individuals during thymic development resulting in a large pool of high avidity T cells in circulation of healthy patients[212].

Mesothelin does not share this method of escape. Initial murine and clinical data provided through CAR-T[147] and GVAX combined with CRS-207 [146] indicate that there is a delay in tumour development but no increase in survival in PDAC. In fact, my data with GVAX indicates that the immune response observed was not reliant on the mesothelin-specific CD8+ T cells (Figure 31B), but rather on other populations stimulated through the GM-CSF secretion. In other murine models targeting mesothelin using a vaccinia virus platform, measurable mesothelin specific responses were observed in circulation but these once again did not translate to survival [213]. This is not limited to mesothelin but has been found with other self antigens as well. Grosso et al investigated the effect of tolerance towards antigens and found a role for Lag 3 in

inducing tolerance. When this pathway was blocked, an anti-target response was measurable but once again did not significantly delay tumour outgrowth over blocking Lag-3 alone[214].

The work in this study has shown that while the oncolytic vaccine AdmesoGFP + MG1meso can induce an anti-mesothelin response characterized by IFNγ secretion and cytotoxicity towards the peptide, this does not translate to an effective protective immune response from Pan02 tumours. A limitation of my study is the inability to confirm that the CD8+ T cells responding to mesothelin have a strong affinity for tumour cells *in vivo*, and we could not test for the role of negative selection in removing high avidity and affinity T cells from circulation, nor did we test the ability of the mesothelin reactive T cells to protect a immune naive mouse from tumour challenge due to lacking a method for effectively sorting or expanding this population from mice.

5 Conclusions

PDAC is one of the deadliest cancers, and new therapeutics are needed. These therapeutics need to address all stages of PDAC, including resectable PDAC. My work clearly demonstrates the successful development of a murine surgical model of PDAC that recapitulates human disease, and which can be used for the study of multiple therapeutics including immunotherapies.

Oncolytic vaccines represent a novel immunotherapeutic that takes advantage of the oncolytic potential of viruses and their ability to induce an inflammatory environment, all while presenting tumour associated antigens to the immune system[109,190]. Unlike whole cell vaccines, OVax require the selection of a specific TAA. I chose to focus on mesothelin as a TAA due to its high expression in multiple cancers, specifically in over 90% of PDAC cases[133]. Furthermore a number of murine studies have progressed to clinical trials with promising early results[108,215]. Using the established heterologous OVax platform with an Adenovirus prime,

and a Maraba MG1 boost, I was able to establish an CD8+ T cell population with mesothelin specificity only after breaking immune tolerance through the depletion of T_{regs}. Furthermore, this vaccination strategy translated to an anti-tumour immune response *ex vivo* and resulted in the recruitment of CD8+ T cells to the site of tumour challenge. However, this did not translate to *in vivo* efficacy, and the AdmesoGFP + MG1meso vaccination failed to protect mice challenged with mesothelin-expressing tumours above the protection provided by T_{reg} depletion alone. This result was found not to rely on the tumour escape mechanisms evaluated, and the observed protection was not dependent on the CD8+ T cells produced through vaccination. Mesothelin does not represent an ideal target TAA for the OVax strategy, potentially due to its inherent properties as a self antigen which result in suboptimal CD8+ T cells present in circulation that are not capable of mounting an efficacious anti-tumour immune response. Future studies to further prove the self antigen theory would be to perform the same vaccination strategy in mesothelin knockout mice, where mesothelin would no longer be a self antigen and therefore no negative selection would have occurred on T cells during thymic development. If these mice were protected from tumour challenge, their CD8+ T cells could then be subsequently adoptively transferred into wild type mice to prove their efficacy at targeting mesothelin. Future OVax strategies should focus on the selection of neoantigens, viral antigens or privileged self antigens to avoid the need to break immune tolerance.

6 Contributions of Collaborators

Our collaborators at McMaster University (Drs Brian Lichty and Kyle Stephenson) kindly provided plasmids encoding codon optimized mesothelin and mesothelin fused to GFP for the development of the Maraba MG1 virus. They also provided the AdmesoGFP virus, which was produced and purified at McMaster University.

7 References

1. Cancer. In: WHO [Internet]. 2018 [cited 2019]. Available: https://www.who.int/cancer/en/

2. Canadian Cancer Society. Canadian Cancer Statistics 2018 [Internet]. 2018. Available: https://www.cancer.ca/en/cancer-information/cancer-101/canadian-cancer-statistics-publication/?region=on

3. Hurton S, MacDonald F, Porter G, Walsh M, Molinari M. The current state of pancreatic cancer in Canada: incidence, mortality, and surgical therapy. Pancreas. 2014;43: 879–885.

4. Pietras K, Ostman A. Hallmarks of cancer: interactions with the tumor stroma. Exp Cell Res. Elsevier; 2010;316: 1324–1331.

5. Hanahan D, Weinberg RA. Hallmarks of cancer: the next generation. Cell. Elsevier; 2011;144: 646–674.

6. Hanahan D, Weinberg RA. The hallmarks of cancer. Cell. 2000;100: 57–70.

7. Crawford Y, Kasman I, Yu L, Zhong C, Wu X, Modrusan Z, et al. PDGF-C mediates the angiogenic and tumorigenic properties of fibroblasts associated with tumors refractory to anti-VEGF treatment. Cancer Cell. 2009;15: 21–34.

8. Dunn GP, Bruce AT, Ikeda H, Old LJ, Schreiber RD. Cancer immunoediting: from immunosurveillance to tumor escape. Nat Immunol. 2002;3: 991–998.

9. Mittal D, Gubin MM, Schreiber RD, Smyth MJ. New insights into cancer immunoediting and its three component phases--elimination, equilibrium and escape. Curr Opin Immunol. 2014;27: 16–25.

10. Schreiber RD, Old LJ, Smyth MJ. Cancer immunoediting: integrating immunity's roles in cancer suppression and promotion. Science. 2011;331: 1565–1570.

11. DuPage M, Cheung AF, Mazumdar C, Winslow MM, Bronson R, Schmidt LM, et al. Endogenous T cell responses to antigens expressed in lung adenocarcinomas delay malignant tumor progression. Cancer Cell. 2011;19: 72–85.

12. DuPage M, Mazumdar C, Schmidt LM, Cheung AF, Jacks T. Expression of tumour-specific antigens underlies cancer immunoediting. Nature. 2012;482: 405–409.

13. Diamond MS, Kinder M, Matsushita H, Mashayekhi M, Dunn GP, Archambault JM, et al. Type I interferon is selectively required by dendritic cells for immune rejection of tumors. J Exp Med. 2011;208: 1989–2003.

14. Gasser S, Orsulic S, Brown EJ, Raulet DH. The DNA damage pathway regulates innate immune system ligands of the NKG2D receptor. Nature. 2005;436: 1186–1190.

15. Iannello A, Thompson TW, Ardolino M, Lowe SW, Raulet DH. p53-dependent chemokine production by senescent tumor cells supports NKG2D-dependent tumor elimination by natural killer

cells. J Exp Med. 2013;210: 2057–2069.

16. Teng MWL, Vesely MD, Duret H, McLaughlin N, Towne JE, Schreiber RD, et al. Opposing roles for IL-23 and IL-12 in maintaining occult cancer in an equilibrium state. Cancer Res. 2012;72: 3987–3996.

17. Koebel CM, Vermi W, Swann JB, Zerafa N, Rodig SJ, Old LJ, et al. Adaptive immunity maintains occult cancer in an equilibrium state. Nature. 2007;450: 903–907.

18. Wu X, Peng M, Huang B, Zhang H, Wang H, Huang B, et al. Immune microenvironment profiles of tumor immune equilibrium and immune escape states of mouse sarcoma. Cancer Lett. 2013;340: 124–133.

19. Sharma P, Hu-Lieskovan S, Wargo JA, Ribas A. Primary, Adaptive, and Acquired Resistance to Cancer Immunotherapy. Cell. 2017;168: 707–723.

20. Hruban RH, Fukushima N. Pancreatic adenocarcinoma: update on the surgical pathology of carcinomas of ductal origin and PanINs. Mod Pathol. 2007;20 Suppl 1: S61–70.

21. Siegel RL, Miller KD, Jemal A. Cancer statistics, 2017. CA Cancer J Clin. 2017;67: 7–30.

22. Cid-Arregui A, Juarez V. Perspectives in the treatment of pancreatic adenocarcinoma. World J Gastroenterol. 2015;21: 9297–9316.

23. Burris HA 3rd, Moore MJ, Andersen J, Green MR, Rothenberg ML, Modiano MR, et al. Improvements in survival and clinical benefit with gemcitabine as first-line therapy for patients with advanced pancreas cancer: a randomized trial. J Clin Oncol. 1997;15: 2403–2413.

24. Mohammad AA. Advanced pancreatic cancer: The standard of care and new opportunities. Oncol Rev. 2018;12: 370.

25. Amrutkar M, Gladhaug IP. Pancreatic Cancer Chemoresistance to Gemcitabine. Cancers . 2017;9. doi:10.3390/cancers9110157

26. Salman B, Zhou D, Jaffee EM, Edil BH, Zheng L. Vaccine therapy for pancreatic cancer. Oncoimmunology. 2013;2: e26662.

27. Torphy RJ, Zhu Y, Schulick RD. Immunotherapy for pancreatic cancer: Barriers and breakthroughs. Ann Gastroenterol Surg. 2018;2: 274–281.

28. Neoptolemos JP, Palmer DH, Ghaneh P, Psarelli EE, Valle JW, Halloran CM, et al. Comparison of adjuvant gemcitabine and capecitabine with gemcitabine monotherapy in patients with resected pancreatic cancer (ESPAC-4): a multicentre, open-label, randomised, phase 3 trial. Lancet. 2017;389: 1011–1024.

29. Gunturu KS, Rossi GR, Saif MW. Immunotherapy updates in pancreatic cancer: are we there yet? Ther Adv Med Oncol. 2013;5: 81–89.

30. Adamska A, Domenichini A, Falasca M. Pancreatic Ductal Adenocarcinoma: Current and Evolving Therapies. Int J Mol Sci. 2017;18. doi:10.3390/ijms18071338

31. Ishiwata T. Pancreatic Ductal Adenocarcinoma: Basic and Clinical Challenges for Better Prognosis. Journal of Carcinogenesis & Mutagenesis. OMICS International; 2013;0: -.

32. Feig C, Gopinathan A, Neesse A, Chan DS, Cook N, Tuveson DA. The pancreas cancer microenvironment. Clin Cancer Res. 2012;18: 4266–4276.

33. Oettle H, Neuhaus P, Hochhaus A, Hartmann JT, Gellert K, Ridwelski K, et al. Adjuvant chemotherapy with gemcitabine and long-term outcomes among patients with resected pancreatic cancer: the CONKO-001 randomized trial. JAMA. 2013;310: 1473–1481.

34. Reni M, Balzano G, Zanon S, Zerbi A, Rimassa L, Castoldi R, et al. Safety and efficacy of preoperative or postoperative chemotherapy for resectable pancreatic adenocarcinoma (PACT-15): a randomised, open-label, phase 2-3 trial. Lancet Gastroenterol Hepatol. 2018;3: 413–423.

35. Gürlevik E, Fleischmann-Mundt B, Brooks J, Demir IE, Steiger K, Ribback S, et al. Administration of Gemcitabine After Pancreatic Tumor Resection in Mice Induces an Antitumor Immune Response Mediated by Natural Killer Cells. Gastroenterology. 2016;151: 338–350.e7.

36. Hwang HK, Murakami T, Kiyuna T, Kim SH, Lee SH, Kang CM, et al. Splenectomy is associated with an aggressive tumor growth pattern and altered host immunity in an orthotopic syngeneic murine pancreatic cancer model. Oncotarget. 2017;8: 88827–88834.

37. Hwang HK, Kang CM, Lee SH, Murakami T, Kiyuna T, Kim SH, et al. Fluorescence-guided Surgery with Splenic Preservation Prevents Tumor Recurrence in an Orthotopic Nude-mouse Model of Human Pancreatic Cancer. Anticancer Res. 2018;38: 665–670.

38. Huynh AS, Abrahams DF, Torres MS, Baldwin MK, Gillies RJ, Morse DL. Development of an orthotopic human pancreatic cancer xenograft model using ultrasound guided injection of cells. PLoS One. 2011;6: e20330.

39. Fernández- Cruz L, Orduña D, Cesar- Borges G, López- Boado MA. Distal pancreatectomy: en- bloc splenectomy vs spleen- preserving pancreatectomy. HPB . 2005;7: 93–98.

40. Sun N, Lu G, Zhang L, Wang X, Gao C, Bi J, et al. Clinical efficacy of spleen-preserving distal pancreatectomy with or without splenic vessel preservation: A Meta-analysis. Medicine . 2017;96: e8600.

41. Warshaw AL. Conservation of the spleen with distal pancreatectomy. Arch Surg. 1988;123: 550–553.

42. Warshaw AL. Distal pancreatectomy with preservation of the spleen. J Hepatobiliary Pancreat Sci. 2010;17: 808–812.

43. Shoup M, Brennan MF, McWhite K, Leung DHY, Klimstra D, Conlon KC. The value of splenic preservation with distal pancreatectomy. Arch Surg. 2002;137: 164–168.

44. Yang F, Jin C, Warshaw AL, You L, Mao Y, Fu D. Total pancreatectomy for pancreatic malignancy with preservation of the spleen. J Surg Oncol. 2019;119: 784–793.

45. Tang CW, Feng WM, Bao Y, Fei MY, Tao YL. Spleen-preserving distal pancreatectomy or distal pancreatectomy with splenectomy?: Perioperative and patient-reported outcome analysis. J Clin Gastroenterol. 2014;48: e62–6.

46. Pendola F, Gadde R, Ripat C, Sharma R, Picado O, Lobo L, et al. Distal pancreatectomy for benign and low grade malignant tumors: Short-term postoperative outcomes of spleen preservation-A systematic review and update meta-analysis. J Surg Oncol. 2017;115: 137–143.

47. Jean-Philippe Adam, Alexandre Jacquin, Christophe Laurent, Denis Collet, Masson B, Fernández-Cruz L, et al. Laparoscopic spleen-preserving distal pancreatectomy: splenic vessel preservation compared with the Warshaw technique. JAMA Surg. 2013;148: 246–252.

48. Talmadge JE, Singh RK, Fidler IJ, Raz A. Murine Models to Evaluate Novel and Conventional Therapeutic Strategies for Cancer. Am J Pathol. 2007;170: 793–804.

49. Frese KK, Tuveson DA. Maximizing mouse cancer models. Nat Rev Cancer. 2007;7: 645–658.

50. Fiebig HH, Maier A, Burger AM. Clonogenic assay with established human tumour xenografts: correlation of in vitro to in vivo activity as a basis for anticancer drug discovery. Eur J Cancer. 2004;40: 802–820.

51. Johnson JI, Decker S, Zaharevitz D, Rubinstein LV, Venditti JM, Schepartz S, et al. Relationships between drug activity in NCI preclinical in vitro and in vivo models and early clinical trials. Br J Cancer. 2001;84: 1424–1431.

52. Clark CE, Beatty GL, Vonderheide RH. Immunosurveillance of pancreatic adenocarcinoma: insights from genetically engineered mouse models of cancer. Cancer Lett. 2009;279: 1–7.

53. Partecke LI, Sendler M, Kaeding A, Weiss FU, Mayerle J, Dummer A, et al. A syngeneic orthotopic murine model of pancreatic adenocarcinoma in the C57/BL6 mouse using the Panc02 and 6606PDA cell lines. Eur Surg Res. 2011;47: 98–107.

54. Little EC, Wang C, Watson PM, Watson DK, Cole DJ, Camp ER. Novel immunocompetent murine models representing advanced local and metastatic pancreatic cancer. J Surg Res. 2012;176: 359–366.

55. Tuveson DA, Zhu L, Gopinathan A, Willis NA, Kachatrian L, Grochow R, et al. Mist1-KrasG12D knock-in mice develop mixed differentiation metastatic exocrine pancreatic carcinoma and hepatocellular carcinoma. Cancer Res. 2006;66: 242–247.

56. Corbett TH, Roberts BJ, Leopold WR, Peckham JC, Wilkoff LJ, Griswold DP Jr, et al. Induction and chemotherapeutic response of two transplantable ductal adenocarcinomas of the pancreas in C57BL/6 mice. Cancer Res. 1984;44: 717–726.

57. Wang B, Shi Q, Abbruzzese J, Xiong Q, Le X, Xie K. A Novel, Clinically Relevant Animal Model of Metastatic Pancreatic Adenocarcinoma Biology and Therapy. Int J Gastrointest Cancer. 2001;29: 37–46.

58. Soares KC, Foley K, Olino K, Leubner A, Mayo SC, Jain A, et al. A preclinical murine model of hepatic metastases. J Vis Exp. 2014; 51677.

59. Leao IC, Ganesan P, Armstrong TD, Jaffee EM. Effective depletion of regulatory T cells allows the recruitment of mesothelin-specific CD8 T cells to the antitumor immune response against a mesothelin-expressing mouse pancreatic adenocarcinoma. Clin Transl Sci. 2008;1: 228–239.

60. Tepel J, Kruse M-L, Kapischke M, Haye S, Sipos B, Kremer B, et al. Adjuvant treatment of pancreatic carcinoma in a clinically adapted mouse resection model. Pancreatology. karger.com; 2006;6: 240–247.

61. Ni X, Yang J, Li M. Imaging-guided curative surgical resection of pancreatic cancer in a xenograft mouse model. Cancer Lett. 2012;324: 179–185.

62. Amedei A, Niccolai E, Prisco D. Pancreatic cancer: role of the immune system in cancer progression and vaccine-based immunotherapy. Hum Vaccin Immunother. 2014;10: 3354–3368.

63. Davis M, Conlon K, Bohac GC, Barcenas J, Leslie W, Watkins L, et al. Effect of pemetrexed on innate immune killer cells and adaptive immune T cells in subjects with adenocarcinoma of the pancreas. J Immunother. 2012;35: 629–640.

64. Pandha H, Rigg A, John J, Lemoine N. Loss of expression of antigen-presenting molecules in human pancreatic cancer and pancreatic cancer cell lines. Clin Exp Immunol. 2007;148: 127–135.

65. Duan X, Deng L, Chen X, Lu Y, Zhang Q, Zhang K, et al. Clinical significance of the immunostimulatory MHC class I chain-related molecule A and NKG2D receptor on NK cells in pancreatic cancer. Med Oncol. 2011;28: 466–474.

66. Hamanaka Y, Suehiro Y, Fukui M, Shikichi K, Imai K, Hinoda Y. Circulating anti-MUC1 IgG antibodies as a favorable prognostic factor for pancreatic cancer. Int J Cancer. 2003;103: 97–100.

67. Cappello P, Tomaino B, Chiarle R, Ceruti P, Novarino A, Castagnoli C, et al. An integrated humoral and cellular response is elicited in pancreatic cancer by alpha-enolase, a novel pancreatic ductal adenocarcinoma-associated antigen. Int J Cancer. 2009;125: 639–648.

68. Cappello P, Tonoli E, Curto R, Giordano D, Giovarelli M, Novelli F. Anti-α-enolase antibody limits the invasion of myeloid-derived suppressor cells and attenuates their restraining effector T cell response. Oncoimmunology. 2016;5: e1112940.

69. Amedei A, Niccolai E, Benagiano M, Della Bella C, Cianchi F, Bechi P, et al. Ex vivo analysis of pancreatic cancer-infiltrating T lymphocytes reveals that ENO-specific Tregs accumulate in tumor tissue and inhibit Th1/Th17 effector cell functions. Cancer Immunol Immunother. 2013;62: 1249–1260.

70. Fukunaga A, Miyamoto M, Cho Y, Murakami S, Kawarada Y, Oshikiri T, et al. CD8+ tumor-infiltrating lymphocytes together with CD4+ tumor-infiltrating lymphocytes and dendritic cells improve the prognosis of patients with pancreatic adenocarcinoma. Pancreas. 2004;28: e26–31.

71. Tewari N, Zaitoun AM, Arora A, Madhusudan S, Ilyas M, Lobo DN. The presence of tumour-associated lymphocytes confers a good prognosis in pancreatic ductal adenocarcinoma: an immunohistochemical study of tissue microarrays. BMC Cancer. 2013;13: 436.

72. Tang Y, Xu X, Guo S, Zhang C, Tang Y, Tian Y, et al. An increased abundance of tumor-infiltrating regulatory T cells is correlated with the progression and prognosis of pancreatic ductal adenocarcinoma. PLoS One. 2014;9: e91551.

73. Rudensky AY. Regulatory T cells and Foxp3 [Internet]. Immunological Reviews. 2011. pp. 260–268. doi:10.1111/j.1600-065x.2011.01018.x

74. Arce Vargas F, Furness AJS, Solomon I, Joshi K, Mekkaoui L, Lesko MH, et al. Fc-Optimized Anti-CD25 Depletes Tumor-Infiltrating Regulatory T Cells and Synergizes with PD-1 Blockade to Eradicate Established Tumors. Immunity. 2017;46: 577–586.

75. Elpek KG, Lacelle C, Singh NP, Yolcu ES, Shirwan H. CD4+CD25+ T regulatory cells dominate multiple immune evasion mechanisms in early but not late phases of tumor development in a B cell lymphoma model. J Immunol. 2007;178: 6840–6848.

76. Golgher D, Jones E, Powrie F, Elliott T, Gallimore A. Depletion of CD25+ regulatory cells uncovers immune responses to shared murine tumor rejection antigens. Eur J Immunol. 2002;32: 3267–3275.

77. Jones E, Dahm-Vicker M, Simon AK, Green A, Powrie F, Cerundolo V, et al. Depletion of CD25+ regulatory cells results in suppression of melanoma growth and induction of autoreactivity in mice. Cancer Immun. 2002;2: 1.

78. Shang B, Liu Y, Jiang S-J, Liu Y. Prognostic value of tumor-infiltrating FoxP3+ regulatory T cells in cancers: a systematic review and meta-analysis. Sci Rep. 2015;5: 15179.

79. Tesi RJ. MDSC; the Most Important Cell You Have Never Heard Of [Internet]. Trends in Pharmacological Sciences. 2019. pp. 4–7. doi:10.1016/j.tips.2018.10.008

80. Mizoguchi A, Bhan AK. A case for regulatory B cells. J Immunol. 2006;176: 705–710.

81. Olkhanud PB, Damdinsuren B, Bodogai M, Gress RE, Sen R, Wejksza K, et al. Tumor-Evoked Regulatory B Cells Promote Breast Cancer Metastasis by Converting Resting CD4+ T Cells to T-Regulatory Cells. Cancer Res. American Association for Cancer Research; 2011;71: 3505–3515.

82. Farren MR, Mace TA, Geyer S, Mikhail S, Wu C, Ciombor K, et al. Systemic Immune Activity Predicts Overall Survival in Treatment-Naïve Patients with Metastatic Pancreatic Cancer. Clin Cancer Res. 2016;22: 2565–2574.

83. Gabitass RF, Annels NE, Stocken DD, Pandha HA, Middleton GW. Elevated myeloid-derived suppressor cells in pancreatic, esophageal and gastric cancer are an independent prognostic factor and are associated with significant elevation of the Th2 cytokine interleukin-13. Cancer Immunol Immunother. 2011;60: 1419–1430.

84. Ikemoto T, Yamaguchi T, Morine Y, Imura S, Soejima Y, Fujii M, et al. Clinical roles of increased populations of Foxp3+CD4+ T cells in peripheral blood from advanced pancreatic cancer patients. Pancreas. 2006;33: 386–390.

85. Zhao F, Obermann S, von Wasielewski R, Haile L, Manns MP, Korangy F, et al. Increase in frequency of myeloid-derived suppressor cells in mice with spontaneous pancreatic carcinoma. Immunology. 2009;128: 141–149.

86. Hiraoka N, Onozato K, Kosuge T, Hirohashi S. Prevalence of FOXP3+ regulatory T cells increases during the progression of pancreatic ductal adenocarcinoma and its premalignant lesions. Clin Cancer Res. 2006;12: 5423–5434.

87. Kurahara H, Shinchi H, Mataki Y, Maemura K, Noma H, Kubo F, et al. Significance of M2-polarized tumor-associated macrophage in pancreatic cancer. J Surg Res. 2011;167: e211–9.

88. Coley WB. The Treatment of Inoperable Sarcoma by Bacterial Toxins (the Mixed Toxins of the Streptococcus erysipelas and the Bacillus prodigiosus). Proc R Soc Med. 1910;3: 1–48.

89. Ehrlich P. Collected Papers: Including a Complete Bibliography. Pergamon Press; 1956.

90. Burnet FM. Immunological surveillance in neoplasia. Transplant Rev. 1971;7: 3–25.

91. Schumacher TN, Schreiber RD. Neoantigens in cancer immunotherapy. Science. 2015;348: 69–74.

92. Brunet J-F, Denizot F, Luciani M-F, Roux-Dosseto M, Suzan M, Mattei M-G, et al. A new member

of the immunoglobulin superfamily—CTLA-4. Nature. 1987;328: 267–270.

93. Allison JP, Krummel MF. The Yin and Yang of T Cell Costimulation [Internet]. Science. 1995. pp. 932–932. doi:10.1126/science.270.5238.932

94. Ishida Y, Agata Y, Shibahara K, Honjo T. Induced expression of PD- 1, a novel member of the immunoglobulin gene superfamily, upon programmed cell death. EMBO J. Wiley Online Library; 1992; Available: https://onlinelibrary.wiley.com/doi/abs/10.1002/j.1460-2075.1992.tb05481.x

95. Larkin J, Chiarion-Sileni V, Gonzalez R, Grob JJ, Cowey CL, Lao CD, et al. Combined Nivolumab and Ipilimumab or Monotherapy in Untreated Melanoma. N Engl J Med. 2015;373: 23–34.

96. Larkin J, Lao CD, Urba WJ, McDermott DF, Horak C, Jiang J, et al. Efficacy and Safety of Nivolumab in Patients With BRAF V600 Mutant and BRAF Wild-Type Advanced Melanoma [Internet]. JAMA Oncology. 2015. p. 433. doi:10.1001/jamaoncol.2015.1184

97. Macherla S, Laks S, Naqash AR, Bulumulle A, Zervos E, Muzaffar M. Emerging Role of Immune Checkpoint Blockade in Pancreatic Cancer. Int J Mol Sci. 2018;19. doi:10.3390/ijms19113505

98. Banerjee K, Kumar S, Ross KA, Gautam S, Poelaert B, Nasser MW, et al. Emerging trends in the immunotherapy of pancreatic cancer. Cancer Lett. 2018;417: 35–46.

99. Koido S, Hara E, Homma S, Namiki Y, Komita H, Takahara A, et al. Dendritic/pancreatic carcinoma fusions for clinical use: Comparative functional analysis of healthy- versus patient-derived fusions. Clin Immunol. 2010;135: 384–400.

100. Saito H, Dubsky P, Dantin C, Finn OJ, Banchereau J, Palucka AK. Cross-priming of cyclin B1, MUC-1 and survivin-specific CD8+ T cells by dendritic cells loaded with killed allogeneic breast cancer cells. Breast Cancer Res. 2006;8: R65.

101. Koido S, Hara E, Homma S, Torii A, Toyama Y, Kawahara H, et al. Dendritic cells fused with allogeneic colorectal cancer cell line present multiple colorectal cancer-specific antigens and induce antitumor immunity against autologous tumor cells. Clin Cancer Res. 2005;11: 7891–7900.

102. Kotteas E, Saif MW, Syrigos K. Immunotherapy for pancreatic cancer. J Cancer Res Clin Oncol. 2016;142: 1795–1805.

103. McCormick KA, Coveler AL, Rossi GR, Vahanian NN, Link C, Chiorean EG. Pancreatic cancer: Update on immunotherapies and algenpantucel-L. Hum Vaccin Immunother. 2016;12: 563–575.

104. Hardacre JM, Mulcahy M, Small W, Talamonti M, Obel J, Krishnamurthi S, et al. Addition of algenpantucel-L immunotherapy to standard adjuvant therapy for pancreatic cancer: a phase 2 study. J Gastrointest Surg. 2013;17: 94–100; discussion p. 100–1.

105. Jaffee EM, Hruban RH, Biedrzycki B, Laheru D, Schepers K, Sauter PR, et al. Novel allogeneic granulocyte-macrophage colony-stimulating factor-secreting tumor vaccine for pancreatic cancer: a phase I trial of safety and immune activation. J Clin Oncol. 2001;19: 145–156.

106. Lutz E, Yeo CJ, Lillemoe KD, Biedrzycki B, Kobrin B, Herman J, et al. A lethally irradiated allogeneic granulocyte-macrophage colony stimulating factor-secreting tumor vaccine for pancreatic adenocarcinoma. A Phase II trial of safety, efficacy, and immune activation. Ann Surg. 2011;253: 328–335.

107. Le DT, Lutz E, Uram JN, Sugar EA, Onners B, Solt S, et al. Evaluation of ipilimumab in combination with allogeneic pancreatic tumor cells transfected with a GM-CSF gene in previously treated pancreatic cancer. J Immunother. 2013;36: 382–389.

108. Le DT, Crocenzi TS, Urum JN, Lutz ER, Laheru DA, Sugar EA, et al. Randomized Phase II study of the safety, efficacy and immune response of GVAX pancreas (with cyclophosphamide) and CRS-207 with or without nivolumab in patients with previously treated metastatic pancreatic adenocarcinoma (STELLAR) [Internet]. Journal for ImmunoTherapy of Cancer. 2015. doi:10.1186/2051-1426-3-s2-p155

109. Russell SJ, Barber GN. Oncolytic Viruses as Antigen-Agnostic Cancer Vaccines. Cancer Cell. 2018;33: 599–605.

110. Chiocca EA, Rabkin SD. Oncolytic viruses and their application to cancer immunotherapy. Cancer Immunol Res. 2014;2: 295–300.

111. Atherton MJ, Lichty BD. Evolution of oncolytic viruses: novel strategies for cancer treatment. Immunotherapy. 2013;5: 1191–1206.

112. Conry RM, Westbrook B, McKee S, Norwood TG. Talimogene laherparepvec: First in class oncolytic virotherapy. Hum Vaccin Immunother. 2018;14: 839–846.

113. Senzer NN, Kaufman HL, Amatruda T. Phase II clinical trial of a granulocyte-macrophage colony-stimulating factor-encoding, second-generation oncolytic herpesvirus in patients with unresectable …. of Clinical Oncology. academia.edu; 2009; Available: http://www.academia.edu/download/33188707/Senzer.pdf

114. Chesney J, Puzanov I, Collichio F, Singh P, Milhem MM, Glaspy J, et al. Randomized, Open-Label Phase II Study Evaluating the Efficacy and Safety of Talimogene Laherparepvec in Combination With Ipilimumab Versus Ipilimumab Alone in Patients With Advanced, Unresectable Melanoma [Internet]. Journal of Clinical Oncology. 2018. pp. 1658–1667. doi:10.1200/jco.2017.73.7379

115. Ribas A, Dummer R, Puzanov I, VanderWalde A, Andtbacka RHI, Michielin O, et al. Oncolytic Virotherapy Promotes Intratumoral T Cell Infiltration and Improves Anti-PD-1 Immunotherapy. Cell. 2018;174: 1031–1032.

116. Tai L-H, Tanese de Souza C, Sahi S, Zhang J, Alkayyal AA, Ananth AA, et al. A mouse tumor model of surgical stress to explore the mechanisms of postoperative immunosuppression and evaluate novel perioperative immunotherapies. J Vis Exp. 2014; doi:10.3791/51253

117. Diaz RM, Galivo F, Kottke T, Wongthida P, Qiao J, Thompson J, et al. Oncolytic immunovirotherapy for melanoma using vesicular stomatitis virus. Cancer Res. 2007;67: 2840–2848.

118. Miller CG, Fraser NW. Requirement of an integrated immune response for successful neuroattenuated HSV-1 therapy in an intracranial metastatic melanoma model. Mol Ther. 2003;7: 741–747.

119. Drake CG. Prostate cancer as a model for tumour immunotherapy. Nat Rev Immunol. 2010;10: 580–593.

120. Gujar SA, Pan DA, Marcato P, Garant KA, Lee PWK. Oncolytic virus-initiated protective immunity against prostate cancer. Mol Ther. 2011;19: 797–804.

121. Krebs P, Barnes MJ, Lampe K, Whitley K, Bahjat KS, Beutler B, et al. NK cell–mediated killing of target cells triggers robust antigen-specific T cell–mediated and humoral responses. Blood. American Society of Hematology; 2009;113: 6593–6602.

122. Bridle BW, Stephenson KB, Boudreau JE, Koshy S, Kazdhan N, Pullenayegum E, et al. Potentiating cancer immunotherapy using an oncolytic virus. Mol Ther. 2010;18: 1430–1439.

123. Pol JG, Zhang L, Bridle BW, Stephenson KB, Rességuier J, Hanson S, et al. Maraba virus as a potent oncolytic vaccine vector. Mol Ther. 2014;22: 420–429.

124. Bridle BW, Clouthier D, Zhang L, Pol J, Chen L, Lichty BD, et al. Oncolytic vesicular stomatitis virus quantitatively and qualitatively improves primary CD8 + T-cell responses to anticancer vaccines. Oncoimmunology. 2013;2: e26013.

125. Pol JG, Acuna SA, Yadollahi B, Tang N, Stephenson KB, Atherton MJ, et al. Preclinical evaluation of a MAGE-A3 vaccination utilizing the oncolytic Maraba virus currently in first-in-human trials. Oncoimmunology. 2019;8: e1512329.

126. Turnstone Biologics, Inc. NCT02879760: Oncolytic MG1-MAGEA3 With Ad-MAGEA3 Vaccine in Combination With Pembrolizumab for Non-Small Cell Lung Cancer Patients [Internet]. Available: https://clinicaltrials.gov/ct2/show/NCT02879760?term=NCT02879760&rank=1

127. Canadian Cancer Trials Group. NCT02285816: MG1 Maraba/MAGE-A3, With and Without Adenovirus Vaccine, With Transgenic MAGE-A3 Insertion in Patients With Incurable MAGE-A3-Expressing Solid Tumours (I214) [Internet]. Available: https://clinicaltrials.gov/ct2/show/NCT02285816?term=NCT02285816&rank=1

128. Guyonneau L, Murisier F, Rossier A, Moulin A, Beermann F. Melanocytes and Pigmentation Are Affected in Dopachrome Tautomerase Knockout Mice. Mol Cell Biol. American Society for Microbiology Journals; 2004;24: 3396–3403.

129. Brun J, McManus D, Lefebvre C, Hu K, Falls T, Atkins H, et al. Identification of genetically modified Maraba virus as an oncolytic rhabdovirus. Mol Ther. 2010;18: 1440–1449.

130. Vavricka CJ, Ray KW, Christensen BM, Li J. Purification and N-glycosylation analysis of melanoma antigen dopachrome tautomerase. Protein J. Springer; 2010;29: 204–212.

131. Zhang M, Ishii K, Hisaeda H, Murata S, Chiba T, Tanaka K, et al. Ubiquitin-fusion degradation pathway plays an indispensable role in naked DNA vaccination with a chimeric gene encoding a syngeneic cytotoxic T lymphocyte epitope of melanocyte and green fluorescent protein. Immunology. 2004;112: 567–574.

132. Steitz J, Brück J, Gambotto A, Knop J, Tüting T. Genetic immunization with a melanocytic self-antigen linked to foreign helper sequences breaks tolerance and induces autoimmunity and tumor immunity. Gene Ther. 2002;9: 208–213.

133. Hassan R, Bera T, Pastan I. Mesothelin: a new target for immunotherapy. Clin Cancer Res. 2004;10: 3937–3942.

134. Hung C-F, Wu TC, Monie A, Roden R. Antigen-specific immunotherapy of cervical and ovarian

cancer. Immunol Rev. 2008;222: 43–69.

135. Zervos E, Agle S, Freistaedter AG, Jones GJB, Roper RL. Murine mesothelin: characterization, expression, and inhibition of tumor growth in a murine model of pancreatic cancer. J Exp Clin Cancer Res. 2016;35: 39.

136. Bera TK, Pastan I. Mesothelin is not required for normal mouse development or reproduction. Mol Cell Biol. 2000;20: 2902–2906.

137. Hassan R, Ho M. Mesothelin targeted cancer immunotherapy. Eur J Cancer. 2008;44: 46–53.

138. Rump A, Morikawa Y, Tanaka M, Minami S, Umesaki N, Takeuchi M, et al. Binding of ovarian cancer antigen CA125/MUC16 to mesothelin mediates cell adhesion. J Biol Chem. 2004;279: 9190–9198.

139. Gubbels JAA, Belisle J, Onda M, Rancourt C, Migneault M, Ho M, et al. Mesothelin-MUC16 binding is a high affinity, N-glycan dependent interaction that facilitates peritoneal metastasis of ovarian tumors. Mol Cancer. 2006;5: 50.

140. Hassan R, Thomas A, Alewine C, Le DT, Jaffee EM, Pastan I. Mesothelin Immunotherapy for Cancer: Ready for Prime Time? J Clin Oncol. 2016;34: 4171–4179.

141. Alewine C, Xiang L, Yamori T, Niederfellner G, Bosslet K, Pastan I. Efficacy of RG7787, a next-generation mesothelin-targeted immunotoxin, against triple-negative breast and gastric cancers. Mol Cancer Ther. 2014;13: 2653–2661.

142. Hollevoet K, Mason-Osann E, Liu X-F, Imhof-Jung S, Niederfellner G, Pastan I. In vitro and in vivo activity of the low-immunogenic antimesothelin immunotoxin RG7787 in pancreatic cancer. Mol Cancer Ther. 2014;13: 2040–2049.

143. Thomas AM, Santarsiero LM, Lutz ER, Armstrong TD, Chen Y-C, Huang L-Q, et al. Mesothelin-specific CD8(+) T cell responses provide evidence of in vivo cross-priming by antigen-presenting cells in vaccinated pancreatic cancer patients. J Exp Med. 2004;200: 297–306.

144. Brockstedt DG, Giedlin MA, Leong ML, Bahjat KS, Gao Y, Luckett W, et al. Listeria-based cancer vaccines that segregate immunogenicity from toxicity. Proc Natl Acad Sci U S A. 2004;101: 13832–13837.

145. Le DT, Brockstedt DG, Nir-Paz R, Hampl J, Mathur S, Nemunaitis J, et al. A live-attenuated Listeria vaccine (ANZ-100) and a live-attenuated Listeria vaccine expressing mesothelin (CRS-207) for advanced cancers: phase I studies of safety and immune induction. Clin Cancer Res. 2012;18: 858–868.

146. Aduro Biotech, Inc. NCT02004262: Safety and Efficacy of Combination Listeria/GVAX Pancreas Vaccine in the Pancreatic Cancer Setting (ECLIPSE) [Internet]. Available: https://clinicaltrials.gov/ct2/show/record/NCT02004262

147. Beatty GL, O'Hara MH, Lacey SF, Torigian DA, Nazimuddin F, Chen F, et al. Activity of Mesothelin-Specific Chimeric Antigen Receptor T Cells Against Pancreatic Carcinoma Metastases in a Phase 1 Trial. Gastroenterology. 2018;155: 29–32.

148. Tai L-H, Auer R. Attacking Postoperative Metastases using Perioperative Oncolytic Viruses and Viral Vaccines. Front Oncol. 2014;4: 217.

149. Market M, Baxter KE, Angka L, Kennedy MA, Auer RC. The Potential for Cancer Immunotherapy in Targeting Surgery-Induced Natural Killer Cell Dysfunction. Cancers . 2018;11. doi:10.3390/cancers11010002

150. Angka L, Khan ST, Kilgour MK, Xu R, Kennedy MA, Auer RC. Dysfunctional Natural Killer Cells in the Aftermath of Cancer Surgery. Int J Mol Sci. 2017;18. doi:10.3390/ijms18081787

151. Tai L-H, de Souza CT, Bélanger S, Ly L, Alkayyal AA, Zhang J, et al. Preventing postoperative metastatic disease by inhibiting surgery-induced dysfunction in natural killer cells. Cancer Res. 2013;73: 97–107.

152. Ananth AA, Tai L-H, Lansdell C, Alkayyal AA, Baxter KE, Angka L, et al. Surgical Stress Abrogates Pre-Existing Protective T Cell Mediated Anti-Tumor Immunity Leading to Postoperative Cancer Recurrence. PLoS One. 2016;11: e0155947.

153. Zhang J, Tai L-H, Ilkow CS, Alkayyal AA, Ananth AA, de Souza CT, et al. Maraba MG1 virus enhances natural killer cell function via conventional dendritic cells to reduce postoperative metastatic disease. Mol Ther. 2014;22: 1320–1332.

154. Diallo J-S, Vähä-Koskela M, Le Boeuf F, Bell J. Propagation, purification, and in vivo testing of oncolytic vesicular stomatitis virus strains. Methods Mol Biol. 2012;797: 127–140.

155. Alkayyal AA, Tai L-H, Kennedy MA, de Souza CT, Zhang J, Lefebvre C, et al. NK-Cell Recruitment Is Necessary for Eradication of Peritoneal Carcinomatosis with an IL12-Expressing Maraba Virus Cellular Vaccine. Cancer Immunol Res. 2017;5: 211–221.

156. Diana A, Wang LM, D'Costa Z, Allen P, Azad A, Silva MA, et al. Prognostic value, localization and correlation of PD-1/PD-L1, CD8 and FOXP3 with the desmoplastic stroma in pancreatic ductal adenocarcinoma. Oncotarget. 2016;7: 40992–41004.

157. Protti MP, De Monte L. Immune infiltrates as predictive markers of survival in pancreatic cancer patients. Front Physiol. 2013;4: 210.

158. Ino Y, Yamazaki-Itoh R, Shimada K, Iwasaki M, Kosuge T, Kanai Y, et al. Immune cell infiltration as an indicator of the immune microenvironment of pancreatic cancer. Br J Cancer. 2013;108: 914–923.

159. Kleeff J, Diener MK, Z'graggen K, Hinz U, Wagner M, Bachmann J, et al. Distal pancreatectomy: risk factors for surgical failure in 302 consecutive cases. Ann Surg. 2007;245: 573–582.

160. Soares KC, Rucki AA, Wu AA, Olino K, Xiao Q, Chai Y, et al. PD-1/PD-L1 blockade together with vaccine therapy facilitates effector T-cell infiltration into pancreatic tumors. J Immunother. 2015;38: 1–11.

161. Takaba H, Takayanagi H. The Mechanisms of T Cell Selection in the Thymus. Trends Immunol. 2017;38: 805–816.

162. Sojka DK, Huang Y-H, Fowell DJ. Mechanisms of regulatory T-cell suppression - a diverse arsenal for a moving target. Immunology. 2008;124: 13–22.

163. Nemunaitis J. Vaccines in cancer: GVAX, a GM-CSF gene vaccine. Expert Rev Vaccines. 2005;4: 259–274.

164. Lemay CG, Rintoul JL, Kus A, Paterson JM, Garcia V, Falls TJ, et al. Harnessing oncolytic virus-mediated antitumor immunity in an infected cell vaccine. Mol Ther. 2012;20: 1791–1799.

165. Horton H, Russell N, Moore E, Frank I, Baydo R, Havenar-Daughton C, et al. Correlation between interferon- gamma secretion and cytotoxicity, in virus-specific memory T cells. J Infect Dis. 2004;190: 1692–1696.

166. Nakiboneka R, Mugaba S, Auma BO, Kintu C, Lindan C, Nanteza MB, et al. Interferon gamma (IFN-γ) negative CD4+ and CD8+ T-cells can produce immune mediators in response to viral antigens. Vaccine. 2019;37: 113–122.

167. Marincola FM, Jaffee EM, Hicklin DJ, Ferrone S. Escape of human solid tumors from T-cell recognition: molecular mechanisms and functional significance. Adv Immunol. 2000;74: 181–273.

168. Sucker A, Zhao F, Real B, Heeke C, Bielefeld N, Maβen S, et al. Genetic evolution of T-cell resistance in the course of melanoma progression. Clin Cancer Res. 2014;20: 6593–6604.

169. Tsung K, Norton JA. In situ vaccine, immunological memory and cancer cure. Hum Vaccin Immunother. 2016;12: 117–119.

170. Le HN, Lee NC, Tsung K, Norton JA. Pre-existing tumor-sensitized T cells are essential for eradication of established tumors by IL-12 and cyclophosphamide plus IL-12. J Immunol. 2001;167: 6765–6772.

171. Gulley JL, Madan RA, Pachynski R, Mulders P, Sheikh NA, Trager J, et al. Role of Antigen Spread and Distinctive Characteristics of Immunotherapy in Cancer Treatment. J Natl Cancer Inst. 2017;109. doi:10.1093/jnci/djw261

172. Stark AP, Sacks GD, Rochefort MM, Donahue TR, Reber HA, Tomlinson JS, et al. Long-term survival in patients with pancreatic ductal adenocarcinoma. Surgery. 2016;159: 1520–1527.

173. Qiu W, Su GH. Development of orthotopic pancreatic tumor mouse models. Methods Mol Biol. 2013;980: 215–223.

174. Tseng WW, Winer D, Kenkel JA, Choi O, Shain AH, Pollack JR, et al. Development of an orthotopic model of invasive pancreatic cancer in an immunocompetent murine host. Clin Cancer Res. 2010;16: 3684–3695.

175. di Magliano MP, Logsdon CD. Roles for KRAS in pancreatic tumor development and progression. Gastroenterology. 2013;144: 1220–1229.

176. Waters AM, Der CJ. KRAS: The Critical Driver and Therapeutic Target for Pancreatic Cancer. Cold Spring Harb Perspect Med. 2018;8. doi:10.1101/cshperspect.a031435

177. Lafaro KJ, Melstrom LG. The Paradoxical Web of Pancreatic Cancer Tumor Microenvironment. Am J Pathol. 2019;189: 44–57.

178. Zheng L. Immune defects in pancreatic cancer. Ann Pancreat Cancer. 2018;1. doi:10.21037/apc.2018.11.01

179. Ahn E, Araki K, Hashimoto M, Li W, Riley JL, Cheung J, et al. Role of PD-1 during effector CD8 T cell differentiation. Proc Natl Acad Sci U S A. 2018;115: 4749–4754.

180. Ahmadzadeh M, Johnson LA, Heemskerk B, Wunderlich JR, Dudley ME, White DE, et al. Tumor antigen–specific CD8 T cells infiltrating the tumor express high levels of PD-1 and are functionally impaired. Blood. American Society of Hematology; 2009;114: 1537–1544.

181. Ngiow SF, Young A, Jacquelot N, Yamazaki T, Enot D, Zitvogel L, et al. A Threshold Level of Intratumor CD8 T-cell PD1 Expression Dictates Therapeutic Response to Anti-PD1 [Internet]. Cancer Research. 2015. pp. 3800–3811. doi:10.1158/0008-5472.can-15-1082

182. Mauri C, Menon M. Human regulatory B cells in health and disease: therapeutic potential. J Clin Invest. 2017;127: 772–779.

183. Zhang Y, Gallastegui N, Rosenblatt JD. Regulatory B cells in anti-tumor immunity. Int Immunol. 2015;27: 521–530.

184. Groot VP, Blair AB, Gemenetzis G, Ding D, Burkhart RA, Yu J, et al. Recurrence after neoadjuvant therapy and resection of borderline resectable and locally advanced pancreatic cancer. Eur J Surg Oncol. 2019; doi:10.1016/j.ejso.2019.04.007

185. Lillemoe KD, Kaushal S, Cameron JL, Sohn TA, Pitt HA, Yeo CJ. Distal pancreatectomy: indications and outcomes in 235 patients. Ann Surg. 1999;229: 693–8; discussion 698–700.

186. Andrén-Sandberg A, Wagner M, Tihanyi T, Löfgren P, Friess H. Technical aspects of left-sided pancreatic resection for cancer. Dig Surg. 1999;16: 305–312.

187. Sasson AR, Hoffman JP, Ross EA, Kagan SA, Pingpank JF, Eisenberg BL. En bloc resection for locally advanced cancer of the pancreas: is it worthwhile? J Gastrointest Surg. 2002;6: 147–57; discussion 157–8.

188. Schwarz RE, Harrison LE, Conlon KC, Klimstra DS, Brennan MF. The impact of splenectomy on outcomes after resection of pancreatic adenocarcinoma. J Am Coll Surg. 1999;188: 516–521.

189. Russell SJ, Peng K-W. Viruses as anticancer drugs. Trends Pharmacol Sci. 2007;28: 326–333.

190. Russell SJ, Peng K-W, Bell JC. Oncolytic virotherapy. Nat Biotechnol. 2012;30: 658–670.

191. Woller N, Gürlevik E, Ureche C-I, Schumacher A, Kühnel F. Oncolytic viruses as anticancer vaccines. Front Oncol. 2014;4: 188.

192. Buonaguro L, Petrizzo A, Tornesello ML, Buonaguro FM. Translating tumor antigens into cancer vaccines. Clin Vaccine Immunol. 2011;18: 23–34.

193. Colella TA, Bullock TN, Russell LB, Mullins DW, Overwijk WW, Luckey CJ, et al. Self-tolerance to the murine homologue of a tyrosinase-derived melanoma antigen: implications for tumor immunotherapy. J Exp Med. 2000;191: 1221–1232.

194. Antony PA, Piccirillo CA, Akpinarli A, Finkelstein SE, Speiss PJ, Surman DR, et al. CD8+ T cell immunity against a tumor/self-antigen is augmented by CD4+ T helper cells and hindered by naturally occurring T regulatory cells. J Immunol. 2005;174: 2591–2601.

195. Gao J-Q, Okada N, Mayumi T, Nakagawa S. Immune cell recruitment and cell-based system for cancer therapy. Pharm Res. 2008;25: 752–768.

196. Bonaventura P, Shekarian T, Alcazer V, Valladeau-Guilemond J, Valsesia-Wittmann S,

Amigorena S, et al. Cold Tumors: A Therapeutic Challenge for Immunotherapy. Front Immunol. 2019;10: 168.

197. Chaudhary B, Elkord E. Regulatory T Cells in the Tumor Microenvironment and Cancer Progression: Role and Therapeutic Targeting. Vaccines (Basel). 2016;4. doi:10.3390/vaccines4030028

198. Facciabene A, Motz GT, Coukos G. T-regulatory cells: key players in tumor immune escape and angiogenesis. Cancer Res. 2012;72: 2162–2171.

199. Gallimore A, Godkin A. Regulatory T cells and tumour immunity - observations in mice and men. Immunology. 2008;123: 157–163.

200. Viehl CT, Moore TT, Liyanage UK, Frey DM, Ehlers JP, Eberlein TJ, et al. Depletion of CD4+CD25+ regulatory T cells promotes a tumor-specific immune response in pancreas cancer-bearing mice. Ann Surg Oncol. 2006;13: 1252–1258.

201. Prasad SJ, Farrand KJ, Matthews SA, Chang JH, McHugh RS, Ronchese F. Dendritic cells loaded with stressed tumor cells elicit long-lasting protective tumor immunity in mice depleted of CD4+CD25+ regulatory T cells. J Immunol. 2005;174: 90–98.

202. Moo-Young TA, Larson JW, Belt BA, Tan MC, Hawkins WG, Eberlein TJ, et al. Tumor-derived TGF-beta mediates conversion of CD4+Foxp3+ regulatory T cells in a murine model of pancreas cancer. J Immunother. 2009;32: 12–21.

203. Dranoff G, Jaffee E, Lazenby A, Golumbek P, Levitsky H, Brose K, et al. Vaccination with irradiated tumor cells engineered to secrete murine granulocyte-macrophage colony-stimulating factor stimulates potent, specific, and long-lasting anti-tumor immunity. Proc Natl Acad Sci U S A. 1993;90: 3539–3543.

204. Okazaki T, Chikuma S, Iwai Y, Fagarasan S, Honjo T. A rheostat for immune responses: the unique properties of PD-1 and their advantages for clinical application. Nat Immunol. Nature Publishing Group, a division of Macmillan Publishers Limited. All Rights Reserved.; 2013;14: 1212.

205. Khallouf H, Märten A, Serba S, Teichgräber V, Büchler MW, Jäger D, et al. 5-Fluorouracil and Interferon-α Immunochemotherapy Enhances Immunogenicity of Murine Pancreatic Cancer Through Upregulation of NKG2D Ligands and MHC Class I. J Immunother . journals.lww.com; 2012;35: 245.

206. McNally A, Hill GR, Sparwasser T, Thomas R, Steptoe RJ. CD4+CD25+ regulatory T cells control CD8+ T-cell effector differentiation by modulating IL-2 homeostasis. Proc Natl Acad Sci U S A. 2011;108: 7529–7534.

207. Weber R, Fleming V, Hu X, Nagibin V, Groth C, Altevogt P, et al. Myeloid-Derived Suppressor Cells Hinder the Anti-Cancer Activity of Immune Checkpoint Inhibitors. Front Immunol. 2018;9: 1310.

208. Bell J. Oncolytic viruses: immune or cytolytic therapy? Mol Ther. 2014;22: 1231–1232.

209. Guevara-Patiño JA, Engelhorn ME, Turk MJ, Liu C, Duan F, Rizzuto G, et al. Optimization of a self antigen for presentation of multiple epitopes in cancer immunity. J Clin Invest. 2006;116: 1382–1390.

210. Houghton AN, Guevara-Patiño JA. Immune recognition of self in immunity against cancer. J Clin Invest. 2004;114: 468–471.

211. Reiser J, Banerjee A. Effector, Memory, and Dysfunctional CD8(+) T Cell Fates in the Antitumor Immune Response. J Immunol Res. 2016;2016: 8941260.

212. Pittet MJ, Zippelius A, Valmori D, Speiser DE, Cerottini J-C, Romero P. Melan-A/MART-1-specific CD8 T cells: from thymus to tumor. Trends Immunol. 2002;23: 325–328.

213. White M, Freistaedter A, Jones GJB, Zervos E, Roper RL. Development of improved therapeutic mesothelin-based vaccines for pancreatic cancer. PLoS One. 2018;13: e0193131.

214. Grosso JF, Kelleher CC, Harris TJ, Maris CH, Hipkiss EL, De Marzo A, et al. LAG-3 regulates CD8+ T cell accumulation and effector function in murine self- and tumor-tolerance systems. J Clin Invest. 2007;117: 3383–3392.

215. Beatty GL, Haas AR, Maus MV, Torigian DA, Soulen MC, Plesa G, et al. Mesothelin-specific chimeric antigen receptor mRNA-engineered T cells induce anti-tumor activity in solid malignancies. Cancer Immunol Res. 2014;2: 112–120.

8 Appendices

8.1 List of Antibodies

Target	Clone	Application	Company/Cat#	Fluorochrome
B-Actin	13E5	Western Blot	Cell Signalling Technologies 4970S	NA
Cas9	7A9	Western Blot	diagenode C15200203	NA
CD8α	2.43	*In vivo* depletion	BioXcell – BE0061	NA
	53-6.7	Flow Cytometry	BD Biosciences 562283	PE-CF594
	53-6.7		BD Pharmingen 561109	PerCPCy5.5
	53-6.7		BD Biosciences 553031	FITC
	4SM15	IHC	eBioscience 14-0808-80	NA
CD4	GK1.5	Flow Cytometry		V450
			BD Biosciences 553730	PE
	EPR19514	IHC	Abcam ab183685	NA
CD3ε	500A2	Flow Cytometry	BD Biosciences 557984	AF700
	145-2C11		Biolegend 100326	PerCP
	Polyclonal	IHC	Abcam ab5690	NA
CD45	30-F11	Flow Cytometry	BD Biosciences 564225	BV786
CD11b	M1/70	Flow Cytometry	eBiosciences 17-0112-81	APC
			eBiosciences 25-0112-82	PeCy7

CD11c	HL3	Flow Cytometry	eBiosciences 12-0114-81	PE
CD19	1D3	Flow Cytometry	BD Biosciences 557399	PE
			eBiosciences 11-0193-81	FITC
CD20	SA271G2	In vivo Depletion	Biolegend 152104	NA
CD25	PC61.5	*In vivo* depletion	BioLegend 102040	NA
		Flow Cytometry	Biolegend 102006	FITC
CD49b	DX5	Flow Cytometry	eBiosciences 17-5971-81	APC
CD69	H1.2F3	Flow Cytometry	eBiosciences 11-0691-81	FITC
CD122	™-B1	Flow Cytometry	eBiosciences 12-1222-81	PE
CD137	IAH2	Flow Cytometry	BD Biosciences 558976	PE
F4/80	T45-2342	Flow Cytometry	BD Horizon 565411	BV421
Foxp3	FJK-16s	Flow Cytometry	eBiosciences 17-5773-80	APC
GFP	Polyclonal	Western Blot	Invitrogen #A-11122	NA
GR-1	RB6-8C5	Flow Cytometry	eBiosciences 11-5931-82	FITC
		In vivo depletion	BioXCell - BE0075	NA
IFNγ	XMG1.2	Flow	eBiosciences 17-7311-	APC

		Cytometry	81	
Ly6C	HK1.4	Flow Cytometry	eBiosciences 17-5932-82	APC
Ly6G	1A8	Flow Cytometry	BD Horizon 562700	PE-CF594
C-ERC/Mesothelin	308	Western Blot	IBL 28127	NA
MHC I (H2Db)	28-14-8	Flow Cytometry	eBioscience 11-5999-82	FITC
MHC I (H2Db/H2Kb)	28-8-6	Flow Cytometry	Biolegend 114605	FITC
NK1.1	PK136	Flow Cytometry	eBioscience 17-5941-82	APC
			eBiosciences 12-0251-81	PE
PD-1	J43	Flow Cytometry	BD Biosciences 562571	APC
			BD Horizon 565942	BV421
TNFα	MP6-XT22	Flow Cytometry	Biolegend 506324	Pe-Cy7
VSV	Polyclonal	Western Blot	Gift from Dr Ilkow	NA

8.2 List of primers used in assays

Procedure	Target	Sequence
Viral Cloning	Mesothelin with Mlu1 FWD	5’ - TCATTTTAATTTGTTACGCGTTGTATGAAAAAACTCATCAACAGCCATCATGAGAAGAGATGCCGAGCAG - 3’
	Mesothelin with Mlu1 REV	5’- AGTTTTTTTCATACAACGCGTTTAAAGCTTAGACAG - 3’
qPCR	Mesothelin FWD	5’ - TCCTGAGTCCCTGATCCAGC - 3’
	Mesothelin REV	5’ - TCACTGTGTCTGGTGAGGTC - 3’
qPCR	Murine β-Actin FWD	5’ - CCCTAAGGCCAACCGTGAA - 3’
	Murine β-Actin REV	5’ - GAGCATAGCCCTCGTAGAT - 3’
qPCR	Murine GAPDH FWD	5’ - GTGGAGTCATACTGGAACATGTAG - 3’
	Murine GAPDH REV	5’ - AATGGTGAAGGTCGGTGTG - 3’
qPCR	Maraba FWD	5’ - GGTGATGGGCAGACTATGAAA- 3’
	Maraba Rev	5’ - CCTAAGGCCAAGAAACAAAAGAG - 3’

8.3 Sequences of viral inserts

muMesothelin

gaattcaagctgctagcgccaccatgagaagagatgccgagcagaaggcctgccccctggcaaagaaccctacaaggtggacgagga
cctgatcttctaccagaactgggagctggaagcctgcgtggacggcaccatgctggccagacagatggacctcgtgaacgagatcccctt
cacctacgagcagctgagcatcttcaagcacaagctggacaagacctacccccagggctaccccgagagcctgattcagcagctgggcc
acttcttcagatacgtgtcccccgaggacatccaccagtggaacgtgaccagccccgacaccgtgaaaaccctgctgaaggtgtccaagg
gccagaagatgaacgcccaggctatcgccctggtggcctgctatctgagaggcggcggacagctggatgaggacatggtcaaggccctg
ggcgacatccccctgagctacctgtgtgacttcagtccacaagacctgcacagcgtgcccagcagcgtgatgtggctcgtgggacctcag
gacctggacaagtgcagccagagacacctgggcctgctgtaccagaaggcttgcagcgccttccagaacgtgtccggcctggaatacttc
gagaagatcaagaccttcctgggcggagccagcgtgaaggacctgagagccctgagccagcacaacgtgtccatggatatcgccacctt
caagagactgcaggtggacagcctcgtgggcctgtctgtggctgaggtgcagaagctgctgggacccaacatcgtggacctgaaaaccg
aagaggacaagagccccgtgcgggactggctgttcagacagcaccagaaggatctggacagactgggcctgggactgcagggcggaa
tccctaacggatacctggtgctggacttcaacgtgcgcgaggccttcagctccagagcctctctgctgggccctggcttcgtgctgatctgga
tccctgctctgctgcccgccctgagactgtctaagctttaagtcgac

muMesothelin-GFP

gaattcaagctgctagcgccaccatgagaagagatgccgagcagaaggcctgccccctggcaaagaaccctacaaggtggacgagga
cctgatcttctaccagaactgggagctggaagcctgcgtggacggcaccatgctggccagacagatggacctcgtgaacgagatcccctt
cacctacgagcagctgagcatcttcaagcacaagctggacaagacctacccccagggctaccccgagagcctgattcagcagctgggcc
acttcttcagatacgtgtcccccgaggacatccaccagtggaacgtgaccagccccgacaccgtgaaaaccctgctgaaggtgtccaagg
gccagaagatgaacgcccaggctatcgccctggtggcctgctatctgagaggcggcggacagctggatgaggacatggtcaaggccctg
ggcgacatccccctgagctacctgtgtgacttcagtccacaagacctgcacagcgtgcccagcagcgtgatgtggctcgtgggacctcag
gacctggacaagtgcagccagagacacctgggcctgctgtaccagaaggcttgcagcgccttccagaacgtgtccggcctggaatacttc
gagaagatcaagaccttcctgggcggagccagcgtgaaggacctgagagccctgagccagcacaacgtgtccatggatatcgccacctt
caagagactgcaggtggacagcctcgtgggcctgtctgtggctgaggtgcagaagctgctgggacccaacatcgtggacctgaaaaccg
aagaggacaagagccccgtgcgggactggctgttcagacagcaccagaaggatctggacagactgggcctgggactgcagggcggaa
tccctaacggatacctggtgctggacttcaacgtgcgcgaggccttcagctccagagcctctctgctgggccctggcttcgtgctgatctgga
tccctgctctgctgcccgccctgagactgtctaagcttgccaccatggtgagcaagggcgaggagctgttcaccggggtggtgcccatcct
ggtcgagctggacggcgacgtaaacggccacaagttcagcgtgtccggcgagggcgagggcgatgccacctacggcaagctgaccct
gaagttcatctgcaccaccggcaagctgcccgtgccctggcccaccctcgtgaccaccctgacctacggcgtgcagtgcttcagccgctac
cccgaccacatgaagcagcacgacttcttcaagtccgccatgcccgaaggctacgtccaggagcgcaccatcttcttcaaggacgacggc
aactacaagacccgcgccgaggtgaagttcgagggcgacaccctggtgaaccgcatcgagctgaagggcatcgacttcaaggaggacg
gcaacatcctggggcacaagctggagtacaactacaacagccacaacgtctatatcatggccgacaagcagaagaacggcatcaaggtg
aacttcaagatccgccacaacatcgaggacggcagcgtgcagctcgccgaccactaccagcagaacaccccccatcggcgacggccccg
tgctgctgcccgacaaccactacctgagcacccagtccgccctgagcaaagaccccaacgagaagcgcgatcacatggtcctgctggag
ttcgtgaccgccgccgggatcactctcggcatggacgagctgtacaagtaaaacgcgtgtcgact

9 Curriculum Vitae

Katherine E Baxter

Education and Training

PhD. Microbiology and Immunology (2014- Expected Completion Spring 2019)
University of Ottawa – Ottawa ON
Supervised by Dr Rebecca Auer and Dr John Bell at the Ottawa Hospital Research Institute.
Thesis: *Development of a heterologous oncolytic vaccine targeting mesothelin for the treatment of pancreatic adenocarcinoma*
Queen Elizabeth Graduate Scholarships in Science & Technology (2017-2018) University of Ottawa Excellence Scholarship (2017-2018)
University of Ottawa Admission Scholarship (2014-2017, 2018-2019)
Dept. of BMI Poster Day 1st prize in PhD Microbiology and Immunology (2017)

Honours BSc: Biopharmaceutical Sciences specialization Genomics (co-op) 2009-2014
University of Ottawa – Ottawa ON
Graduated Magna Cum Laude, Dean's Honour list. Received Undergraduate Admission Scholarship

Languages:
Native/Bilingual Proficiency in English and French

Skills
General Skills:
Development, planning and execution of a PhD level project
Supervision and training of undergraduate students
Analysis software including statistical analysis (Excel, GraphPad, R) as well as genome analysis software (KEGG, David, Gene Ontology)
Collaboration on multiple teams, including within the lab as well as between multiple labs to further scientific projects and apply to grants
Experience writing manuscripts, scholarship applications and patents.
Lab Skills:
Tissue culture experience, and CL2 level work with murine tissues and human specimens
Animal Work: Extensive work with animal models, including in vivo immune assays, injection techniques and development of a surgery model. Work in multiple tumour models. NIAUT Certification.
Immune Assays: Extensive work with immune-based assays including ELISA, ELISpot, flow cytometry, T cell based assays, cytotoxic assays, in vivo depletions, IHC and many more
RNA/DNA/Protein work: Extraction, manipulation and characterization of RNA, DNA and protein including PCR, qRT-PCR, microarray, restriction digest, and Western Blot characterization and related analysis.
Bacterial Work: Work in bacterial culture, transformation, growth and phenotype microarrays

Virus experience: Development of viral backbones and rescue. Transductions, growth curves, cytotoxicity assays and in vivo work.
CRISPR/Cas9 editing

Leadership Skills

Leadership in developing a branch of a cancer charity
Community outreach
Co-ordination of large-scale events
Motivation of student interest in participating and learning about cancer and cancer research

Experience

Graduate Student - The Ottawa Hospital Research Institute (2014-expected completion Spring 2019)

Supervised by Dr Rebecca Auer and Dr John Bell

Developing a murine surgical model of pancreatic cancer, and characterizing the immune infiltration and microenvironment of the tumour

Developing a heterologous prime-boost oncolytic vaccine platform, and characterizing the adaptive and innate immune responses stimulated through vaccination

Understanding the mechanisms of developing an efficacious, or non-efficacious oncolytic vaccine platform *in vivo*

Flow cytometry, RNA/DNA extraction, PCR and qRT-PCR, ELISAs and other fluorometric assays, tissue culture, protein extraction/Western blot, IHC, CrisprCas9 editing, oncolytic virus engineering/characterization/growth, animal work, student supervision.

Research Assistant/Honours Student - Health Canada (2013-2014)

Studied the effects of various nanoparticles on tissues and human cells to establish biomarkers of toxicity and inflammation.

Human and murine mRNA and microRNA extraction, microarrays, qPCR, statistical and data analysis of microarray profiles.

Research Technician/Co-op student - Apopharma Non-Clinical Discovery (2012)

Work as part of a team to measure effects of in-production pharmaceuticals on murine tissues

Use of various immunoassays including ELISAs and IHC

Research Technician/Co-op student - Laboratory of Foodborne Zoonoses, PHAC (2012)

Analysis of pathogenic *E.coli* through DNA, PCR and tissue microarrays

Use of bacterial techniques and assays, DNA extraction, PCR. Part of a Canada-wide team.

Research Technician/Co-op student - HPFB, Health Canada (2012)

Development of an *in vitro* model of Parkinson's-like neurons for the regulatory testing of new therapeutics

Tissue culture work, MTT and LDH assays

Additional Work Experience:

Teaching Assistant (2018)
General Intermediary Metabolism, Faculty of Science
Tutoring (2009-2014)

Tutoring high school and university level math, science and French

Service/Leadership Roles

Founding Member, RIOT Ottawa Branch, Canadian Cancer Society (2016-current)
Coordinator – Advertising, Organization and Teacher Recruitment, Let's Talk Cancer, Ottawa (2016-current)
Volunteer, Team COVCo, Terry Fox Foundation (2014-current);

Publications

Spleen preserving distal pancreatectomy preserves immune function in a surgical model of pancreatic adenocarcinoma. Baxter KE. Tanese de Souza C, Tai LH, Yaghini P, Daneshmand M, Kennedy MA, Auer RC. Journal for Immunotherapy of Cancer. *In review.*

The self-antigen mesothelin is not an ideal target of the oncolytic prime-boost platform. Baxter KE. Tanese de Souza C, Tai LH, Alkayyal AA, Stephenson KB, Bell JC, Lichty BD, Kennedy MA, Auer RC. *In preparation.*

The potential for cancer immunotherapy in targeting surgery-induced natural killer cell dysfunction. Market M, Baxter KE, Angka L, Kennedy MA, Auer RC. *Cancers*. 2018 11(1). Pii:E2. doi: 10.3390/cancers11010002.

Phosphodiesterase-5 inhibition reduces postoperative metastatic disease by targeting surgery-induced myeloid derived suppressor cells. Tai LH, Alkayyal AA, Leslie AL, Sahi S, Bennett S, Tanese de Souza C, Baxter KE, Angka L, Xu R, Kennedy MA, Auer RC. *OncoImmunology*. 2018 7(6): e1431082

Surgical Stress Abrogates Pre-Existing Protective T Cell Mediated Anti-Tumor Immunity Leading to Postoperative Cancer Recurrence. Ananth AA, Tai LH, Lansdell C, Alkayyal AA, Baxter KE, Angka L, Zhang J, Tanese de Souza C, Stephenson KB, Parato K, Bramson JL, Bell JC, Lichty BD, Auer RC. *PLoS One*. 2016; 11(5): e0155947

Patents

Patent Pending: MG1 mesothelin, prime-boost platform. Application in preparation with Turnstone Biologics

First Author Posters Presented at Conferences

Third CRI-CIMT- EATI-AACR International Cancer Immunotherapy Conference Mainz, Germany 2017
Summit for Cancer Immunotherapy Ottawa ON (2017)
Summit for Cancer Immunotherapy CCIC/BioCanRx Halifax NS (2016)
Terry Fox Research Institute (TFRI) Annual Scientific Meeting Vancouver BC (2016)